ABSTRACT

Orbits, Pseudo Orbits, and the Characteristic Polynomial
of q-nary Quantum Graphs

Victoria K. Hudgins, Ph.D.

Mentor: Jonathan M. Harrison, Ph.D.

Quantum graphs provide a simple model of quantum mechanics in systems with complex geometry and can be used to study quantum chaos. We evaluate the variance of the coefficients of a quantum binary graph's associated characteristic polynomial, which is related to the quantum graph's spectrum. This variance can be written as a finite sum over pairs of short pseudo orbits on the graph with the same topological and metric lengths. To account for all pairs of this type, we first count the numbers of primitive periodic orbits and primitive pseudo orbits on general q-nary graphs by exploiting properties of Lyndon words. We then classify the primitive pseudo orbits on binary graphs by their numbers of self-intersections, the number of repetitions of each self-intersection, and the lengths of self-intersections, in order to determine the contributions of primitive pseudo orbit pairs to the variance. By arranging the sum in a way that considers the contribution of each primitive pseudo orbit paired with all possible partners, we can evaluate the sum over all pairs of primitive pseudo orbits and then use the graph's ergodicity to asymptotically determine the variance in the

limit of large binary graphs. The Bohigas-Giannoni-Schmit conjecture suggests spectral statistics of generic quantum graphs are typically modeled by those of random matrices, in the limit of large graphs. However, we show that, for families of binary graphs, there is a uniform family-specific deviation from random matrix behavior in the variance of coefficients of the characteristic polynomial. Related results for the variance of the coefficients of the characteristic polynomial for general q-nary quantum graphs are also investigated.

Orbits, Pseudo Orbits, and the Characteristic Polynomial
of q-nary Quantum Graphs

by

Victoria K. Hudgins, B.S., M.S.

A Dissertation

Approved by the Department of Mathematics

Dorina Mitrea, Ph.D., Chairperson

Submitted to the Graduate Faculty of
Baylor University in Partial Fulfillment of the
Requirements for the Degree
of
Doctor of Philosophy

Approved by the Dissertation Committee

Jonathan M. Harrison, Ph.D., Chairperson

Fritz Gesztesy, Ph.D.

Klaus Kirsten, Ph.D.

Mark Sepanski, Ph.D.

Brian Simanek, Ph.D.

B. F. L. Ward, Ph.D.

Accepted by the Graduate School

August 2020

J. Larry Lyon, Ph.D., Dean

Page bearing signatures is kept on file in the Graduate School.

TABLE OF CONTENTS

LIST OF FIGURES

LIST OF TABLES

ACKNOWLEDGMENTS

First and foremost, a huge thank you to my advisor, Dr. Jon Harrison. When you completed your Pizza Seminar talk on binary graphs and Lyndon words five years ago, I turned to the graduate students nearby and exclaimed, "That was so cool! We have to read more about Lyndon words!" When they laughed, I knew that my interest in this was unique. I cannot thank you enough for trusting me to help move that project forward, for investing your time in giving me a broad mathematical physics education, and for always taking the time to discuss my very real concerns about pursuing a career in mathematics. You have pushed the limits of my thinking and have always been there to support me.

To the mathematics department at Baylor University – thank you to all the faculty, staff, and my fellow graduate students who have helped me wrestle with mathematical concepts, streamlined my teaching to make time for research, and offered an encouraging word in the last six years. In particular, thanks to my committee – Dr. Fritz Gesztesy, Dr. Klaus Kirsten, Dr. Mark Sepanski, Dr. Brian Simanek, and Dr. B.F.L. Ward – for your encouragement over the years (especially in those first couple rough colloquium talks) and for all the time that you have spent revising and polishing this dissertation. Thank you to my cohort – Peter Coogan, Dr. Jennifer Loe, Dr. Isaac Michael, and Dr. John Miller – I could never have survived the first semester without your willingness to let me just watch you solve problems without contributing. Thank you to the original Mathematical Maidens – Dr. Katie Elliott, Dr. Tiffany Jones,

Dr. Jennifer Loe, and Dr. Erica Swindle – I don't think I could have survived the last few months of writing without having seen each of you go through this before me and your continued friendship. Thank you to Taylor Poe and Jack Rebrovich – while the 2020 pandemic quarantine gave me unprecedented freedom to sit at home and write all day everyday, it was your checkups, shared walks in the sunshine, and your willingness to listen to me rant and celebrate through these last four months that gave me the sanity I needed to get this done.

Thank you to my Waco community – particularly the ladies of IF:Baylor and the members of the Mount Lebanon SDA Church – for your unceasing support and friendship over the last six years. Thank you to my pseudo-parents all over, for praying me past each obstacle, whether you are near or far.

Thank you to all my former math teachers – in particular, Anita Minty, Marilynn Peeke, and Dr. Larry Ray – you have inspired, pushed, and encouraged me, even on this graduate school journey, long after having spent time in your classrooms.

Last, but by no means least, thank you to my family. Your love, your desire to understand what I've been doing, your encouragement even when I haven't communicated it well, your prayers, your spiritual, emotional, mental, and financial support – these have all enabled me to keep going when times were difficult. Every investment has mattered and has not gone unnoticed.

"Rejoice always; pray without ceasing; in everything give thanks;

for this is God's will for you in Christ Jesus."

1 Thessalonians 5:18

To my mother
Without you, this would not exist

CHAPTER ONE

Literature Review

1.1 Quantum Graphs

1.1.1 Graph Theory

It is hard to overstate the usefulness of graph theory, as this branch of mathematics has found applications in many areas of science over the centuries. Graph theory was invented by the Swiss mathematician Leonhard Euler in 1736 [51, 70, 113], when he ventured to solve a popular problem of the day known as the Königsberg Bridges Problem. The Pregel River ran through the the city of Königsberg, Prussia (located on the modern site of Kaliningrad, Russia) and created an island called Kneiphof. This island was connected to the north, south, and east banks of the river by a total of seven walking bridges, see figure 1.1. The Königsberg Bridges Problem posed the

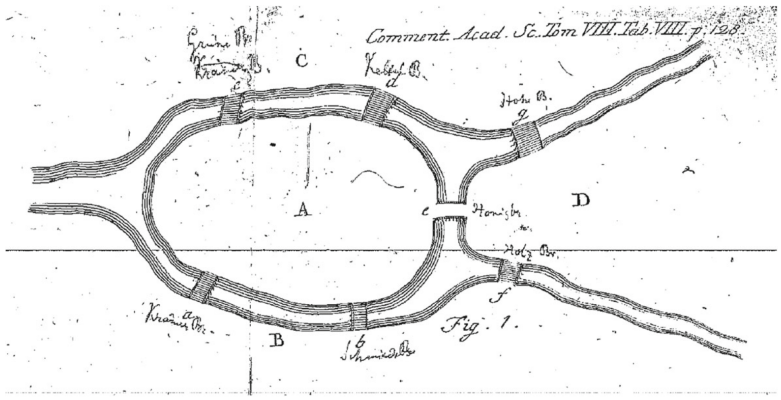

Figure 1.1. Euler's sketch of the Königsberg Bridges Problem, 1736 [50, 113]

question: is it possible for one to begin at any of the four landmasses and cross each bridge precisely once? In particular, is it possible to do this and end at the same place at which one began?

Euler considered the problem by reducing each landmass to a point with a label A, B, C, or D and replacing each bridge with a line labeled a, b, c, d, e, f, or g, as in figure 1.2. By concatenating landmass and bridge labels alternately, Euler could

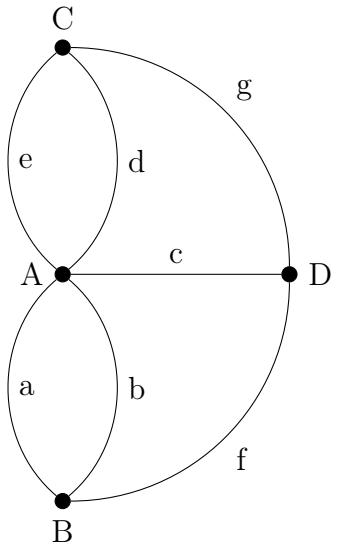

Figure 1.2. A graph-theoretic rendering of the Königsberg Bridges Problem

represent possible walks through the city. In particular, Euler's paper goes further than listing all possible paths and solving by brute force; rather, he derives necessary and sufficient conditions under which a problem of this type has a solution. Much of what follows in subsequent chapters is concerned with problems of a similar nature to Euler's second question, with walks that begin and end at the same point, so we will focus on that case here.

Euler showed that a walk that begins and ends at the same point and uses each bridge exactly once, an *Eulerian circuit*, exists if and only if the number of bridges connected to each region of land is even. One can easily see this is a necessary condition by imagining that one is an observer stationed at a particular landmass. If a walker enters your region via a particular bridge, then the walker must leave that region via another bridge, so the bridges connected to that region are used up in pairs. And if the walker begins in your landmass, they will leave on a bridge, use up a pair of bridges each time they visit, and there must be a single bridge remaining in order for the walker to return to his starting region. Consequently, there is no Eulerian circuit that solves the Königsberg Bridges Problem, as the number of bridges adjacent to each region of land is odd.

Euler states in this same paper that he finds this solution interesting because, while the problem is geometric in nature, the solution does not involve any traditional geometric measures. This makes the result a pre-cursor to the modern field of topology. Moreover, the reader familiar with graph theory will recognize Euler's reduction of landmasses to points (or *vertices*) and of bridges to lines (or *edges*) as a representation of the problem as a *graph*, a set of vertices connected by edges.

A related problem finds routes that visit each vertex precisely once, rather than using each edge. These are referred to as *Hamiltonian paths* (or *Hamiltonian circuits* when they start and end at the same vertex) for Sir William Hamilton who, in 1859, sold the idea for a game entitled Around the World [70]. A regular dodecahedron was drawn in two dimensions with each of its twenty vertices labeled by a letter A through T, as in figure 1.3. Each letter represented a major city around the world,

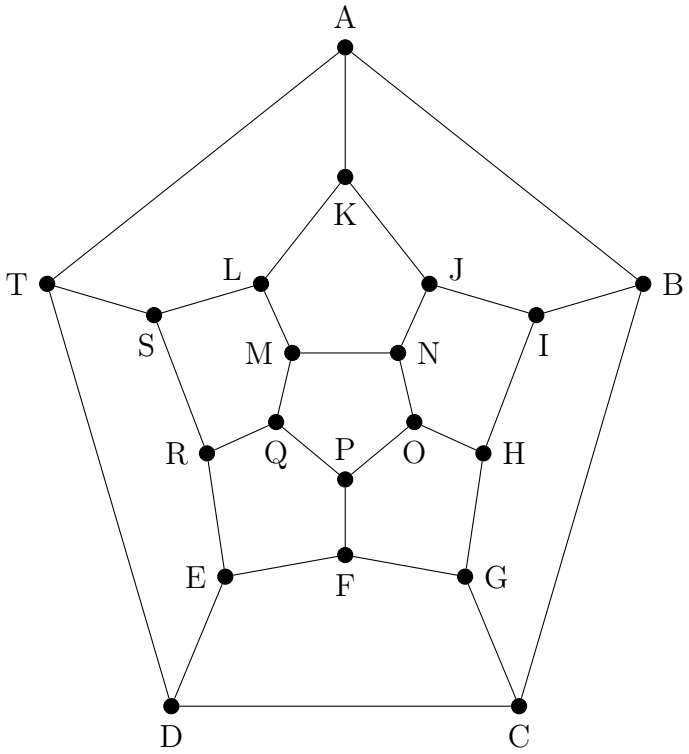

Figure 1.3. Hamilton's Around the World game

and the goal was to determine a route that would pass through each city exactly once. While this problem is intimately connected to the first example, it turns out to be much more difficult to solve [4].

More generally, graph theory is used to study any sort of networking problem, including traffic flows [102, 109, 114], activity of the brain [74, 83], social networking [33, 105], sports analysis [36], and much more [41, 128, 135]. It is also deeply connected to the famous Four-Color Theorem, which states that every map of countries, states, provinces, etc. can be colored in such a way that any countries adjacent to one another are colored differently and at most four colors are used. This was first hypothesized in 1852 by Francis Guthrie and proven in 1977 by Appel and Haken [1, 42, 70].

1.1.2 Origins of Quantum Graphs and Applications

Linus Pauling, who is consistently ranked as one of the most influential scientists of all time [73], was an American chemist. He earned two Nobel prizes, one in chemistry in 1954 and the other for peace in 1962, and is generally considered to be the first to study quantum graphs [11, 61]. In his 1936 paper, "The Diamagnetic Anisotropy of Aromatic Molecules", Pauling sought to calculate the magnetic anisotropy of aromatic hydrocarbons, magnetic effects associated to these molecules dependent on the direction or axis considered. Pauling states [106],

> Our problem is equivalent to that of calculating the magnetic effect of the currents induced in a conducting network.... In order to simplify the calculation we shall first consider rectilinear hexagonal nets, and then make a small correction by replacing the outermost lines by circular arcs.

The "rectilinear hexagonal net" to which he refers is the network or graph, pictured in figure 1.4. A key difference between Pauling's model and the classical graph theory of section 1.1.1 is that here Pauling is thinking of the "rectilinear hexagonal net" as a net of wires embedded in the plane. Thus, the edges of the graph are not simply denoting relationships between vertices, but can be thought of as intervals of the real line. Following this idea, he then considers the Hamiltonian function for an electron in a constant magnetic field of strength H parallel to the z-axis. A differential operator paired with a graph that consists of intervals joined at vertices is what is now called a *quantum graph*.

Pauling's model was quickly denounced by other chemists; first by Kathleen Lonsdale [92], who pointed out that it did not account for differences in isomers. While the model did not survive for this application, it has evolved over the last eighty-four

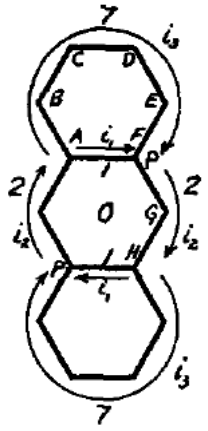

Figure 1.4. Pauling's diagram of the induced currents in anthracene [106]

years and been applied to many fields. As the relevant time-independent Schrödinger equation is an ordinary differential equation [80], quantum graphs yield simple, yet non-trivial, problems. The edges or wires of the graph are thought of as being widthless, which is not an unreasonable assumption at the atomic and subatomic levels.

Some examples of applications include mesoscopic systems, waveguides, and Anderson localization; see [18, 61, 84] for a survey of these examples and more. Mesoscopic systems are systems whose dimensions are measured by only a few nanometers and cannot be treated purely by classical or quantum physics, such as quantum wires or quantum dots, and have been successfully modeled by quantum graphs [2, 38]. Quantum graphs have been used to study acoustic and electromagnetic waveguides, which restrict transmission of a wave to one dimension with minimal loss of energy [52] and quantum waveguides, which study the dynamics of quantum particles constrained to tubular structures or networks [30, 31, 133]. They have also been used to study Anderson localization, or the absence of wave diffusion in a disordered medium [3].

Quantum graphs have also attracted significant attention in the study of quantum chaos, and were first proposed as a model of quantum chaos in a series of papers by Kottos and Smilansky [79, 80, 81, 82]. These seminal works established an exact trace formula for the quantum spectrum, which we will explore in greater detail in section 1.2.4. This produced an explosion of interest in quantum graphs as models of quantum chaos in the last two decades, a sampling of which will also be discussed in section 1.2.4. A comprehensive survey of results can be found in [18, 61]. To understand the impact of these results, we turn now to an overview of quantum chaos.

1.2 Quantum Chaos

1.2.1 Chaotic Dynamics

A dynamical system is a triple consisting of a phase space, a set of times, and a rule that describes how the phase space evolves over time. For example, the phase space can be a manifold, with the evolution through time described by a diffeomorphism; the phase space can be topological so that the evolution through time is described by a homeomorphism; or, the phase space could be a measure space with its evolution described by a measure-preserving transform. Some examples include a physical system containing N particles where the state space is $\mathbb{R}^{6N}$, which stores the position and momentum in each of three directions for each particle, governed by Hamilton's equations. Another example is the Bernoulli shift map on the product space of bi-infinite sequences of elements from a finite set, each with a positive weight such that the sum of the weights is one [107].

A standard example that illustrates the difference between regular and chaotic motion in a dynamical system is that of billiards. We start with a bounded planar domain with piecewise smooth boundaries and let a particle within this domain move in a straight line over time, with the stipulation that when the particle reaches the boundary, the angle of reflection will be equal to the angle of incidence [23]. We often refer to the domain itself as a *billiard*. Two examples of billiards are pictured in figure 1.5, a circular billiard and a *Sinai billiard*, a square region with a circle missing at the center.

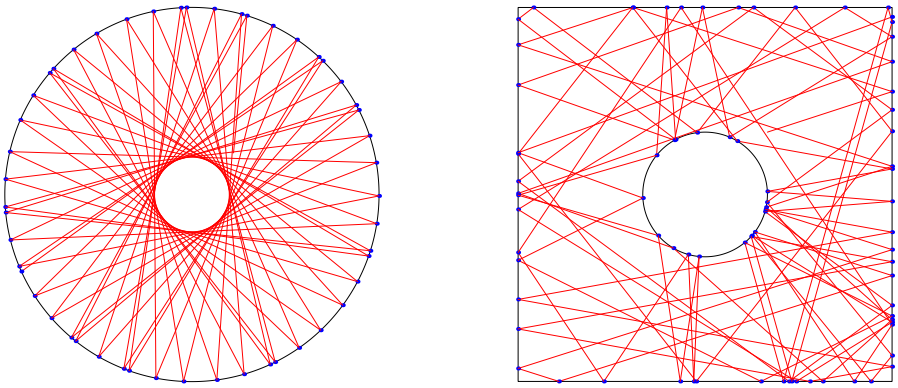

Figure 1.5. A circular billiard (left) and a Sinai billiard (right), each with a part of a billiard trajectory. The trajectory in the Sinai billiard is ergodic, whereas the trajectory in the circular billiard is not.

There many notions of chaotic motion in a dynamical system, including, but not limited to: sensitivity of trajectories to initial conditions, ergodicity, mixing, and entropy [107]. The reader familiar with basic notions of chaos is probably familiar with the idea of trajectories sensitive to initial conditions. If two particles begin at the same point on the circular billiard and travel at the same speed with velocity

vectors separated by an angle $\epsilon > 0$, then the two trajectories will diverge linearly with time; for the Sinai billiard, the same setup will yield trajectories that diverge exponentially over time [23]. However, for our purposes it is more useful to consider ergodicity and mixing as indicators of chaos.

Informally, in the context of billiards, *ergodicity* means that a typical trajectory densely fills the billiard. Portions of typical trajectories are shown for both the circular and Sinai billiards in figure 1.5. The portion of a trajectory shown for the Sinai billiard will densely fill the region as the time evolution continues, so the Sinai billiard is ergodic. However, a typical trajectory on the circular billiard avoids a smaller circular region at the center of the billiard. Depending on the initial angle, typical trajectories will not avoid the same circular region at the center of the billiard, but they will, in general, not be space-filling.

Now consider coloring n particles in some region of the billiard red, and color n particles blue in a second region, of the same size as the first region. Fix an initial velocity vector for each particle and evolve each particle in each region for a long period of time. After evolving each point for the same length of time, consider the ratio of red to blue particles in a third region of the billiard. If the numbers of red and blue particles are equal in this third region, and this occurs for all choices of regions in the billiard, then the billiard is mixing. Informally then, a billiard is *mixing*, if after a long time, particles that began in the same region are equally likely to end anywhere. The Sinai billiard in figure 1.5 is not only ergodic, but mixing. Ergodicity of a system does not necessarily imply mixing, but mixing implies ergodicity [112].

Ergodicity and mixing as notions of chaos will make more sense than exponential divergence of trajectories in the graph setting, as the classical dynamics defined for a graph will be probabilistic in nature. In particular, the dynamics will be defined by a Markov chain such that the directed edges (which we will call *bonds*) of a graph are the phase space, with the edge denoting position and the edge's direction denoting momentum [18]. We return to this in section 1.2.4.

1.2.2 Quantum Mechanics

Quantum mechanics explains the behavior of atomic and subatomic particles. The laws of classical Hamiltonian mechanics do not apply on the atomic and subatomic levels. A fundamental concept in quantum mechanics is wave-particle duality, which asserts that at this small scale particles behave both like classical particles and like waves. While this concept is widely accepted today, it took many physicists, including Planck, Einstein, de Broglie, and Schrödinger several decades to develop [69, 103, 122]. Following this idea, around 1925 the Schrödinger equation, where quantum states are described by a wavefunction, became a popular formulation of quantum mechanics. In this description, the absolute value squared of a wave function is a probability distribution for the position of a particle in the system [69].

Quantum mechanics is very different from classical mechanics, yet both describe reality and there must be agreement between them. Niels Bohr proposed a Correspondence Principle that asserts classical mechanics is the limit of quantum mechanics as objects increase in size. With slightly more rigor, Bohr's Correspondence Principle claims that quantum mechanics transitions to classical mechanics in the classical limit

of Planck's constant $\hbar \to 0$, which corresponds to the limit of large energies or large quantum numbers [67, 69, 103, 122].

In a series of papers published 1967-1971 [63, 64, 65, 66], Martin Gutzwiller explores this connection, and writes the density of quantum states for small values of $\hbar$ as a sum over all periodic orbits in the corresponding classical system. This is the trace of the semiclassical Green's function and is called a *trace formula*. Here, a periodic orbit refers to a smoothly closed trajectory [65], which begins and ends at the same point. In particular, Gutzwiller's trace formula can be used to formulate the density of quantum states for the Schrödinger equation on a billard domain, as in figure 1.5, as a sum over trajectories that are periodic. This connects the quantum spectrum to the classical periodic orbits of the system and as such is an important tool in *semiclassical quantum mechanics* [123], which is the study of quantum mechanics when Planck's constant $\hbar$ is small.

1.2.3 Random Matrices and the BGS Conjecture

In 1992, Martin Gutzwiller [67] attempted to describe quantum chaos by dividing up the study of mechanics into three areas, though admitting that in practicality these divisions are non-existent, see figure 1.6. These divisions are regular classical systems, chaotic systems, and quantum systems. The study of dynamical systems has increasingly involved studying connections between regular and chaotic systems, and a major tool for doing this is the Kolmogorov-Arnold-Moser (KAM) theorem, which identifies when perturbations cause regular dynamics to become chaotic [129]. The major connection between regular classical systems and quantum systems is

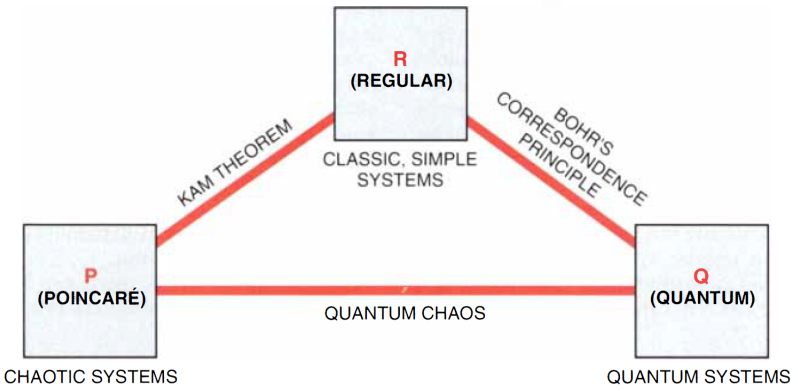

Figure 1.6. Gutzwiller's diagram for understanding categories of mechanics [67].

Bohr's Correspondence Principle, as introduced in section 1.2.1. It demonstrates that classical mechanics can be obtained from quantum mechanics in the classical limit of Planck's constant $\hbar \to 0$. The relationships between classically chaotic systems and quantum systems is the field of *quantum chaos*. For an overview of some problems being addressed as of 2019, see [134].

One example used to study these connections is to consider a Schrödinger equation on a classically chaotic billiard domain, such as the Sinai billiard in figure 1.5, on which we saw that typical classical billiard trajectories are ergodic and mixing. If one considers the Laplacian with Dirichlet boundary conditions on the Sinai billiard, then the problem amounts to solving a time-independent Schrödinger equation that represents a free particle in the domain. In general, computing the spectrum of the Laplacian on a generic chaotic domain is difficult [23], but for the Sinai billiard, there is a simple closed form [26], which was crucial in the original statement of the BGS Conjecture, which we will describe shortly. These general difficulties highlight the value of trace formulas, such as the one derived by Gutzwiller, that characterize the

quantum spectrum in terms of classical periodic orbits. Moreover, trace formulas aid in answering questions of an asymptotic nature, relating the behavior of large eigenvalues to the classical periodic orbits of the billiard flow.

Surprisingly, universal features arise in the spectrum of both regular and chaotic quantum systems, first noted by Berry and Tabor for regular systems and by Bohigas, Giannoni, and Schmit for chaotic systems. If a general dynamical system is regular, then its spectrum is uncorrelated and displays Poisson statistics [22]. If, however, a system is chaotic, then its spectrum is correlated and the spectral statistics resemble those of an ensemble of random matrices (the ensemble is determined by the symmetries of the quantum system) [26]. Both the principles identified by Berry-Tabor and Bohigas-Giannoni-Schmit (BGS) are still considered conjectures, in the sense that they can only be shown for specific statistics in specific systems, but a lot of numerical evidence and convincing proofs exist [10, 25, 29, 49, 57, 89, 91, 94, 95, 96, 100, 101, 110, 115]. It is interesting to note, however, that not all systems agree with these conjectures [8], including the application that we consider in this thesis.

A typical semiclassical approach to obtain spectral statistics that satisfy the BGS conjecture is to write the spectral statistic in terms of a trace formula for the spectrum; for example, applying Gutzwiller's result [66]. Many spectral statistics, such as the form factor (the Fourier transform of the two-point correlation function), turn into a double sum over pairs of orbits of the same length. In 1985, Berry showed that the first type of pair that interferes constructively to contribute to the spectral rigidity are pairs of identical orbits, or of mutually time-reversed orbits [21], and these pairs produce the constant term in a series expansion in powers of $\hbar$. Another development

in these proofs came from Sieber and Richter in 2001. In investigating the spectral form factor, Sieber and Richter realized that orbits with a self-intersection, or figure of eight shaped orbits, have partner orbits of the same length where one of the loops is run in the opposite direction from that of the original orbit [120, 121], as in figure 1.7. These orbits interfere with one another constructively and produce the linear term

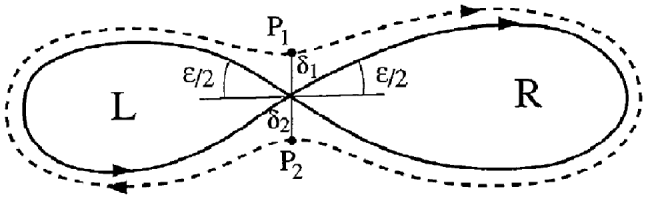

Figure 1.7. A figure of eight shaped orbit as drawn by Sieber and Richter [121].

in the expansion in powers of $\hbar$. Müller et al. continued to develop this approach by considering orbits with multiple self-intersections and obtained the whole form factor expansion for small values of $\hbar$ [100, 101]. The same authors also introduced computations with *pseudo orbits*, which are collections of periodic orbits, to this sort of problem in [72, 99]. However, these results do not fully explain the correspondence with the eigenvalue statistics of random matrix ensembles, as the calculations do not show that the contribution from other orbit pairs sums to zero. However, heuristic arguments suggest that the orbit pairs not evaluated are uncorrelated and should not contribute.

Random matrices were first introduced by Wishart in 1928 [55, 132]. Their popularity increased throughout the 1950s after Wigner [130] proposed using them as a model to understand statistical behaviour of slow neutron resonances in nuclear

physics [55, 98]. In 1955, Wigner was also the first to investigate the Gaussian ensembles of random matrices [131].

The Gaussian ensembles of random matrices consist of Hermitian matrices whose independent elements are independently distributed Gaussian random variables, and whose probability distribution is invariant under unitary, orthogonal, or symplectic transformations; thus, the ensembles are known as the Gaussian Unitary (GUE), Gaussian Orthogonal (GOE), and Gaussian Symplectic (GSE) Ensembles, respectively. When one considers that quantum systems either lack time-reversal invariance, or are time-reversal invariant with the square of the time-reversal operator either 1 or -1 [55, 68, 98], the corresponding Hamiltonian matrix operator is Hermitian (a complex square matrix that is equal to its conjugate transpose), symmetric (a real-valued square matrix that is equal to its transpose, a special case of Hermitian matrices), or Hermitian quaternionic (a symmetric square Hermitian matrix composed of quaternions). Dyson introduced the classification of random matrix ensembles by their time-invariant properties. The three possibilities discussed correspond to the GUE, GOE, or GSE, respectively [44, 45, 46, 47, 48].

The seminal paper outlining the BGS Conjecture [26] begins with a comparison of the level fluctuations of the quantum spectrum for the Sinai billiard with the level fluctuations of the eigenvalues of the Gaussian Orthogonal Ensemble of random matrices. After numerical analysis of the Sinai billiard's spectrum, Bohigas-Giannoni-Schmit conjecture that, in general, the quantum spectra of time-reversal invariant classically chaotic systems can be universally modeled by the level fluctuations of the Gaussian Orthogonal Ensemble; moreover, they conclude by proposing that quantum

systems lacking time-reversal invariance should have spectra modeled by the Gaussian Unitary Ensemble. It has since been observed that time-reversal invariant quantum systems that lack rotational symmetry have spectra modeled by the Gaussian Symplectic Ensemble [98].

1.2.4 Quantum Chaos on Graphs

For a quantum graph that pairs a metric graph with a self-adjoint differential operator (the Hamiltonian), the standard way to define an associated classical dynamical system on the graph is to convert the quantum evolution operator governing scattering of plane-waves at the graph vertices into a Perron-Frobenius operator governing transition probabilities between bonds of the graph [9, 18, 61, 78]. To do this, one lets the state space of the quantum graph dynamics be the set of directed edges (which we will call *bonds*) on the graph, where the choice of edge is position and the direction of the edge is momentum. Then one takes the absolute value squared of the scattering coefficients at a vertex to obtain the transition probabilities between adjacent bonds at that vertex. Thus, the classical dynamics of the quantum graph is a Markov chain, as the likelihood of transitioning to a particular bond depends only on the current state.

Given some initial state (some bond), after time $t \in \mathbb{N}_0$, each bond has some probability of being occupied with a total probability of one across all bonds. For connected graphs there is only one invariant probability distribution, the constant distribution, under the discrete Markov process. The classical dynamics is ergodic if the probability of occupying a particular bond averaged over time approaches the

invariant probability distribution [9, 61, 80]. One may also show for some graphs that the Markov process is mixing, which is the stronger chaotic property that any initial probability distribution converges to the invariant distribution under the Markov process in the large time limit [61]. For a quantum graph to be ergodic and/or mixing, it must be connected. However, a connected graph is not necessarily mixing. Consider a graph with V vertices and $E = V - 1$ edges, with an edge between some central vertex and each of the other vertices, a *star graph*; see figure 1.8. We will

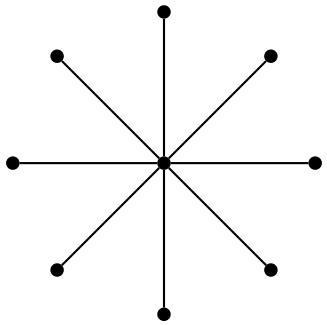

Figure 1.8. A star graph with nine vertices and eight edges.

think here of the star graph having both an incoming and an outgoing bond associated to each edge at the central vertex. The classical dynamics for a quantum star graph are ergodic, but not mixing, as at each time step of the Markov chain, the state is either an incoming or outgoing bond at v, and the transition probability to a bond of the same type is always zero [61].

In 1984, Roth derived a trace formula using the heat kernel of a quantum graph [116]. In a series of pioneering papers begun in 1997, Kottos and Smilansky were the first to connect quantum graph models to the study of quantum chaos [79, 80, 81, 82]. They characterize the probabilistic ergodic classical dynamics of a quantum graph, as

well as derive a trace formula for the density of states of a quantum graph's spectrum via a scattering approach. The trace formula is derived by expressing the density of states in terms of traces of powers of the scattering matrix and then writing the traces in terms of periodic orbits on the graph [18]. By *periodic orbits* we mean the graph's *circuits*, or sequences of vertices and edges on the graph that start and end at the same vertex, where rotations of these sequences are considered to be the same circuit. Of course these are generalizations of Eulerian circuits from the Königsberg Bridges Problem or Hamiltonian circuits from the Around the World game in section 1.1.1. For a general quantum system, Gutzwiller's trace formula is a semi-classical approximation valid in the limit $\hbar \to 0$, while on a quantum graph the trace formula exactly relates the quantum spectrum to the classical orbits independent of $\hbar$.

In 2002 and 2003, Berkolaiko, Schanz, and Whitney [19, 20] extended Berry's diagonal approximation [21] of a quantum graph's form factor to include diagrams of self-intersecting periodic orbits (orbits with repeated vertices) in analog to Sieber-Richter [120, 121] and found pairs of periodic orbits that yield higher order approximations to the form factor. This approach on graphs was subsequently extended by Müller et. al. [100, 101] in 2004 and 2005 to higher order contributions in general systems; here the quantum graph result came first and inspired the general result.

Another result that expresses a spectral property of a quantum graph, the coefficients of a generic graph's characteristic polynomial, in terms of orbits was obtained by Band, Harrison, and Joyner [5] in analogy to the results of Müller et. al. [72, 99]. The formula expresses the n-th coefficient as a sum over pseudo orbits (collections of periodic orbits) with n bonds. Our results in Chapters Four and Five will apply

similar ideas to those introduced by Berkolaiko-Schanz-Whitney [19, 20] and Müller et al. [100, 101] to the pseudo orbit formula.

The application of quantum graph models to the study of quantum chaos by Kottos and Smilansky ignited an explosion of interest. Results on particular graphs appeared quickly; a complete expansion of the form factor for star graphs is obtained in [12, 13] by Berkolaiko, Bogolmony, and Keating; binary graphs are considered in [124], and line-graphs are considered in [104]. An exact trace formula for the spectrum of the Dirac operator on graphs is derived and the spectrum is shown to approach GSE statistics in the semiclassical limit in [27, 28] by Bolte and Harrison.

Another topic in quantum chaos that has been studied on graphs is that of quantum ergodicity, which is the property that, in the limit of increasing energies, the eigenstates of a quantized ergodic classical Hamiltonian tend to equidistribute over the appropriate energy shell. It has been shown by Berkolaiko, Keating, and Winn [15, 16, 75] that star graphs are not quantum ergodic, which is used to show that, in general, billiards with the addition of a point singularity (called Šeba billiards) are not quantum ergodic either. However, quantum graphs constructed from interval maps do exhibit quantum ergodicity [14]. Quantum ergodicity is discussed more generally on graphs in [60]. Another important related topic is the analysis of spectral statistics via supersymmetric techniques introduced by Gnutzmann and Altland [59]. An extensive exposition of this topic can be found in [61].

Binary and q-nary graphs will be defined rigorously in section 2.5, but for now it suffices to say that a binary graph will have an even number of vertices and twice as many bonds such that, at each vertex, there are two incoming and two outgoing bonds. More generally, a q-nary graph has a number of vertices that is a multiple of q and has q times as many bonds, with q incoming and q outgoing bonds at each vertex.

The subset of q-nary graphs in which the number of vertices is precisely a power of q are called de Bruijn graphs [40]. The study of these graphs began with the search for the shortest possible circular superstring that contains all strings of a given length r. By enumerating these strings of length r over a q-nary alphabet and labeling each of the q^r vertices with one of these strings (see figure 1.9), de Bruijn showed that the solution to this problem is exactly the problem of finding a Hamiltonian circuit. This

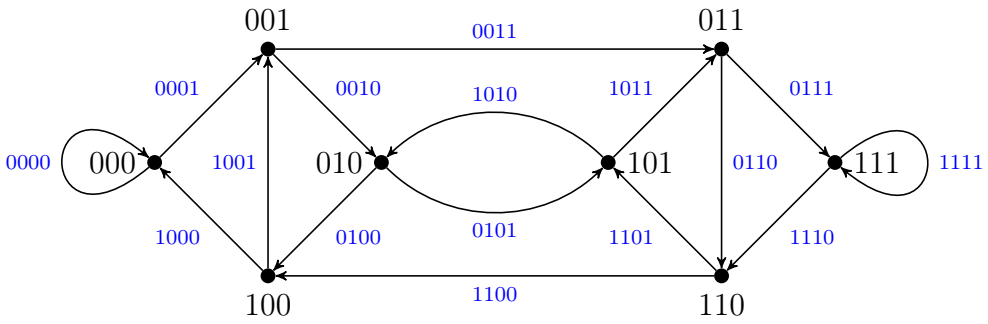

Figure 1.9. A binary de Bruijn graph with binary strings of length three labeling the vertices and binary strings of length four labeling the edges.

is a hard problem computationally (and this was a growing concern when published in 1946), but he also showed that this problem can always be converted to a search

for an Eulerian circuit by labeling edges between vertices with a string of length $r+1$. An edge exists from vertex u to vertex v if the first r digits of the edge label are the vertex label of u and the last r digits of the edge label are the vertex label of v. Thus, the solution to finding a superstring is precisely Euler's solution to the Königsberg Bridges Problem, and also happens to be much simpler computationally than finding a Hamiltonian circuit.

The q-nary graph models have proven useful in biology, as shown by Pevzner and many others. They can be used to assemble short-read sequences of DNA into a single genome [37, 97]. They have proven useful in antibody sequencing [7], synteny block reconstruction for highly duplicated genomes [108], and RNA assembly [62].

Some work for quantum q-nary graphs has also been done. Several results are the work of Gregor Tanner in a series of papers [124, 125, 126] that investigate the spectral statistics of binary and q-nary quantum graphs, in particular the form factor and the autocorrelation function for a quantum graph's spectral determinant, where he uses binary and q-nary graphs as examples for both. The averaged autocorrelation function of the spectral determinant is defined in [126] by the generating function for the square moduli of the secular coefficients, producing an intimate connection between these results and the results we will obtain regarding the variance of the coefficients of the characteristic polynomial. We will see the same convergence (see figure 1.10) for a particular family of binary graphs to the limit $\lim_{n\to\infty}\langle|a_n|^2\rangle = 5/8$ for sequences of graphs with increasing vertex number when we investigate the sum over pseudo orbits for this variance. In [6], Band, Harrison, and Sepanski apply the

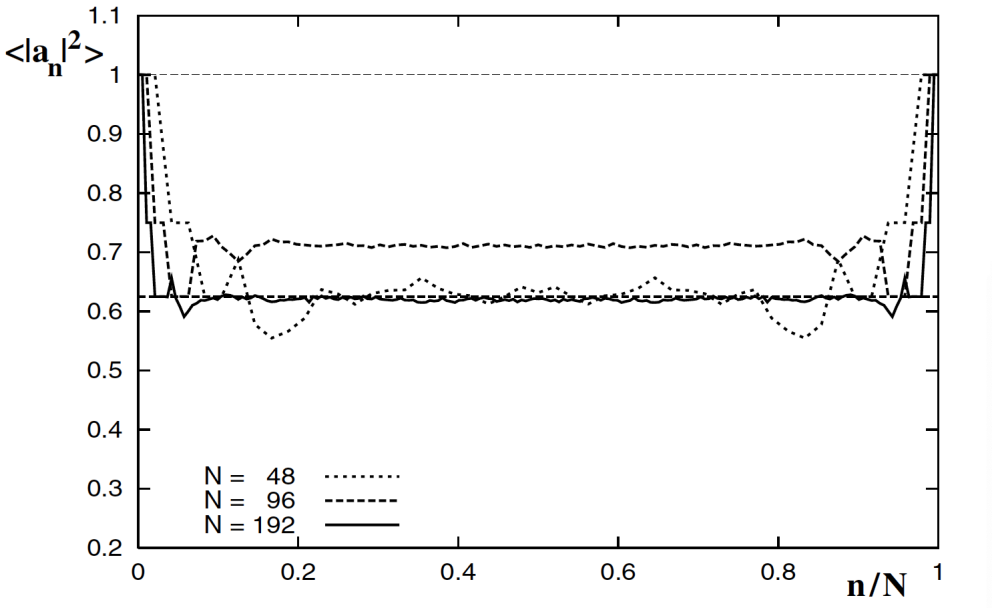

Figure 1.10. Convergence of the binary family with $N = 3 \cdot 2^r$ vertices to the asymptotic result $\langle |a_n|^2 \rangle = 5/8$ in the limit $r \to \infty$ as shown by Tanner [126].

formula of Band, Harrison, and Joyner [5] for the coefficients of a graph's characteristic polynomial to de Bruijn graphs.

In this thesis, we will continue the application of the Band-Harrison-Joyner formula studying the variance of a q-nary quantum graph's characteristic polynomial's coefficients written as a double sum over the graph's primitive pseudo orbits; in particular, we will find the limit of this variance for families of binary graphs for large coefficients and increasingly large graphs within the family in Chapter Four. These results will agree with Tanner [126] and diverge from random matrix theory. To do this, we will first need to count the numbers of primitive pseudo orbits of a given length on a binary graph; in Chapter Three we do this for all q-nary graphs. Preliminary results for determining the variance of a general q-nary graph's characteristic

polynomial's coefficients via a finite sum over pairs of pseudo orbits will be presented in Chapter Five.

CHAPTER TWO

Background

This chapter sets up the basic notation and ideas necessary to understand the results described in Chapters Three, Four, and Five. In section 2.1, we outline some fundamentals of graph theory, in particular the notation needed to discuss directed graphs, as well as define periodic and pseudo orbits on a graph. In section 2.2, we discuss two ways to quantize a metric graph and obtain a quantum graph, and we write the characteristic polynomial of a quantum graph as a finite sum over the graph's pseudo orbits. Section 2.3 reviews the basics properties of permutations and the symmetric group S_n used later. Section 2.4 defines words and, in particular, Lyndon words over a finite alphabet. It also introduces results regarding the factorization of words into Lyndon words and corresponding Lyndon tuples, and the standard factorization of Lyndon words themselves. The last section, section 2.5, defines q-nary graphs. It also explores the connection between words and labelings of de Bruijn graphs, and discusses the vertex scattering matrices that we assign to the vertices of q-nary graphs to quantize them.

2.1 Graph Theory

A *graph* Γ consists of a set of vertices $\mathcal{V}$ and a set of edges $\mathcal{E}$. We will only consider finite graphs with finite vertex and edge sets. Thus, a *vertex* belongs to the set $\mathcal{V} = \{0, 1, 2, \ldots, V-1\}$, and the size of the set of vertices is $|\mathcal{V}| = V$. An *edge* is an unordered pair of vertices $e = \{i, j\} \in \mathcal{E}$; two vertices i and j are *adjacent* if

$\{i, j\}$ is an edge. An edge $e = \{i, i\}$ is called a *loop*. The number of edges in Γ is $|\mathcal{E}| = E$. An example of a graph is given in figure 2.1. To any graph we can associate

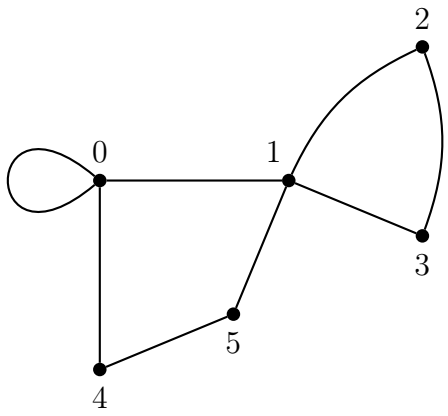

Figure 2.1. A graph with six vertices and eight edges.

an *adjacency matrix* A_V, a square matrix with dimension V such that $(A_V)_{i,j} = 1$ if vertices i and j are adjacent, and $(A_V)_{i,j} = 0$ otherwise. For the graph in figure 2.1, the adjacency matrix is

$$A_V = \begin{pmatrix} 1 & 1 & 0 & 0 & 1 & 0 \\ 1 & 0 & 1 & 1 & 0 & 1 \\ 0 & 1 & 0 & 1 & 0 & 0 \\ 0 & 1 & 1 & 0 & 0 & 0 \\ 1 & 0 & 0 & 0 & 0 & 1 \\ 0 & 1 & 0 & 0 & 1 & 0 \end{pmatrix} . \tag{2.1.1}$$

Note that this matrix is *symmetric*, as $(A_V)_{i,j} = (A_V)_{j,i}$; this symmetry is due to the fact that the edges are unordered pairs. The *degree* of a vertex v is the number of vertices adjacent to it,

$$d_v = \sum_{j=0}^{V-1} (A_V)_{v,j} = \sum_{i=0}^{V-1} (A_V)_{i,v} . \tag{2.1.2}$$

A *path* or a *walk* is a sequence of vertices $p = v_0 v_1 \cdots v_n$ such that $\{v_i, v_{i+1}\} \in \mathcal{E}$ for all $0 \leq i < n$. Thus, the sequence of vertices and the edges between adjacent pairs can be traversed in the order given. A path is of *length* n if it contains n edges. If for every pair of vertices i, j there is a path of some length that starts at vertex i and ends at vertex j, then the graph Γ is *connected*. In particular, the graph Γ is connected if, for every pair of vertices i and j, there exists some power n such that the i, j-th entry of $(A_V)^n$ is nonzero; then the number of paths of length n between vertices i and j is $(A_V)^n_{i,j}$.

If an edge has a direction associated to it, then we will refer to the directed edge $b = (i, j)$ as a *bond*, where the pair of vertices (i, j) is ordered; the set of all bonds $\mathcal{B}$ has size $|\mathcal{B}| = B$. The *origin* and *terminus* of a bond can be specified by functions $o, t : \mathcal{B} \to \mathcal{V}$; for some bond $b = (i, j)$, the origin of b is $o(b) = i$ and the terminus of b is $t(b) = j$. The *reversal* of a bond $b = (i, j)$ is given by $\bar{b} = (j, i)$. The terms directed graph or digraph generally refer to graphs that may have a mixture of directed and undirected edges; however, for the purposes of this thesis, we assume that a *directed graph* or *digraph* has only bonds and no undirected edges. A natural way to turn a generic graph into a directed graph is to replace each edge with two bonds, one running in either direction; the edge $e = \{i, j\}$ would be replaced with the bond $b = (i, j)$ and its reversal $\bar{b} = (j, i)$, making the size of the bond set $B = 2E$. We will denote a bond's direction on a graph with arrows; see figure 2.2.

For a directed graph, we say two vertices i and j are *adjacent* if either (i, j) or (j, i) is in the set of bonds $\mathcal{B}$. The *adjacency matrix* A_V is defined such that $(A_V)_{i,j} = 1$ if there is a bond $(i, j) \in \mathcal{B}$ and $(A_V)_{i,j} = 0$ otherwise. The adjacency matrix for the

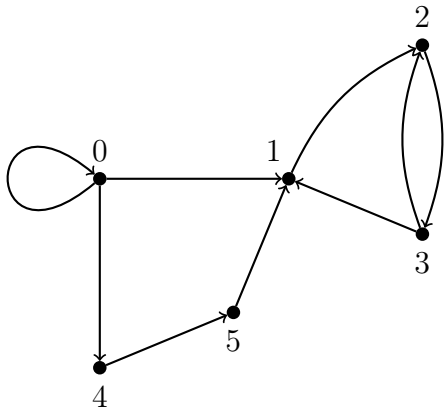

Figure 2.2. A directed graph with six vertices and nine edges.

digraph in figure 2.2 is

$$A_V = \begin{pmatrix} 1 & 1 & 0 & 0 & 1 & 0 \\ 0 & 0 & 1 & 0 & 0 & 0 \\ 0 & 0 & 0 & 1 & 0 & 0 \\ 0 & 1 & 1 & 0 & 0 & 0 \\ 0 & 0 & 0 & 0 & 0 & 1 \\ 0 & 1 & 0 & 0 & 0 & 0 \end{pmatrix} . \tag{2.1.3}$$

We define the *outgoing bonds* at v as the subset of $\mathcal{B}$ that have $o(b) = v$, and the *incoming bonds* at v as the subset of $\mathcal{B}$ that have $t(b) = v$. We will use $\mathcal{B}_v$ to denote the set of all bonds adjacent to v, both incoming and outgoing. The *incoming degree* of a vertex v is the number of bonds that terminate at v,

$$d_v^{in} = \sum_{j=0}^{V-1} (A_V)_{v,j} = \sum_{\substack{b \in \mathcal{B}_v \\ t(b)=v}} 1 , \tag{2.1.4}$$

and the *outgoing degree* of a vertex v is the number of bonds that originate at v,

$$d_v^{out} = \sum_{i=0}^{V-1} (A_V)_{i,v} = \sum_{\substack{b \in \mathcal{B}_v \\ o(b)=v}} 1 . \tag{2.1.5}$$

Then the *degree* of a vertex v is the sum $d_v = d_v^{in} + d_v^{out}$.

A *path* or a *walk* on a directed graph is a sequence of vertices $p = v_0 v_1 \cdots v_n$ such that $(v_i, v_{i+1}) \in \mathcal{B}$ for all $0 \leq i < n$ and is of *length* n as it contains n bonds. As with undirected graphs, we will call a directed graph *connected* if for every pair of vertices i, j, there is a path of some length between them. Thus, the graph Γ is again connected if for every pair of vertices i and j, there exists some power n such that the i, j-th entry of $(A_V)^n$ is nonzero. We note that the directed graph in figure 2.2 is not connected, as there is no path from vertex four to vertex zero.

For both directed and undirected graphs, a path $p = v_0 v_1 \cdots v_{n-1} v_0$ that begins and ends at the same vertex is a *closed path* or *closed walk* or *circuit*. A *periodic orbit* γ is an equivalence class of closed paths under rotation; for some closed path $p_0 = v_0 v_1 \cdots v_{n-1} v_0$ belonging to a periodic orbit γ, each of the paths $p_1 = v_1 v_2 \cdots v_{n-1} v_0 v_1$, $p_2 = v_2 v_3 \cdots v_{n-1} v_0 v_1 v_2, \ldots,\ p_{n-1} = v_{n-1} v_0 v_1 \cdots v_{n-1}$ belong to γ also. The n-th rotation of p_0 is $p_n = p_0$. Let n' be the smallest number of rotations such that $p_{n'} = p_0$. If $n' = n$, then the periodic orbit γ is *primitive*. If $n' < n$, then the periodic orbit γ is a *repetition* of a shorter closed path γ' of length n', and the *repetition number* of γ, or the number of repetitions of the shorter path γ', is $r_\gamma = n/n'$. For a periodic orbit γ containing n bonds, the *topological length* is the number of bonds B_γ in γ.

Any collection of periodic orbits $\bar{\gamma} = \{\gamma_1, \gamma_2, \ldots, \gamma_{m_{\bar{\gamma}}}\}$ is a *pseudo orbit*, and we denote the number of periodic orbits in $\bar{\gamma}$ by $m_{\bar{\gamma}}$. In analogy to periodic orbits, we let the topological length of $\bar{\gamma}$ be the sum of the topological lengths of the orbits it contains,

$$B_{\bar{\gamma}} = \sum_{\gamma_j \in \bar{\gamma}} B_{\gamma_j} \ . \tag{2.1.6}$$

The collection $\bar{\gamma} = \{\gamma_1, \gamma_2, \ldots, \gamma_M\}$ is a *primitive pseudo orbit* if it contains only primitive periodic orbits such that $\gamma_i \neq \gamma_j$ for $1 \leq i < j \leq m_{\bar{\gamma}}$. A pseudo orbit is *irreducible* if the collection of periodic orbits contains each bond on the graph at most once. Note that, irreducible pseudo orbits are primitive; however, a primitive pseudo orbit need not be irreducible. In Chapter Three we will derive an algorithm that counts the number of primitive periodic orbits of any length and the number of primitive pseudo orbits of length $n > p$ on q-nary graphs with $V = p \cdot q^r$ vertices.

2.2 Quantum Graphs

2.2.1 Definitions of Quantum Graphs

As the graphs we consider in subsequent chapters are digraphs, we will write our quantum graph definitions using digraph notation. As noted in section 1.1.2, a key feature of a quantum graph is that the graph is viewed as a network of wires between adjacent vertices, rather than only adjacency relations between vertices. To make a directed graph a *metric graph*, we associate a positive length L_b to each bond b and consider the interval $[0, L_b]$. While it is reasonable to consider bonds of semi-infinite length in a quantum graph, we will consider only the case of finite bond lengths. Given a metric graph, we assign a coordinate $x_b \in [0, L_b]$ to each bond such that the coordinate increases in the direction of the bond. Thus, $x_b = 0$ at $o(b)$ and $x_b = L_b$ at $t(b)$. We do not require here that for any bond b, its reversal $\bar{b}$ is also in the graph.

A periodic orbit γ on a metric graph has not only a topological length, but a *metric length*, the sum of the lengths of the bonds in γ, given by

$$L_\gamma = \sum_{b \in \gamma} L_b \ . \tag{2.2.1}$$

For a pseudo orbit $\bar{\gamma} = \{\gamma_1, \gamma_2, \ldots, \gamma_{m_{\bar{\gamma}}}\}$, let the metric length of $\bar{\gamma}$ be

$$L_{\bar{\gamma}} = \sum_{\gamma_j \in \bar{\gamma}} L_{\gamma_j} \ . \tag{2.2.2}$$

As in [79, 80, 81, 82], we will assume henceforward that the graph's bond lengths are *incommensurate*, meaning that the set of bond lengths is rationally independent. Thus, if we know the metric length of a periodic or pseudo orbit, we know which bonds were used in the orbit and how many times.

Once we have a metric graph, we can assign functions to the intervals associated to the bonds; a function f on the metric graph will be a B-tuple of functions on each interval. We consider functions from the Hilbert space

$$L^2(\Gamma) = \bigoplus_{b=1}^{B} L^2([0, L_b]), \tag{2.2.3}$$

with the inner product

$$\langle f, g \rangle = \sum_{b \in \mathcal{B}} \int_0^{L_b} f(x)\overline{g(x)} \, \mathrm{d}x. \tag{2.2.4}$$

Observables we wish to measure are described by self-adjoint operators acting on functions in the Hilbert space. One such observable is the *Hamiltonian*, $\mathcal{H}$, where

$$\mathcal{H} : f_b(x_b) \to -\frac{\mathrm{d}^2}{\mathrm{d}x_b^2} f_b(x_b) + V(x_b) f_b(x_b), \tag{2.2.5}$$

with domain consisting of functions in the second Sobolev space

$$H^2(\Gamma) = \bigoplus_{b=1}^{B} H^2([0, L_b]), \tag{2.2.6}$$

satisfying appropriate vertex conditions such that the operator $\mathcal{H}$ is self-adjoint; one example of such vertex conditions are the Neumann-like (standard/Kirchoff) vertex conditions.

To define standard vertex conditions, we let $f_b(v)$ denote the value of the function f_b at the vertex v; so if $o(b) = v$, then $f_b(v) = f_b(0)$, and if $t(b) = v$, then $f_b(v) = f_b(L_b)$. Similarly, $\dfrac{\mathrm{d}f_b}{\mathrm{d}x_b}(v) = \dfrac{\mathrm{d}f_b}{\mathrm{d}x_b}(0)$ when $v = o(b)$, and $\dfrac{\mathrm{d}f_b}{\mathrm{d}x_b}(v) = -\dfrac{\mathrm{d}f_b}{\mathrm{d}x_b}(L_b)$ when $v = t(b)$. In the *standard vertex conditions*, a function f on the metric graph Γ is continuous at the vertices, $f_{b_1}(v) = f_{b_2}(v)$ for all bonds $b_1, b_2 \in \mathcal{B}_v$, and the outgoing derivatives of f at vertex v sum to zero,

$$\sum_{b \in \mathcal{B}_v} \frac{\mathrm{d}f_b}{\mathrm{d}x_b}(v) = 0 \ . \tag{2.2.7}$$

We note that these vertex conditions are called Neumann-like because at a vertex of degree one, the condition reduces to a Neumann boundary condition. A metric graph with an associated differential operator (that is typically self-adjoint) is a *quantum graph*.

Solving the eigenproblem

$$\mathcal{H}f = Ef \ , \tag{2.2.8}$$

one obtains wavefunctions, f, on Γ for which the energy, E, of the system is constant. The point spectrum of $\mathcal{H}$ is the set of all energies that the quantum graph can attain.

The standard vertex conditions are a special case of the *δ-type* vertex conditions, where the function f is continuous at each vertex v, and the outgoing derivatives of f at vertex v satisfy

$$\sum_{b \in \mathcal{B}_v} \frac{\mathrm{d}f_b}{\mathrm{d}x_b}(v) = \alpha_v f(v) \ . \tag{2.2.9}$$

At a vertex of degree two, these δ-type vertex conditions correspond to a Schrödinger equation with a Dirac δ potential on an interval. The δ-type vertex conditions interpolate between Neumann and Dirichlet vertex conditions. To obtain Neumann vertex conditions, let $\alpha_v = 0$. Dirichlet vertex conditions, which require that the function vanish at a vertex, are obtained by dividing both sides of (2.2.9) by α_v and letting $\alpha_v \to \infty$ [17]. In practice, Dirichlet vertex conditions are not generally considered on quantum graphs, as they disconnect the set of intervals. All self-adjoint vertex conditions were classified by Kostrykin and Schrader [18, 77] and alternative formulations were provided by Kuchment et al. [56, 85] and Cheon et al. [35].

2.2.2 The Secular Equation of a Quantum Graph

Now we derive a secular equation, from which one can determine the spectrum of a graph. Here we consider an undirected graph as a directed graph Γ, where to each edge $e = \{i, j\}$ we associate the bond $b = (i, j)$ and its reversal $\bar{b} = (j, i)$; thus, Γ has $B = 2E$ bonds. The derivation will be the same if we begin with a directed graph with only a single bond between any pair of vertices and double the number of bonds by adding the reversal of each bond to the set of bonds. We assume that $L_{\bar{b}} = L_b$ and that the relation $x_{\bar{b}} = L_b - x_b$ holds on the coordinates along the intervals associated

to bonds and their reversals. We consider solutions to the eigenproblem

$$-\frac{\mathrm{d}^2 f_b}{\mathrm{d}x_b^2} = k^2 f_b(x_b) \ , \tag{2.2.10}$$

the time-independent Schrödinger equation describing a free particle on each interval. At each vertex, we will think of outgoing plane waves as living on the interval labeled by outgoing bond b and incoming plane waves as living on the interval labeled by incoming bond $\bar{b}$, so solutions will be linear combinations of plane waves for $k \neq 0$ (see [86, 87]),

$$f(x_b) = a_b \mathrm{e}^{\mathrm{i}kx_b} + a_{\bar{b}} \mathrm{e}^{-\mathrm{i}kx_{\bar{b}}} = a_b \mathrm{e}^{\mathrm{i}kx_b} + \mathrm{e}^{\mathrm{i}kL_b} a_{\bar{b}} \mathrm{e}^{-\mathrm{i}kx_b} \ , \tag{2.2.11}$$

where the second equality is a result of the relation $x_{\bar{b}} = L_b - x_b$.

For a vertex v with a plane wave e^{-ikx_b} approaching v on the incoming bond b, the wave will scatter when it reaches v into outgoing waves on all outgoing bonds adjacent to v. Then we can write solutions along the bonds adjacent to v as

$$\begin{cases} f_b(x_b) = \mathrm{e}^{-\mathrm{i}kx_b} + \sigma^{(v)}_{b,b} \mathrm{e}^{\mathrm{i}kx_b} \text{ on } b \\ f_{b'}(x_{b'}) = \sigma^{(v)}_{b',b} \mathrm{e}^{\mathrm{i}kx_b} \text{ for } b' \neq b \ , \end{cases} \tag{2.2.12}$$

where x_b-coordinates are measured from the vertex v on each bond, f satisfies the vertex conditions, and the coefficients $\sigma^{(v)}_{b',b}$ are called the *scattering coefficients* at v. We note that $\sigma^{(v)}_{b',b} = 0$ for all bonds $b \in \mathcal{B}_v$ that are not outgoing at v. Collecting the scattering coefficients $\sigma^{(v)}_{b',b}$ into a $d_v \times d_v$ matrix, we obtain the *scattering matrix*, $\sigma^{(v)}(k)$, that depends on the wave number k. This scattering matrix can be shown to be unitary for all vertex conditions that define a self-adjoint operator [18, 77]. For

the negative Laplacian with Neumann vertex conditions (2.2.7), the scattering matrix [80] is k-independent,

$$\sigma^{(v)}_{b',b} = \frac{2}{d_v} - \delta_{b',b} \ . \tag{2.2.13}$$

The *bond scattering matrix* $S(k)$ is a $2E \times 2E$ matrix that collects all the vertex scattering amplitudes,

$$S_{b',b}(k) = \delta_{t(b),v} \ \delta_{o(b'),v} \ \sigma^{(v)}_{b',b}(k), \tag{2.2.14}$$

indicating that b is an incoming bond at vertex v and b' is outgoing at v. Note that, an incoming plane wave $\mathrm{e}^{\mathrm{i}kx_b}$ scatters to b' having acquired a phase $\mathrm{e}^{\mathrm{i}kL_b}$ from equation (2.2.11).

Now if

$$\vec{a} = (a_1, \ldots, a_B, a_{\bar{1}}, \ldots, a_{\bar{B}})^T \tag{2.2.15}$$

is a vector of all $2E$ plane wave coefficients of an eigenfunction of the Laplacian, then the coefficients of the plane waves must be in a steady state; thus,

$$\vec{a} = S(k)\mathrm{e}^{\mathrm{i}kL}\vec{a} \tag{2.2.16}$$

for $L = \mathrm{diag}(L_1, \ldots, L_E, L_1, \ldots, L_E) = \mathrm{diag}(L_1, \ldots, L_B)$, a diagonal matrix of all bond lengths. We refer to the matrix $U(k) = S(k)\mathrm{e}^{\mathrm{i}kL}$ as the *quantum evolution map*. Rewriting (2.2.16), we obtain

$$(I - S(k)\mathrm{e}^{\mathrm{i}kL})\vec{a} = \vec{0} \tag{2.2.17}$$

and note that (2.2.17) has a nontrivial solution if and only if

$$\det(I - S(k)\mathrm{e}^{\mathrm{i}kL}) = 0; \tag{2.2.18}$$

equation (2.2.18) is called a *secular equation* of the quantum graph Γ. Solutions k of the secular equation (2.2.18) are the square roots of the eigenvalues k^2 of the graph Laplacian. A similar derivation for a Schrödinger operator with non-zero potential can be found in [117].

A commonly used alternative approach originated by Tanner [124] to define a quantum graph is to specify the unitary quantum evolution map $U(k) = S(k)\mathrm{e}^{\mathrm{i}kL}$, rather than beginning with a differential operator and vertex conditions. The matrix $S(k)$ will be defined following (2.2.14), so to determine $U(k)$, we need only specify a unitary vertex scattering matrix $\sigma^{(v)}(k)$ at each vertex. We define the spectrum of the graph to be the values k^2 that satisfy

$$\det(I - U(k)) = 0 \ , \tag{2.2.19}$$

in analogy to the spectrum of the Laplacian given by the secular equation (2.2.18). We note that a k-dependent choice of vertex scattering matrix does not, in general, result in a real spectrum. However, if the vertex scattering matrix is chosen to be independent of the wave number k, the spectrum is real [18, 32, 61].

Popular choices of vertex scattering matrices include the Neumann matrix (2.2.13), which encodes the Neumann vertex conditions for a generic graph and favors backscattering over other transitions, and the Discrete Fourier Transform (DFT) matrix

$$\sigma^{(v)}_{b',b} = \frac{1}{\sqrt{q}}\mathrm{e}^{2\pi\mathrm{i}\cdot b'b/q} \ . \tag{2.2.20}$$

The DFT matrix is a natural choice of scattering matrix, as the probability of scattering from an incoming bond b to an outgoing bond b' is democratic, in the sense that the probability of scattering from b to b' is

$$|\sigma^{(v)}_{b',b}|^2 = \begin{cases} 1/q & \text{if } t(b) = o(b') \ , \\ 0 & \text{otherwise} \ . \end{cases} \tag{2.2.21}$$

Unitary matrices that retain democratic forward scattering probabilities but prohibit backscattering are called *equitransmitting matrices* [71]; then,

$$|\sigma^{(v)}_{b',b}|^2 = \begin{cases} \frac{1}{d_v - 1} & \text{if } b' \neq b \ , \\ 0 & \textit{otherwise} \ . \end{cases} \tag{2.2.22}$$

For some dimensions it is also possible to generate unitary scattering matrices with the democratic property (2.2.21) from vertex conditions of a self-adjoint Laplace operator on a metric graph [127]. See [18, 61, 71, 88] for more on these types of scattering matrices. While it is standard to index $\sigma^{(v)}$ by the outgoing and incoming bonds, $\sigma^{(v)}_{b',b}$, we can also index by the terminal and original points on these bonds, respectively, $\sigma^{(v)}_{t(b'),o(b)}$, since $t(b) = o(b') = v$ when $\sigma^{(v)}_{b',b}$ is non-zero.

As the vertex scattering matrix $\sigma^{(v)}(k)$ and the bond scattering matrix $S(k)$ will be k-independent in what follows, we will henceforward suppress the dependence on the spectral parameter k and refer to $\sigma^{(v)}$ and S. Now we can define the *stability amplitude* of a periodic orbit, γ, as the product of scattering coefficients along γ,

$$A_\gamma = S_{b_2,b_1} S_{b_3,b_2} \cdots S_{b_n,b_{n-1}} S_{b_1,b_n} \ . \tag{2.2.23}$$

Additionally, the stability amplitude of a pseudo orbit $\bar{\gamma}$ is

$$A_{\bar{\gamma}} = \prod_{\gamma_j \in \bar{\gamma}} A_{\gamma_j} \ . \tag{2.2.24}$$

When the bond scattering matrix is k-independent, we also have a Weyl law for the average number of eigenvalues in an interval. Let $N^{sp}(k)$ count the number of eigenvalues of $U(k)$ that are less than k^2 and let $N^{alg}(k_1, k_2)$ count the number of roots of the secular equation (2.2.19) in the interval (k_1, k_2). Then $N^{sp}(k) = N^{alg}(0, k) + c$, where c is the multiplicity of the zero eigenvalue. Note that, c is not necessarily the multiplicity of the root zero of (2.2.19). The Weyl Law is [18],

Lemma 2.2.1. For a graph with a k-independent bond scattering matrix S,

$$N^{alg}(k_1, k_2) = \frac{\mathrm{Tr}(L)}{2\pi}(k_2 - k_1) + R \ , \tag{2.2.25}$$

where $\mathrm{Tr}(L)$ is the trace of the diagonal matrix of bond lengths L and thus, is the total metric length of the graph. The constant R is uniformly bounded in k_1 and k_2.

2.2.3 The Characteristic Polynomial of a Quantum Graph

In general, any square matrix M of dimension N has a characteristic polynomial,

$$\det(\zeta I - M) = \sum_{n=0}^{N} a_n \zeta^{N-n} \ . \tag{2.2.26}$$

A discrete graph has a characteristic polynomial,

$$\det(\zeta I - A) = \sum_{n=0}^{V} a_n \zeta^{V-n} \ , \tag{2.2.27}$$

where A is the graph's $V \times V$ adjacency matrix. The characteristic polynomial of a generic quantum graph with $B = 2E$ bonds is

$$F_\zeta(k) = \det(\zeta I - U(k)) = \sum_{n=0}^{B} a_n(k)\zeta^{B-n} \ . \tag{2.2.28}$$

Note that $U(k) = S\mathrm{e}^{\mathrm{i}kL}$ is the graph's quantum evolution map, so $F_1(k) = 0$ is the graph's secular equation (2.2.19), which encodes the graph's spectrum. As our bond scattering matrix S is k-independent in what follows, we will also henceforward suppress the dependency of the coefficients $a_n(k)$ on k.

As the quantum evolution map is unitary, its inverse is its conjugate transpose. Thus, there is a Riemann-Siegel lookalike formula [80] that connects pairs of coefficients of $F_\zeta(k)$,

$$a_n = a_B \bar{a}_{B-n} \ . \tag{2.2.29}$$

Using the fact that $U^{-1} = U^*$,

$$F_\zeta(k) = \det(\zeta I - U(k)) = \det(-\zeta U(k)) \det(\zeta^{-1} I - U^*(k)) \ . \tag{2.2.30}$$

Then writing the last determinant as a polynomial (2.2.28),

$$F_\zeta(k) = \det(-\zeta U(k)) \sum_{n=0}^{B} \bar{a}_n(k)(\zeta^{-1})^{B-n} \ . \tag{2.2.31}$$

Factoring out $-\zeta$ from the matrix determinant in (2.2.31), and using $B = 2E$,

$$F_\zeta(k) = (-\zeta)^B \det(U(k)) \sum_{n=0}^{B} \bar{a}_n(k)\zeta^{n-B} = \det(U(k)) \sum_{n=0}^{B} \bar{a}_n(k)\zeta^n \ . \tag{2.2.32}$$

Hence, as $a_B = \det(U(k))$, we obtain (2.2.29).

In [5], Band, Harrison, and Joyner derive a formula for the n-th coefficient of the characteristic polynomial, writing it as a sum over primitive pseudo orbits of topological length $B_\gamma = n$ (2.1.6). The contribution of a particular pseudo orbit $\bar{\gamma}$ to a coefficient is determined by the number of periodic orbits $m_{\bar{\gamma}}$ in $\bar{\gamma}$, the metric length (2.2.2) of $\bar{\gamma}$, and the stability amplitude (2.2.24) of $\bar{\gamma}$. A pseudo orbit of length zero, $\bar{0}$, is a pseudo orbit containing no periodic orbits. Clearly $m_{\bar{0}} = B_{\bar{0}} = L_{\bar{0}} = 0$ and we set $A_{\bar{0}} = 1$. Now we have the following theorem from [5]. (This proof can be found in the appendix of [5]; the proof in the main body of the paper is for a sum over irreducible pseudo orbits.)

Theorem 2.2.1. The coefficients $a_n(k)$ of the characteristic polynomial $F_\zeta(k)$ with $U(k) = S\mathrm{e}^{\mathrm{i}kL}$ are given by

$$a_n = \sum_{\bar{\gamma}|B_{\bar{\gamma}}=n} (-1)^{m_{\bar{\gamma}}} A_{\bar{\gamma}} \mathrm{e}^{\mathrm{i}kL_{\bar{\gamma}}} \ , \tag{2.2.33}$$

where $\bar{\gamma}$ is a primitive pseudo orbit on the quantum graph for which $U(k)$ is the quantum evolution operator.

Proof. Recall the matrix identity

$$\det(I - U(k)) = \exp \mathrm{Tr} \ln(I - U(k)) = \exp \mathrm{Tr} \left(- \sum_{j=1}^{\infty} \frac{[U(k)]^j}{j} \right) \ , \tag{2.2.34}$$

which holds for $k + \mathrm{i}\epsilon$ in the limit $\epsilon \to 0$. Applying (2.2.34) to the characteristic polynomial $F_\zeta(k)$, we obtain

$$F_\zeta(k) = \zeta^B \det(I - \zeta^{-1} U(k)) = \zeta^B \exp \left(- \sum_{j=1}^{\infty} \frac{\zeta^{-1} T_j}{j} \right) \ , \tag{2.2.35}$$

where $T_j = \mathrm{Tr}([U(k)]^j)$. The traces of the j-th powers of the quantum evolution map $U(k) = S\mathrm{e}^{\mathrm{i}kL}$ can be expressed as sums over periodic orbits,

$$T_j = \sum_{b_1,\ldots,b_j=1}^{B} U_{b_2,b_1} U_{b_3,b_2} \cdots U_{b_1,b_j} \tag{2.2.36}$$

$$= \sum_{b_1,\ldots,b_j=1}^{B} (S_{b_2,b_1}\mathrm{e}^{\mathrm{i}kL_{b_2}})(S_{b_3,b_2}\mathrm{e}^{\mathrm{i}kL_{b_3}}) \cdots (S_{b_1,b_j}\mathrm{e}^{\mathrm{i}kL_{b_1}}) \tag{2.2.37}$$

$$= \sum_{b_1,\ldots,b_j=1}^{B} S_{b_2,b_1} S_{b_3,b_2} \cdots S_{b_1,b_j} \mathrm{e}^{\mathrm{i}k(L_{b_1}+L_{b_2}+\cdots L_{b_j})} \ . \tag{2.2.38}$$

If we let the summation indices correspond to the bonds of the graph, then we have periodic orbits $\gamma = (b_1, b_2, \ldots, b_j)$. Thus,

$$T_j = \sum_{\gamma | B_\gamma = j} \frac{j}{r_\gamma} A_\gamma \mathrm{e}^{\mathrm{i}kL_\gamma} \ , \tag{2.2.39}$$

as there are j/r_γ distinct cyclic rotations of γ.

Inserting (2.2.39) into (2.2.35), we obtain

$$F_\zeta(k) = \zeta^B \exp\left(-\sum_{j=1}^{\infty} \sum_{\gamma | B_\gamma = j} \zeta^{-j} \frac{A_\gamma \mathrm{e}^{\mathrm{i}kL_\gamma}}{r_\gamma} \right) \ . \tag{2.2.40}$$

Equivalently, we can fix a primitive periodic orbit π and sum over its rotations, so that

$$F_\zeta(k) = \zeta^B \exp\left(-\sum_{\pi \text{ primitive}} \sum_{r=1}^{\infty} \zeta^{-rB_\pi} \frac{A_\pi^r \mathrm{e}^{\mathrm{i}krL_\pi}}{r} \right) \ . \tag{2.2.41}$$

Using the series expansion of $\ln(1-x)$ and properties of logarithms, we have

$$F_\zeta(k) = \zeta^B \exp\left(\sum_{\pi \text{ primitive}} \ln(1 - \zeta^{-B_\pi} A_\pi \mathrm{e}^{\mathrm{i}kL_\pi} \right) \tag{2.2.42}$$

$$= \zeta^B \prod_{\pi \text{ primitive}} (1 - \zeta^{-B_\pi} A_\pi \mathrm{e}^{\mathrm{i}kL_\pi}) \ . \tag{2.2.43}$$

If we expand the infinite product in (2.2.43), we would have a series where each term is associated to a collection of primitive periodic orbits without repetition, i.e., a primitive pseudo orbit. Of course, the characteristic polynomial has only finite powers of ζ; in particular,

$$F_\zeta(k) = \zeta^B \sum_{n=0}^{B} a_n \zeta^{-n} \ , \tag{2.2.44}$$

so many of the contributions from primitive pseudo orbits will cancel, and the result follows. □

First, we examine the mean values of the coefficients of the characteristic polynomial averaged over the spectral parameter k,

$$\langle a_n \rangle_k = \sum_{\bar{\gamma} | B_{\bar{\gamma}} = n} (-1)^{m_{\bar{\gamma}}} A_{\bar{\gamma}} \lim_{K \to \infty} \frac{1}{K} \int_0^K \mathrm{e}^{\mathrm{i}kL_{\bar{\gamma}}} \, \mathrm{d}k \ . \tag{2.2.45}$$

As characteristic polynomials are monic and using the Rieman-Siegel formula (2.2.29), trivially $\langle a_0 \rangle_k = \langle a_B \rangle_k = 1$; this can also be obtained by evaluating a_0 over the primitive pseudo orbit $\bar{0}$, as defined above. For $0 < n < B$, the mean value of the n-th coefficient is $\langle a_n \rangle_k = 0$ as $L_{\bar{\gamma}} \neq 0$.

Hence, the first non-trivial moment of the coefficients of the characteristic polynomial is the variance. The variance can be written as a sum over pairs of primitive pseudo orbits;

$$\langle |a_n|^2 \rangle_k = \sum_{\substack{\{\bar{\gamma},\bar{\gamma}'\}: \\ B_{\bar{\gamma}}=B_{\bar{\gamma}'}=n}} (-1)^{m_{\bar{\gamma}}+m_{\bar{\gamma}'}} A_{\bar{\gamma}} \bar{A}_{\bar{\gamma}'} \lim_{K\to\infty} \frac{1}{K} \int_0^K e^{\mathrm{i}k(L_{\bar{\gamma}}-L_{\bar{\gamma}'})} \, \mathrm{d}k \tag{2.2.46}$$

$$= \sum_{\substack{\{\bar{\gamma},\bar{\gamma}'\}: \\ B_{\bar{\gamma}}=B_{\bar{\gamma}'}=n}} (-1)^{m_{\bar{\gamma}}+m_{\bar{\gamma}'}} A_{\bar{\gamma}} \bar{A}_{\bar{\gamma}'} \delta_{L_{\bar{\gamma}},L_{\bar{\gamma}'}} \ . \tag{2.2.47}$$

Thus, only pairs of primitive pseudo orbits of both the same topological and metric lengths will contribute to $\langle |a_n|^2 \rangle_k$. As the graph's bond lengths are incommensurate, each pseudo orbit in a pair of primitive pseudo orbits $\{\bar{\gamma}, \bar{\gamma}'\}$ that contributes to (2.2.47) must visit each bond the same number of times.

We must find pairs of primitive pseudo orbits having the same topological and metric lengths in order to get nonzero contributions to (2.2.47). The simplest way in which to obtain pairs of this type is to pair a primitive pseudo orbit with itself, called the *diagonal contribution*. If a graph has time-reversal symmetry, then pairing a pseudo orbit with its reversal would be considered to also be part of the diagonal contribution; however, for all the examples we consider, the graphs lack time-reversal symmetry. This diagonal contribution to the variance is expected to be a significant contribution, as diagonal pairings can be considered for every primitive pseudo orbit. As $(-1)^{2m_{\bar{\gamma}}}$ is positive for every diagonal pair $\{\bar{\gamma}, \bar{\gamma}\}$, the diagonal contribution to (2.2.47) is given by

$$\langle |a_n|^2 \rangle_{\mathrm{diag}} = \sum_{\bar{\gamma}|B_{\bar{\gamma}}=n} |A_{\bar{\gamma}}|^2 \ . \tag{2.2.48}$$

We will further simplify this contribution for quantum q-nary graphs in section 2.5 and evaluate it in Chapter Three as an application of counting primitive periodic and primitive pseudo orbits.

2.3 The Symmetric Group S_n

In this section and section 2.4 we will discuss some results that allow for analysis of families of q-nary quantum graphs (as in sections 2.2 and 1.3). Both permutations and Lyndon words will be used extensively throughout the upcoming chapters to analyze the variance of the coefficients of the characteristic polynomial. The following content and related notions can be found in [90, 118].

The *symmetric group* S_n consists of all bijections from the set $\{1, 2, \ldots, n\}$ to itself. The group is equipped with a multiplication operation that composes these functions; thus, sequences of permutations are applied to the set $\{1, 2, \ldots, n\}$ from right to left. The elements of the group are called *permutations* and are notated in three common ways. First, a permutation $\pi \in S_n$ can be represented by a two-line notation that shows where elements map,

$$\begin{pmatrix} 1 & 2 & \cdots & n-1 & n \\ \pi(1) & \pi(2) & \cdots & \pi(n-1) & \pi(n) \end{pmatrix} . \tag{2.3.1}$$

If the permutation $\pi \in S_6$ of six elements is given by

$$\pi(1) = 2,\ \pi(2) = 3,\ \pi(3) = 1,\ \pi(4) = 5, \pi(5) = 4,\ \pi(6) = 6 , \tag{2.3.2}$$

then the two line form of π is

$$\pi = \begin{pmatrix} 1 & 2 & 3 & 4 & 5 & 6 \\ 2 & 3 & 1 & 5 & 4 & 6 \end{pmatrix} . \tag{2.3.3}$$

Of course, the first line is fixed, so we could just as easily represent the permutation by a second form, a one-line notation, that neglects the first line of the previous notation. Then the one-line notation associated to the example (2.3.2) is $\pi = 231546$. The third notation, which we will discuss next, also only has one line and traditionally requires use of parentheses, so it is standard to drop the parentheses in this one-line notation, so as not to confuse the two.

If we iterate applications of the map π on some element $i \in \{1, 2, \ldots, n\}$, elements of the infinite sequence $i, \pi(i), \pi^2(i), \pi^3(i), \ldots$ cannot all be distinct. Let r be the smallest natural number such that $\pi^r(i) = i$; then,

$$(i, \pi(i), \pi^2(i), \ldots, \pi^{r-1}(i)) \tag{2.3.4}$$

is a *cycle*. This means that for distinct elements $a_1, a_2, \ldots, a_k \in \{1, 2, \ldots, n\}$ with $k \leq n$, a cycle $\rho = (a_1\ a_2\ \cdots\ a_k)$ is such that $\rho(a_i) = a_{i+1}$ for $i = 1, \ldots, k-1$ and $\rho(a_k) = a_1$; also, $\rho(a) = a$ for any $a \notin \{a_1, a_2, \ldots, a_k\}$. A cycle on k elements is called a *k-cycle*.

Let π be a permutation that consists of the cycles $\pi_1, \pi_2, \ldots, \pi_m$. If an element $a \in \{1, 2, \ldots, n\}$ is fixed by all the cycles of π, so $\pi_i(a) = a$ for all $i = 1, \ldots, m$, then a is a *fixed point* of the permutation π. A set of cycles $\pi_1, \pi_2, \ldots, \pi_m$ is *disjoint* if for every element $a \in \{1, 2, \ldots, n\}$ such that $\pi_i(a) \neq a$ for some $i = 1, 2, \ldots, m$, then $\pi_j(a) = a$ for all $j \neq i$.

It is well understood [90] that every permutation in the symmetric group S_n can be written as a product of disjoint cycles and that disjoint cycles commute. We will primarily use this third notation, the *disjoint cycle decomposition*, to represent

a permutation, $\pi = \pi_1\pi_2\cdots\pi_m$ where the cycles π_i are disjoint. We note that it is standard to leave fixed points out of the disjoint cycle decomposition of a permutation. For the example (2.3.2), the disjoint cycle decomposition of π is $\pi = (1\ 2\ 3)(4\ 5)$, composed of a 3-cycle $\pi_1 = (1\ 2\ 3)$, a 2-cycle $\pi_2 = (4\ 5)$, and the 1-cycle $\pi_3 = (6)$ which yields the fixed point 6. The *identity permutation* $e = (1)(2)\cdots(n)$ is the permutation whose disjoint cycle decomposition is the product of all 1-cycles.

It is also well-known [90] that every permutation in S_n for $n \geq 2$ can be written as a product of 2-cycles, called *transpositions*, which follows from the fact that a k-cycle $(a_1\ a_2\ \cdots\ a_k)$ can be written as a product of $k-1$ transpositions, $(a_1\ a_2\ \cdots\ a_k) = (a_1\ a_2)(a_2\ a_3)\cdots(a_{k-1}\ a_k)$. Note that a product of transpositions is not unique. For the example (2.3.2), we can write $\pi = (1\ 2)(2\ 3)(4\ 5)(5\ 6)(5\ 6)$; however, we may also write $\pi = (1\ 2)(2\ 3)(4\ 5)(5\ 6)(5\ 6)(4\ 6)(4\ 6)$. However, both of these products contain an odd number of transpositions. In particular, there is no permutation that can be written as both a product of an even number of transpositions and a product of an odd number of transpositions [90]. Thus, we call a permutation *even (odd)* if it is the product of an even (odd) number of transpositions and define the *sign* of a permutation by a function $\text{sgn} : S_n \to \{-1, 1\}$, by

$$\text{sgn}(\pi) = \begin{cases} 1 & \text{if } \pi \text{ is a product of an even number of transpositions,} \\ -1 & \text{otherwise,} \end{cases} \tag{2.3.5}$$

for $\pi \in S_n$.

As a k-cycle can be written as a product of $k-1$ transpositions, it is even (odd) if and only if k is odd (even). Thus, we can determine the sign of a permutation

by considering the lengths of cycles in its disjoint cycle decomposition. We saw that π from the example (2.3.2) was odd from its transposition products; moreover, its disjoint cycle decomposition has a 3-cycle, a 2-cycle, and a 1-cycle, or two even cycles and an odd cycle. Thus, $\pi = (1\ 2\ 3)(4\ 5)$ is odd, as it contains an odd number of odd cycles. The following proposition shows that we can relate the sign of a permutation to the number of cycles in its disjoint cycle decomposition.

Proposition 2.3.1. Let $\sigma \in S_n$. Denote by $T(\sigma)$ the total number of cycles in the disjoint cycle decomposition of the permutation σ, and

$$\operatorname{sgn}(\sigma) = (-1)^{n+T(\sigma)} \ . \tag{2.3.6}$$

Proof. This proof is due to Klingsberg [76]. Let $E(\sigma)$ and $O(\sigma)$ denote the numbers of even-length and odd-length cycles in the disjoint cycle decomposition of σ, respectively, so the total number of cycles in σ is $T(\sigma) = E(\sigma) + O(\sigma)$. Here we will consider fixed-points as cycles of length one, so that the number of fixed points in σ is included in $O(\sigma)$. Let $l(\rho)$ denote the length of a cycle ρ of σ. Then

$$\ell = \sum_{\rho:\ l(\rho) \text{ is even}} l(\rho) + \sum_{\rho:\ l(\rho) \text{ is odd}} l(\rho) \ . \tag{2.3.7}$$

Now the first sum in (2.3.7) is clearly even, so n is even if and only if the second sum is even, which occurs if and only if the number of terms in the sum, $O(\sigma)$, is even. Therefore, $O(\sigma) \equiv n \pmod 2$.

Now since cycles of even (odd) length can only be written as an odd (even) number of transpositions and are therefore odd (even), it follows that a permutation σ is even

(odd) if and only if $E(\sigma)$ is even (odd). Thus, $\text{sgn}(\sigma) = (-1)^{E(\sigma)}$. As a result,

$$\text{sgn}(\sigma) = (-1)^{T(\sigma)-O(\sigma)} = (-1)^{T(\sigma)-n} = (-1)^{T(\sigma)+n} \ . \tag{2.3.8}$$

□

The alternating group A_n is the subgroup of S_n containing only the even permutations of S_n and contains exactly half the elements of S_n [90]. It will be useful subsequently to know that the numbers of odd and even permutations in S_n are the same.

2.4 Words and Lyndon Words

As in section 2.3, we continue discussing classic results that will allow for analysis of families of q-nary quantum graphs (as in sections 2.2 and 1.3). Permutations will be used to represent primitive pseudo orbits in subsequent chapters, but they will not be sufficient to label all primitive pseudo orbits. Here we cover results about words and Lyndon words that will be used in Chapter Three and extended to Lyndon tuples in Chapters Four and Five; Lyndon tuples will allow us to label all primitive pseudo orbits and thus to analyze the variance of the coefficients of the characteristic polynomial (2.2.47). The content of this section and related notions can be found in [34, 43, 53, 54, 93].

Let the set $\mathcal{A}$ be an *alphabet* [93]. We refer to the elements of the alphabet as *letters* or *digits*. In upcoming examples, we will use the finite alphabet $\mathcal{A} = \{0, 1, \ldots, q-1\}$. A *word* w over the alphabet $\mathcal{A}$ is a finite sequence of elements from $w = (a_0, a_1, \ldots, a_{\ell-1})$ with $a_i \in \mathcal{A}$ for $i = 0, \ldots, \ell - 1$. We denote the set of all words

over the alphabet $\mathcal{A}$ by $\mathcal{A}^*$. This set has the operation of concatenation associated to it so that, for $a_i, b_j \in \mathcal{A}$ for $1 \leq i \leq \ell, 1 \leq j \leq m$,

$$(a_0, a_1, \ldots, a_{\ell-1})(b_0, b_1, \ldots, b_{m-1}) = (a_0, a_1, \ldots, a_{\ell-1}, b_0, b_1, \ldots, b_{m-1}) \ . \tag{2.4.1}$$

As this operation is associative, we will simply write words as the concatenation of their letters, $w = a_0 a_1 \cdots a_{\ell-1}$. The *length* of a word w is the number of letters in it, $|w| = \ell$. An *ℓ-word* is a word of length ℓ for $\ell \geq 0$. Thus, we may consider a letter $a \in \mathcal{A}$ to be a word of length one. Moreover, we let the empty sequence be the *empty word*, which has length zero, and we denote it by ε. For any word w, $\varepsilon w = w\varepsilon = w$.

A word $x \in \mathcal{A}^*$ is a *factor* of the word $w \in \mathcal{A}^*$ if there exist words $u, v \in \mathcal{A}^*$ such that $w = uxv$; any concatenation of words yielding a word w is called a *factorization* of w. The factor x is a *proper factor* of w if $x \neq w$. If w is given by $w = uv$, then u is a *prefix* of w and v is a *suffix* of w. If $u \neq w$, then u is a *proper prefix* of w; similarly, v is a *proper suffix* of w if $v \neq w$.

A word is *primitive* if it cannot be written as multiple concatenations of a shorter word. Two words x and y are *conjugate* if there exist words $u, v \in \mathcal{A}^*$ such that $x = uv$ and $y = vu$. A set of words that are pairwise conjugate is an equivalence class of $\mathcal{A}^*$ as any word in the class can be obtained by a cyclic permutation of the letters of another.

The alphabet $\mathcal{A}$ has a natural total order; for example, if $\mathcal{A} = \{0, 1, \ldots, q-1\}$, then we set $0 \lhd 1 \lhd \cdots \lhd q-1$. We extend this ordering to a total order on $\mathcal{A}^* \backslash \{\varepsilon\}$, called the *lexicographic* or *dictionary order*, where for any two words $w, w' \in \mathcal{A}^* \backslash \{\varepsilon\}$, $w \lhd w'$ if and only if either

a) $w' = wx$ for some $x \in \mathcal{A}^* \backslash \{\varepsilon\}$, or,

b) $w = xuy$ and $w' = xvz$ with $u \lhd v$ for $u, v \in \mathcal{A}$ and $x, y, z \in \mathcal{A}^*$.

A *Lyndon word* is a primitive word that is the least lexicographically in its conjugacy class; thus, a word w is a Lyndon word if and only if for all $u, v \in \mathcal{A}^* \backslash \{\varepsilon\}$ such that $w = uv$, also $w = uv \lhd vu$. We denote the set of all Lyndon words over $\mathcal{A}$ by $\mathcal{L}$, and include the alphabet $\mathcal{A}$ itself as Lyndon words of length one.

We will use Lyndon words extensively to label periodic and pseudo orbits in Chapters Three, Four, and Five, so here we include some standard results taken from [43, 54, 93] that will be relevant to our work.

Proposition 2.4.1. A non-empty word w is a Lyndon word if and only if it is strictly smaller than each of its proper suffixes.

Proof. If w is strictly less than each of its proper suffixes, then $w = uv$ with u, v non-empty, and $uv \lhd v$. Therefore, $uv \lhd vu$ and w is a Lyndon word.

If $w = uv$ is a Lyndon word for u, v non-empty words, then $uv \lhd vu$. Note that u cannot begin with the prefix v, as then $v \lhd u$ and w is not a Lyndon word. Thus, $uv \lhd v$. □

If $w \in \mathcal{L} \backslash \mathcal{A}$, a Lyndon word that is not a single letter, and if $w = rs$ such that $r, s \in \mathcal{L}$ and s is of maximal length, then the pair (r, s) is the *standard factorization* of w. We note the following related characterizations.

Proposition 2.4.2. For a Lyndon word $w \in \mathcal{L}\backslash\mathcal{A}$, with $w = rs$ for $r, s \in \mathcal{L}$, then (r, s) is the standard factorization of w if and only if s is the smallest proper suffix of w lexicographically.

Proof. Suppose s is the smallest proper suffix of w in lexicographic order. If $r \in \mathcal{A}$, then s is of maximal length. If $r \notin \mathcal{A}$, then $r = ab$ for some non-empty words a, b. Suppose $w = rs = abs$ such that $a, bs \in \mathcal{L}$. As $bs \in \mathcal{L}$, bs is smaller lexicographically than any of its proper suffixes by proposition 2.4.1. But $s \lhd bs$, as both are proper suffixes of w, a contradiction. Thus, s is of maximal length.

Suppose s is of maximal length such that both r and s are in $\mathcal{L}$. If $r \in \mathcal{A}$, then $s \in \mathcal{L}$ implies, by proposition 2.4.1, that s is strictly less than all its proper suffixes, making it the least of all the proper suffixes of w. If $r \notin \mathcal{A}$, then suppose that s is not the smallest proper suffix of w lexicographically. As $s \in \mathcal{L}$, s is smaller than each of its proper suffixes by proposition 2.4.1, so there exist non-empty words a and b so that $r = ab$ and $w = abs$ with bs the smallest proper suffix of w. As bs is the smallest proper suffix of w, we have already proven that bs must be of maximal length so that both $a, bs \in \mathcal{L}$, a contradiction. Therefore, s is the smallest proper suffix of w. □

Proposition 2.4.3. A non-empty word $w \in \mathcal{L}$ if and only if $w \in \mathcal{A}$ or $w = rs$ with $r, s \in \mathcal{L}$ and $r \lhd s$. If there exists a pair (r, s) with $w = rs$ such that $s, w \in \mathcal{L}$ and s is of maximal length, then $r \in \mathcal{L}$ and (r, s) is the standard factorization of w with $r \lhd rs \lhd s$.

A classic result of Chen, Fox, and Lyndon [6, 34, 43, 53, 54, 93], states that every non-empty word in $\mathcal{A}^*\backslash\mathcal{A}$ has a unique factorization as a non-increasing sequence of

Lyndon words in lexicographic order. In particular, in Chapters Three, Four, and Five, we will rely on the subset of words with strictly decreasing decomposition to label primitive pseudo orbits, as in [6].

Theorem 2.4.1. Every non-empty word w can be uniquely formed by concatenating a non-increasing sequence of Lyndon words in lexicographic order. So

$$w = l_1 l_2 \dots l_k \ , \tag{2.4.2}$$

where $l_1, \dots, l_k \in \mathcal{L}$ and $l_i \trianglerighteq l_{i+1}$, for $i = 1, \dots, k-1$, using the lexicographic order.

It will also be useful in Chapters Four and Five to consider not only Lyndon words, but tuples of Lyndon words. In fact, the Lyndon tuples over a multiset, that we will subsequently define, are generalizations of permutations from the symmetric group.

To define a multiset [53, 54], we consider the finite alphabet $\mathcal{A} = \{1, 2, \dots, \mu\}$. A *multiset* M over $\mathcal{A}$ is given by pairing the alphabet with a function $f : \mathcal{A} \to \mathbb{N}_0$. The multiplicity of a letter $a \in \mathcal{A}$ in M is given by $f(a)$, and the cardinality of M is

$$\sum_{a \in \mathcal{A}} f(a) = \ell \ . \tag{2.4.3}$$

For simplicity, we will denote $M = [1^{m_1}, 2^{m_2}, \dots, \mu^{m_\mu}]$, where $m_a = f(a)$ for $a \in \mathcal{A}$. Then consider an ℓ-word $w = a_0 a_1 \dots a_{\ell-1}$ that uses each element of M exactly once; thus, the length of the word $|w| = \ell$ is the cardinality of M. Recalling theorem 2.4.1, there is a unique Lyndon factorization of $w = l_k \dots l_2 l_1$ such that l_i is a Lyndon word for $i = 1, \dots, k$, and $l_k \trianglerighteq \cdots \trianglerighteq l_2 \trianglerighteq l_1$. For those words with a strictly decreasing factorization such that $l_k \triangleright \cdots \triangleright l_2 \triangleright l_1$, we let the *Lyndon tuple* of w over M be

$\text{tup}(w) = (l_1, l_2, \ldots, l_k)$. We denote the set of all Lyndon tuples over the set M by $\mathcal{L}(M)$.

For any non-empty ℓ-word w with $\text{tup}(w) = (l_1, l_2, \ldots, l_k) \in \mathcal{L}(M)$, we define the *Lyndon index* of w to be the number $i_{\mathcal{L}}(w) = \ell - k$. A non-empty ℓ-word w with $\text{tup}(w) = (l_1, l_2, \ldots, l_k) \in \mathcal{L}(M)$ is called *even (odd)* if its Lyndon index $i_{\mathcal{L}}(w)$ is even (odd). Note that, we are only assigning a notion of parity to ℓ-words that have a strictly decreasing Lyndon word decomposition.

The following theorem of Faal [54] says that the set of even (or odd) Lyndon tuples is exactly half the size of the set of all Lyndon tuples, so there are the same numbers of odd and even Lyndon tuples. We will reserve the proof of this theorem for Chapter Four, as the tools used to prove it will be re-used in subsequent proofs regarding the primitive pseudo orbits of a binary graph.

Theorem 2.4.2. Let $\mathcal{A} = \{1, 2, \ldots, \mu\}$ be a finite ordered alphabet and

$$M = [1^{m_1}, 2^{m_2}, \ldots, \mu^{m_\mu}] \tag{2.4.4}$$

be a multiset over $\mathcal{A}$ of cardinality $\ell > 1$. Then, the number of even ℓ-words over M is the same as the number of odd ℓ-words over M.

Last, we note that these results for Lyndon tuples over multisets are indeed generalizations of permutations, in the sense that they are sets of bijections from a set to itself. If we consider the multiset $M = [1, 2, \ldots, \mu]$ over an alphabet $\mathcal{A} = \{1, 2, \ldots, \mu\}$ such that the multiplicity of each element is one, then the number of μ-words over M is $\mu!$, the number of permutations of μ elements. Each word has a strictly decreasing Lyndon decomposition, as all elements of the multiset have multiplicity one. Thus, to

each of the $\mu!$ words there is a unique associated Lyndon tuple; the Lyndon tuples are in bijection with the permutations of S_μ. Let the word w correspond to the Lyndon tuple $\mathrm{tup}(w) = (l_1, l_2, \ldots, l_k)$. Each Lyndon word is some concatenation of letters, $l_i = a_{1i}a_{2i}\cdots a_{ci}$ that corresponds to a c_i-cycle $(a_{1i}\ a_{2i}\cdots a_{ci})$ in the disjoint cycle decomposition of a permutation π_w.

2.5 q-nary Graphs

Here we define the q-nary graphs as described in section 1.3. These include the de Bruijn graphs with $V = q^r$ vertices [40], which generalize to graphs with $V = p \cdot q^r$. Quantum de Bruijn graphs were studied in [6, 124, 125, 126] with generalizations in the binary case ($q = 2$) included in [124, 125, 126]. All of the results in subsequent chapters will be for families of q-nary graphs.

A *q-nary graph* is a directed graph with $V = p \cdot q^r$ vertices and $B = p \cdot q^{r+1}$ bonds, where p and q are relatively prime positive integers, $r \in \mathbb{N}$, and $q \geq 2$, see [6, 124, 125, 126]. Numbering the vertices $0, \ldots, V-1$, the $V \times V$ adjacency matrix has the form,

$$(A_V)_{i,j} = \begin{cases} \delta_{qi,j} + \delta_{qi+1,j} + \cdots + \delta_{qi+q-1,j} & 0 \leq i < V/q \\ \delta_{qi-V,j} + \delta_{qi+1-V,j} + \cdots + \delta_{qi+q-1-V,j} & V/q \leq i < 2V/q \\ \vdots & \vdots \\ \delta_{qi-(q-1)V,j} + \delta_{qi+1-(q-1)V,j} + \cdots + \delta_{qi+q-1-(q-1)V,j} & (q-1)V/q \leq i < V \end{cases}, \tag{2.5.1}$$

where $\delta_{i,j}$ is the Kronecker delta function and $0 \leq j < V$. More succinctly,

$$(A_V)_{i,j} = \delta_{qi \pmod V,j} + \delta_{qi+1 \pmod V,j} + \cdots + \delta_{qi+q-1 \pmod V,j} \ . \tag{2.5.2}$$

The formula (2.5.1) for the adjacency matrix indicates that all entries of one are in consecutive columns, with q per row. For example, the binary graph with 2^2 vertices, see figure 2.3, has the adjacency matrix,

$$A_4 = \begin{pmatrix} 1 & 1 & 0 & 0 \\ 0 & 0 & 1 & 1 \\ 1 & 1 & 0 & 0 \\ 0 & 0 & 1 & 1 \end{pmatrix} \ . \tag{2.5.3}$$

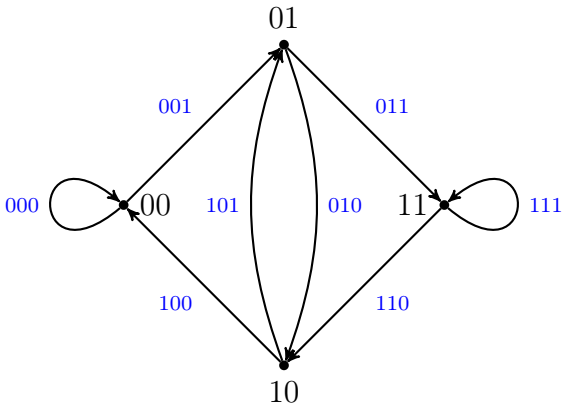

Figure 2.3. The binary graph with $V = 2^2$ vertices and $B = 2^3$ bonds

Families of q-nary graphs with fixed $q \geq 2$ and $p = 1$, or $V = q^r$ for some $r \in \mathbb{N}$, are called *de Bruijn graphs*, as in [6, 40, 124, 125, 126] and as introduced in section 1.3. Three examples of de Bruijn graphs are shown in figures 1.9, 2.3, and 2.4; the first two are binary graphs and the third is ternary. As these de Bruijn graphs have q^r vertices, we label the vertices with the numbers $0, 1, \ldots, V-1$ written in base q. These numbers in base q are r-words over the alphabet $\mathcal{A} = \{0, 1, \ldots, q-1\} = \mathbb{Z}_q$. To see this, consider linear combinations of powers of q,

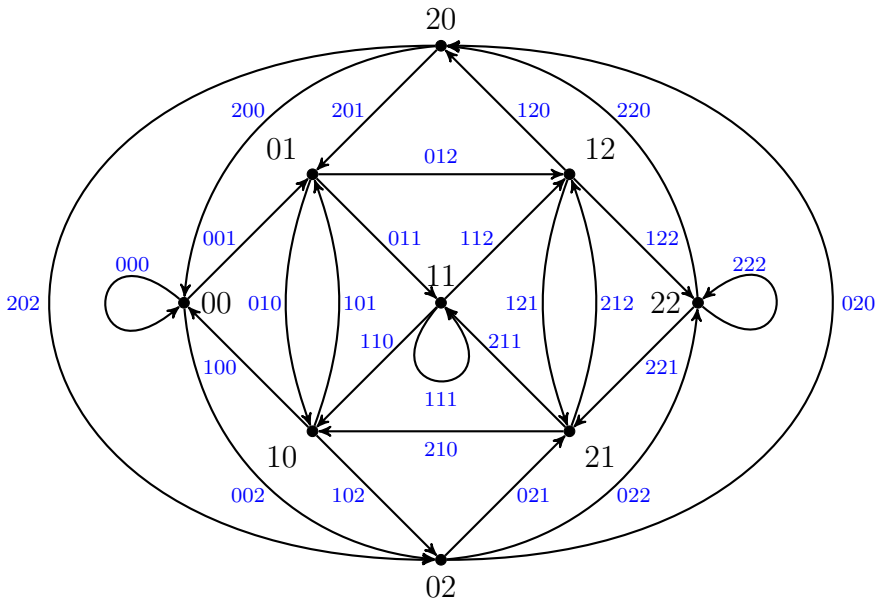

Figure 2.4. The ternary graph with $V = 3^2$ vertices and $B = 3^3$ bonds [6].

$$w = \sum_{i=0}^{r-1} a_i \cdot q^{r-1-i} \ , \tag{2.5.4}$$

with $a_i \in \mathbb{Z}_q$ for all $i = 0, \ldots, r-1$. Then label the vertex by the r-word

$$w = a_0 a_1 \cdots a_{r-1} \ . \tag{2.5.5}$$

Note that a q-nary graph with $V = p \cdot q^r$ such that $p \neq 1$ cannot be labeled in this way; for graphs of this type, we label the vertices $0, 1, \ldots, q-1$, as in figure 2.5.

Once this vertex labeling is made, we can label the bonds with the numbers $0, 1, \ldots, B-1$ written in base q in such a way that the bond labels encode the vertex adjacency relations. As there are q outgoing bonds at each vertex, we let a vertex labeled by $a_0 a_1 \ldots a_{r-1}$ be connected by an outgoing bond to each of the q vertices labeled by $a_1 a_2 \ldots a_{r-1} a_r$, for every choice of $a_r \in \mathbb{Z}_q$. This corresponds to the adjacency relation (2.5.1). To see this, let the vertices i and j be given by,

$$i = a_0 q^{r-1} + a_1 q^{r-2} + \cdots a_{r-2} q + a_{r-1} \ , \tag{2.5.6}$$

$$j = a_1 q^{r-1} + a_2 q^{r-2} + \cdots a_{r-1} q + a_r \ , \tag{2.5.7}$$

for any $a_r \in \mathbb{Z}_q$. Then $qi + w_r \pmod{V} \equiv j$, so $A_{i,j} = 1$. Thus we label bonds with $(r+1)$-words in such a way that the bond labeled $a_0 a_1 \ldots a_{r-1} a_r$ connects the vertex labeled $a_0 a_1 \ldots a_{r-1}$ to the vertex labeled $a_1 \ldots a_{r-1} a_r$ (see also [6]).

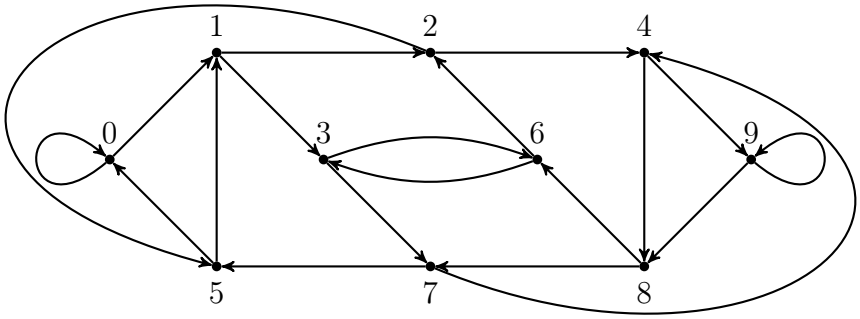

Figure 2.5. The binary graph with $V = 5 \cdot 2$ vertices and $B = 5 \cdot 2^2$ bonds

Moreover, this labeling extends to path labels on q-nary graphs. Consider a q-nary word $w = a_0 a_1 \cdots a_{n+r-1}$ of length $n + r$. Taking consecutive groups of digits of length r, we get a sequence of $n + 1$ labels that represent adjacent vertices,

$$a_0 a_1 \cdots a_{r-1} \to a_1 a_2 \cdots a_r \to \cdots \to a_n a_{n+1} \cdots a_{n+r-1} \ , \tag{2.5.8}$$

with a bond connecting each vertex in the sequence (as the origin) to the next vertex (as the terminus), and thus the sequence represents a path of length n. Note that we could also take consecutive groupings of digits of length $r + 1$ to get a sequence of n labels that represent bonds and obtain the same path.

To label a closed path, we observe that a word of length n labels a closed path of length n when one lets the groupings of r digits labeling vertices cycle back to the beginning as necessary. Consider a q-nary word $w = a_0 a_1 \cdots a_{n-1}$ of length n. Taking consecutive groups of digits of length r that cycle back to the beginning, we get a sequence of $n+1$ labels that represent vertices,

$$a_0 a_1 \cdots a_{r-1} \to a_1 a_2 \cdots a_r \to \cdots \to a_n a_1 \cdots a_{r-2} \to a_0 a_1 \cdots a_{r-1} \ , \tag{2.5.9}$$

and we can see that the sequence of vertex labels begins and ends on the same vertex, with a bond connecting each vertex in the sequence (as the origin) to the next vertex (as the terminus); thus, this sequence, therefore w labels a closed path of length n.

It is important to note that all paths and closed paths can be labeled in this way. Given a path $p = v_0 v_1 \cdots v_n$, the vertex labels are

$$a_0 a_1 \cdots a_{r-1},\ a_1 a_2 \cdots a_r,\ \cdots,\ a_{n-r+1} a_{n-r+2} \cdots a_n \ , \tag{2.5.10}$$

and the word that labels the path is $w = a_0 a_1 \cdots a_n$.

In the chapters that follow, we will choose the $d_v^{out} \times d_v^{in}$ vertex scattering matrix $\sigma^{(v)}$ at each vertex v of a quantum q-nary graph to be the unitary $q \times q$ Discrete Fourier Transform (DFT) matrix, in keeping with [6, 18, 124, 125, 126]. For the primitive q-th root of unity $\omega = \mathrm{e}^{2\pi \mathrm{i}/q}$, the scattering matrix is given by

$$\sigma^{(v)} = \frac{1}{\sqrt{q}} \begin{pmatrix} 1 & 1 & 1 & \cdots & 1 \\ 1 & \omega & \omega^2 & \cdots & \omega^{q-1} \\ 1 & \omega^2 & \omega^4 & \cdots & \omega^{2(q-1)} \\ \vdots & \vdots & \vdots & & \vdots \\ 1 & \omega^{q-1} & \omega^{2(q-1)} & \cdots & \omega^{(q-1)(q-1)} \end{pmatrix} \ , \tag{2.5.11}$$

or more succinctly by (2.2.20). As discussed previously, this matrix makes scattering from any incoming bond b to each outgoing bond b' at a vertex v equally likely.

For q-nary quantum graphs equipped with the Discrete Fourier Transform vertex scattering matrix (2.5.11), the square modulus of every non-zero scattering coefficient is $1/q$; thus for these graphs, $|A_{\bar{\gamma}}|^2 = q^{-n}$ if $\bar{\gamma}$ is a pseudo orbit of topological length n. Considering the form of the diagonal contribution (2.2.48), we need only to count the number of primitive pseudo orbits of length n in order to determine the diagonal contribution to the n-th coefficient's variance. We denote by $\mathrm{PPO}_V(n)$ the number of primitive pseudo orbits of length n on a q-nary graph with V vertices; so,

$$\langle |a_n|^2 \rangle_{\mathrm{diag}} = \left(\frac{1}{q}\right)^n \cdot \mathrm{PPO}_V(n) \ . \tag{2.5.12}$$

In Chapter Three we will determine $\mathrm{PPO}_V(n)$ for q-nary graphs with $V = p \cdot q^r$ vertices.

We will see that Lyndon words can be used to uniquely label primitive periodic orbits for q-nary graphs with $V = q^r$ vertices in Chapter Three, as in [6]. In particular, we will develop these previous results to use Lyndon words to count the number of primitive periodic orbits for q-nary graphs with $V = p \cdot q^r$ vertices. Then we will use permutations from the symmetric group or Lyndon tuples over multisets to label primitive pseudo orbits on q-nary graphs. Having specified a vertex scattering matrix for the vertices of a q-nary graph Γ and applied labelings to count primitive pseudo orbits of Γ, then we will be able to use these results to evaluate the variance of the coefficients of Γ's characteristic polynomial.

CHAPTER THREE

Counting Primitive Periodic and Pseudo Orbits on q-nary Graphs

In this chapter, we will develop a method for counting the numbers of primitive periodic orbits and primitive pseudo orbits on q-nary graphs. Both have previously been calculated in [6] for de Bruijn graphs, when the number of vertices on the graph is $V = q^r$, so we will summarize these results and then derive an algorithm for counting primitive periodic orbits and primitive pseudo orbits when the number of vertices is $V = p \cdot q^r$ for $p > 1$ and p relatively prime to q. The algorithm will relate the number of primitive periodic orbits of length n to the number of q-nary Lyndon words of length n by considering the trace of the n-th power of the graph's adjacency matrix. The number of primitive pseudo orbits will be counted by computing their generating function. As an application, we evaluate the diagonal contribution to the variance (2.2.47) for graphs with $V = p \cdot q^r$ vertices.

3.1 Counting Primitive Periodic Orbits

3.1.1 Primitive Periodic Orbits on q-nary de Bruijn Graphs

To count the number of primitive periodic orbits of length n on a q-nary de Bruijn graph with V vertices, $\mathrm{PO}_V(n)$, we relate this quantity to the number of q-nary Lyndon words of length n. Recall from section 2.4 that a Lyndon word is a word that is strictly less in lexicographic order than all of its cyclic permutations [93]. For example, the binary word 00011 is a Lyndon word because it comes before all of its

rotations, 00110, 01100, 11000, and 10001, in dictionary order. An example of a word that is not a Lyndon word would be 0101, because two rotations will result in the same word and neither is less than the other in dictionary order.

Recall from section 2.5 that, when $V = q^r$, closed paths of length n can be labeled by words of length n over a q-nary alphabet. In particular, the word 00011 corresponds to a closed path of length five. If $V = 2^3$, then the digits are read in consecutive groupings of $r = 3$ to denote the labels of the vertices that the path corresponding to 00011 traverses. Thus,

$$000 \to\ 001 \to\ 011 \to\ 110 \to\ 100 \to 000 \tag{3.1.1}$$

on the de Bruijn graph with eight vertices, see figure 1.9 in section 1.3.

An equivalence class of closed paths under rotation is a periodic orbit; thus, a periodic orbit can be represented by a word and all its rotations. If an equivalence class of words under rotation has a unique smallest word in lexicographic order, then this word will uniquely identify a periodic orbit. In addition, as a primitive periodic orbit is not a repetition of a shorter orbit, these words correspond to primitive periodic orbits and are not equivalent to any of their rotations; thus, a Lyndon word uniquely identifies a primitive periodic orbit. The Lyndon word 00011 uniquely corresponds to the primitive periodic orbit that contains the closed paths labeled by 00011, 00110, 01100, 11000, and 10001.

Therefore, when $V = q^r$, the graph's primitive periodic orbits of length n are in bijection with q-nary Lyndon words of length n, so $\mathrm{PO}_V(n) = \mathrm{L}_q(n)$. Note that this bijection does not directly depend on the number of vertices, only that the graph is

a q-nary de Bruijn graph, so $V = p \cdot q^r$ vertices where $p = 1$. Thus, we will suppress the values of p and r and write,

$$\mathrm{PO}_q(n) = \mathrm{L}_q(n) \ . \tag{3.1.2}$$

3.1.2 Primitive Periodic Orbits on General q-nary Graphs

In the case that $V = p \cdot q^r$ with $p \neq 1$ and p relatively prime to q, we can still relate $\mathrm{PO}_V(n)$ to $\mathrm{L}_q(n)$, but there is no longer a straightforward bijection between periodic orbits and Lyndon words. However, we will see that the number of primitive periodic orbits will remain independent of r, so we change notation from $\mathrm{PO}_V(n)$ to $\mathrm{PO}_{p,q}(n)$ henceforward. To show how $\mathrm{PO}_{p,q}(n)$ relates to $\mathrm{L}_q(n)$ for any value of p, we start from the trace of the n-th power of the graph's adjacency matrix. In order to show the r-independence, we show that the non-zero eigenvalues of the adjacency matrix are unaffected by changes in r; increasing r only increases the multiplicity of the eigenvalue zero.

Let A_V be the $V \times V$ adjacency matrix of the q-nary graph with $V = p \cdot q^r$ vertices. Then we consider A_V as a $q \times q$ block matrix with blocks of dimensions $V/q \times V/q$, where we label the q blocks in the last row of A_V by B^μ for $\mu = 0, 1, \ldots, q-1$. Considering that each row of blocks in A_V is identical (see (2.5.1) and (2.5.2)), we can write the last row of A_V as

$$[A_V]_{i,m} = \delta_{qi,m} + \delta_{qi+1,m} + \cdots + \delta_{qi+q-1,m} \ , \tag{3.1.3}$$

where $0 \leq i < V/q$ and $0 \leq m < V$. To access the μ-th block within this row of blocks, we use the column index range $\mu V/q \leq m < (\mu+1)V/q$. Thus, we can let

$0 \leq i, j < V/q$ for each block matrix B^μ with $\mu = 0, 1, \ldots, q-1$ and write

$$B^\mu_{i,j} = \delta_{qi,j+\mu V/q} + \delta_{qi+1,j+\mu V/q} + \cdots + \delta_{qi+q-1,j+\mu V/q} \ . \tag{3.1.4}$$

For simplicity of notation in the following lemma, we let

$$A_p = \sum_{\mu=0}^{q-1} B^\mu \ , \tag{3.1.5}$$

where $B^0, \ldots, B^{q-1}$ are $p \times p$ blocks in A_{pq}.

Lemma 3.1.1. For a q-nary graph with $V = p \cdot q^r$ vertices, the nonzero eigenvalues of the adjacency matrix A_V are also eigenvalues of A_p with identical multiplicity; furthermore, the multiplicity of zero as an eigenvalue of A_V is at least $V - p$.

Proof. Consider the matrix $A_V - \lambda \mathrm{I}_V$, for $V = p \cdot q^r$ with $r \geq 1$, as a $q \times q$ block matrix with blocks of size $V/q \times V/q$. Considering the form of A_V (2.5.1) and (2.5.2), we note that subtracting the q-th row of blocks from each of the first $q-1$ rows above it will eliminate all entries of one from the upper rows of blocks. Doing so also creates block diagonal matrices containing the parameter λ along the diagonal in the q-th column of blocks; as making linear combinations of rows does not affect the determinant, $\det(A_V - \lambda \mathrm{I}_V)$ can be written

$$\begin{vmatrix} \mathrm{diag}(-\lambda) & 0 & 0 & \cdots & 0 & \mathrm{diag}(\lambda) \\ 0 & \mathrm{diag}(-\lambda) & 0 & \cdots & 0 & \mathrm{diag}(\lambda) \\ 0 & 0 & \mathrm{diag}(-\lambda) & 0 & \cdots & \mathrm{diag}(\lambda) \\ \vdots & \ddots & \ddots & \ddots & \ddots & \vdots \\ 0 & \cdots & 0 & 0 & \mathrm{diag}(-\lambda) & \mathrm{diag}(\lambda) \\ B^0 & B^1 & B^2 & \cdots & B^{q-2} & B^{q-1} - \lambda \mathrm{I}_{V/q} \end{vmatrix} . \tag{3.1.6}$$

Next, take each of the first $q-1$ columns and add them to the q-th column; this block-triangularizes the matrix and the last block contains the sum of all the B^μ

blocks. However, entry-wise this sum is

$$\sum_{\mu=0}^{q-1} B^{\mu}_{i,j} = \sum_{\mu=0}^{q-1}\sum_{\kappa=0}^{q-1} \delta_{qi+\kappa,j+\mu V/q} = \sum_{\kappa=0}^{q-1} \delta_{(qi+\kappa) \pmod{(V/q)},j} = \left[A_{V/q}\right]_{i,j} \ ; \tag{3.1.7}$$

so $\det(A_V - \lambda \mathrm{I}_V)$ is

$$\begin{vmatrix} \mathrm{diag}(-\lambda) & 0 & 0 & \cdots & 0 & 0 \\ 0 & \mathrm{diag}(-\lambda) & 0 & \cdots & 0 & 0 \\ 0 & 0 & \mathrm{diag}(-\lambda) & 0 & \cdots & 0 \\ \vdots & \ddots & \ddots & \ddots & \ddots & \vdots \\ 0 & \cdots & 0 & 0 & \mathrm{diag}(-\lambda) & 0 \\ B^0 & B^1 & B^2 & \cdots & B^{q-2} & A_{V/q} - \lambda \mathrm{I}_{V/q} \end{vmatrix} . \tag{3.1.8}$$

As the determinant of a block-triangular matrix is the product of the determinants of the diagonal blocks,

$$\det(A_V - \lambda \mathrm{I}_V) = (-\lambda)^{(q-1)V/q} \det(A_{V/q} - \lambda \mathrm{I}_{V/q}) \ . \tag{3.1.9}$$

Thus, the only non-zero eigenvalues of A_V are those of $A_{V/q}$. Therefore, the only non-zero eigenvalues of A_V for $V = p \cdot q^r$ with $r \geq 1$ are those of A_p, by induction on r. □

Now that we know the non-zero eigenvalues of A_V for $V = p \cdot q^r$ with $r \geq 1$ are precisely the non-zero eigenvalues of A_p, we of course wish to determine these. To determine the eigenvalues of A_p, we will first write A_p in an alternate form that will allow us to apply results for eigenvalues of a generalized permutation matrix.

A permutation matrix is a square matrix that has precisely one entry of one in each row and column and zeros elsewhere. It follows that the $p \times p$ identity matrix I_p is a permutation matrix and one could think of other permutation matrices as being

obtained from the identity matrix by permutations $\pi \in S_p$ of its rows (or columns) [118]. See section 2.3 for more information about the permutation group.

A generalized permutation matrix is a square matrix that has precisely one non-zero entry in each row and column. These matrices always factor as a product of a diagonal matrix containing the nonzero entries and a permutation matrix [58]. This permutation matrix is associated to some permutation π which decomposes into disjoint cycles. Let $(i_1\ i_2\ \ldots\ i_c)$ be a c-cycle of π for $1 \leq c \leq p$, and let the nonzero entries of the generalized permutation matrix in these columns be denoted by $a_{i_1}, a_{i_2}, \ldots, a_{i_c}$. Then a factor of the characteristic polynomial associated to the generalized permutation matrix is given in, [58], by

$$\left(\lambda^c - \prod_{j=1}^{c} a_{i_j}\right) . \tag{3.1.10}$$

We now let S be the $p \times p$ permutation matrix

$$S = \begin{pmatrix} 0 & 1 & 0 & \ldots & 0 \\ 0 & 0 & 1 & \ldots & 0 \\ \vdots & \vdots & \ddots & \ddots & \vdots \\ 0 & 0 & \ldots & 0 & 1 \\ 1 & 0 & \ldots & 0 & 0 \end{pmatrix} , \tag{3.1.11}$$

and note that $S^p = I_p$. Note also that S is a circulant matrix, as for $i = 0, \ldots, p-1$, the i-th row of S is i rotations of the 0-th row. It can be shown that circulant matrices are diagonalized by Discrete Fourier matrices of the same dimensions [39] (see definition in (2.5.11)), and we will utilize this fact in the next lemma. We also define the $p \times p$ matrix H, which has a single non-zero entry;

$$H_{i,j} = \begin{cases} 1 & \text{if } i = j = 0 \\ \\ 0 & \text{otherwise} \end{cases}, \tag{3.1.12}$$

where $0 \leq i, j \leq p-1$. Using H will allow for an entry-by-entry construction of A_p via matrix multiplication. We now write A_p as

$$A_p = \left(\sum_{h=0}^{p-1} S^{p-h} H S^{qh} \right) \left(I + S + S^2 + \cdots + S^{q-1} \right) . \tag{3.1.13}$$

When H is left-multiplied by S^{p-h}, entries in the $(p-h) \pmod p$-th row are determined; subsequent right-multiplication by S^{qh} sends a non-zero entry in the $(p-h) \pmod p$-th row to the column labeled by $qh \pmod p$. As the original adjacency matrix A_V had q consecutive entries, the right multiplication by the matrices $I, S, S^2, \ldots, S^{q-1}$ duplicates the first entry in the next $q-1$ consecutive columns in A_p, with wrapping back to the first column as necessary. Note that, if $p < q$, then some of these entries will overlap and A_p may contain non-zero entries that are greater than one.

A classic theorem of Birkhoff [24] states that any doubly stochastic matrix can be decomposed into a weighted sum over permutation matrices. While this is not the decomposition that we have just used, we do point out that there is a long history of decomposing matrices using permutation matrices. Now we can use this form of A_p to find its eigenvalues.

Lemma 3.1.2. The matrix A_p has a simple eigenvalue of q and all other eigenvalues are comprised of complete sets of roots of unity.

Proof. Let F be a $p \times p$ Discrete Fourier Transform matrix; then,

$$F^{-1}SF = D = \mathrm{diag}(1, \xi, \xi^2, \ldots, \xi^{p-1}) \ , \tag{3.1.14}$$

where $\xi = \mathrm{e}^{2\pi \mathrm{i}/p}$, the primitive p-th root of unity. Let $\tilde{A}_p$ be the matrix given by $F^{-1}A_pF$; so,

$$\tilde{A}_p = F^{-1}\left(\sum_{h=0}^{p-1} S^{p-h}HS^{qh}\right)(I + S + S^2 + \cdots + S^{q-1})F \tag{3.1.15}$$

$$= F^{-1}\left(\sum_{h=0}^{p-1} S^{p-h}HS^{qh} + S^{p-h}HS^{qh+1} + \cdots S^{p-h}HS^{qh+q-1}\right)F \tag{3.1.16}$$

$$= F^{-1}\left(\sum_{h=0}^{p-1}\sum_{\kappa=0}^{q-1} S^{p-h}HS^{qh+\kappa}\right)F \ . \tag{3.1.17}$$

As $\tilde{A}_p$ is obtained by a similarity transform of A_p, they have the same eigenvalues. Now making the substitution $S = FDF^{-1}$, we have

$$\tilde{A}_p = \sum_{h=0}^{p-1}\sum_{\kappa=0}^{q-1} D^{p-h}F^{-1}HFD^{qh+\kappa} \ . \tag{3.1.18}$$

Now we note that $(F^{-1}H)F = \dfrac{1}{p}\cdot \mathbf{1}_p$, as

$$F^{-1}HF = \frac{1}{\sqrt{p}}\begin{pmatrix} 1 & 0 & \ldots & 0 \\ 1 & 0 & \ldots & 0 \\ \vdots & \vdots & \ddots & \vdots \\ 1 & 0 & \ldots & 0 \end{pmatrix}\frac{1}{\sqrt{p}}\begin{pmatrix} 1 & 1 & 1 & \cdots & 1 \\ 1 & \xi & \xi^2 & \cdots & \xi^{p-1} \\ 1 & \xi^2 & \xi^4 & \cdots & \xi^{2(p-1)} \\ \vdots & \vdots & \vdots & \vdots & \vdots \\ 1 & \xi^{p-1} & \xi^{2(p-1)} & \ldots & \xi^{(p-1)(p-1)} \end{pmatrix} \ . \tag{3.1.19}$$

So

$$\tilde{A}_p = \frac{1}{p}\left(\sum_{h=0}^{p-1}\sum_{k=0}^{q-1} D^{p-h}\mathbf{1}_p D^{qh+k}\right) \ , \tag{3.1.20}$$

and the i,j-th entry of $\tilde{A}_p$ for $0 \le i,j \le p-1$ is

$$[\tilde{A}_p]_{i,j} = \frac{1}{p}\sum_{h=0}^{p-1}(\xi^i)^{p-h}(\xi^j)^{qh}\sum_{k=0}^{q-1}(\xi)^{jk} \tag{3.1.21}$$

$$= \frac{1}{p}(1+\xi^j+\xi^{2j}+\cdots+\xi^{(q-1)j})\sum_{h=0}^{p-1}\xi^{ip-ih+qjh} \tag{3.1.22}$$

$$= \frac{1}{p}(1+\xi^j+\xi^{2j}+\cdots+\xi^{(q-1)j})\sum_{h=0}^{p-1}\xi^{h(qj-i)} \tag{3.1.23}$$

$$= \begin{cases} 1+\xi^j+\xi^{2j}+\cdots+\xi^{(q-1)j} & \text{if } qj-i \mod p \equiv 0 \\ 0 & \text{otherwise} \end{cases}, \tag{3.1.24}$$

where $\xi^{ip} = 1$ since ξ is the primitive p-th root of unity.

We now show that $\tilde{A}_p$ is a generalized permutation matrix, which we then use to find its characteristic polynomial and eigenvalues. Consider two columns of $\tilde{A}_p$ numbered $j_1, j_2 \in \{0, 1, \ldots, p-1\}$, such that $j_1 \neq j_2$. Thus, $j_1 \not\equiv j_2 \mod p$ and so $qj_1 \not\equiv qj_2 \mod p$. Then considering row numbers $i_1, i_2 \in \{0, 1, \ldots, p-1\}$ such that both $qj_1 - i_1 \pmod p \equiv 0$ and $qj_2 - i_2 \pmod p \equiv 0$ implies that $i_1 \neq i_2$. Thus, given any column, it has a single nonzero entry in a row unique from any other column's row with nonzero entry. By a similar argument, we can also show that each row has a single nonzero element, so $\tilde{A}_p$ is a generalized permutation matrix.

In order to determine the characteristic polynomial of $\tilde{A}_p$, we must know the cycle structure of the permutation $\pi \in S_p$ associated to $\tilde{A}_p$. To determine which entries of $\tilde{A}_p$ are contained in a c-cycle of π for some $1 \leq c \leq p$, consider powers of $\tilde{A}_p$. According to the definition of $\tilde{A}_p$ in (3.1.24), the only non-zero entry of column j occurs in row $qj \pmod p$. If we multiply $\tilde{A}_p$ by itself, the non-zero entry in column j of $[\tilde{A}_p]^2$ will be determined by the position of the non-zero entry in column qj

(mod p); the only non-zero entry in this column is in row $q^2 j \pmod p$. It will take c iterations of $\tilde{A}_p$ for the non-zero entry in column j to return to row $qj \pmod p$. Consequently, the condition that a c-cycle belongs to the disjoint cycle decomposition of the permutation π associated to $\tilde{A}_p$ is

$$q^c j \equiv j \pmod p \ , \tag{3.1.25}$$

for some column number j and some positive integer c.

Now we multiply the entries as defined in (3.1.24) in the columns numbered

$$j,\ qj \pmod p,\ q^2 j \pmod p, \ldots,\ q^{c-1} j \pmod p \tag{3.1.26}$$

to obtain a divisor of the characteristic polynomial of $\tilde{A}_p$, in the form of equation (3.1.10),

$$\left[\lambda^c - \left(\sum_{h=0}^{q-1} (\xi^j)^h \right) \left(\sum_{h=0}^{q-1} (\xi^{qj})^h \right) \cdots \left(\sum_{h=0}^{q-1} (\xi^{q^{c-1} j})^h \right) \right] \ . \tag{3.1.27}$$

Every $\tilde{A}_p$ will contain a 1-cycle associated to the first entry, as $qj \equiv j \pmod p$ for $j = 0$, and the non-zero entry in this first entry is always $1 + \xi^0 + (\xi^0)^2 + \cdots (\xi^0)^{q-1} = q$. Thus, the first part of the lemma is proved, as the characteristic polynomial of $\tilde{A}_p$ will always have a divisor $(\lambda - q)$.

It remains to show that any other cycle in the permutation associated to $\tilde{A}_p$ produces a divisor $(\lambda^c - 1)$ of the characteristic polynomial, producing eigenvalues that are complete sets of c-th roots of unity. Again the divisor will have the form (3.1.27), and we first show that

$$\left[\left(\sum_{h=0}^{q-1} (\xi^j)^h \right) \left(\sum_{h=0}^{q-1} (\xi^{qj})^h \right) \cdots \left(\sum_{h=0}^{q-1} (\xi^{q^{c-1} j})^h \right) \right] = \sum_{h=0}^{q^c - 1} (\xi^j)^h \ . \tag{3.1.28}$$

Note that if $c = 1$, then this statement is trivially true, as the left-hand side contains only the first factor. Assume that (3.1.28) is true for $c-1$ with $c \geq 2$. Then we know that

$$\left(\sum_{h=0}^{q-1}(\xi^j)^h\right)\left(\sum_{h=0}^{q-1}(\xi^{qj})^h\right)\cdots\left(\sum_{h=0}^{q-1}(\xi^{q^{c-2}j})^h\right) = \left(\sum_{h=0}^{q^{c-1}-1}(\xi^j)^h\right) \ . \tag{3.1.29}$$

Multiplying both sides of this equation by $\left(\sum_{\kappa=0}^{q-1}(\xi^{q^{c-1}j})^\kappa\right)$ yields q times as many terms on the right-hand side as were previously there, and the right-hand side reads

$$\sum_{\kappa=0}^{q-1}\sum_{h=0}^{q^{c-1}-1}\xi^{j(\kappa q^{c-1}+h)} = \sum_{\kappa=0}^{q-1}\sum_{l=\kappa q^{c-1}}^{(\kappa+1)q^{c-1}-1}\xi^{jl} = \sum_{l=0}^{q^c-1}\xi^{jl} \ , \tag{3.1.30}$$

where the change of variables $l = \kappa q^{c-1} + h$ yields the formula (3.1.28).

It follows from (3.1.25) that $(q^c - 1)j \equiv 0 \pmod{p}$ for all j in a particular cycle of length c. As ξ is the primitive p-th root of unity, and since p consecutive powers of a p-th root of unity sum to zero, for $j \neq 0$,

$$\sum_{h=1}^{q^c-1}(\xi^j)^h = 0 \ . \tag{3.1.31}$$

Thus, the characteristic polynomial has divisors $(\lambda^c - 1)$ for each cycle of length $c \geq 2$ of the permutation π associated to the generalized permutation matrix $\tilde{A}_p$. For fixed points of π, the characteristic polynomial has a divisor $(\lambda - 1)$, except in the case of the guaranteed cycle of length one which corresponds to the first column of $\tilde{A}_p$ and yields a divisor $(\lambda - q)$ of the characteristic polynomial. □

Combining lemmas 3.1.1 and 3.1.2, we now see that, A_p has no eigenvalues of zero and therefore, zero is an eigenvalue of A_V with multiplicity $V - p$.

It is clear that A_V (2.5.1) should always have an eigenvalue of q, as the corresponding eigenvector is simply a vector of ones. In addition, this agrees with previous results [125] for $p = 1$, as $A_1 = [q]$, implying that all other eigenvalues of A_V are zero when $p = 1$. Thus, ordering the eigenvalues $|\lambda_0| \geq |\lambda_1| \geq |\lambda_2| \geq \cdots |\lambda_{V-1}|$ of A_V, the spectral gap of A_V is

$$|\lambda_0| - |\lambda_1| = \begin{cases} q, & p = 1 \\ q - 1 & \text{otherwise} \end{cases} ; \tag{3.1.32}$$

note that when $p \neq 1$, $\lambda_1 = 1$.

Summing the n-th power of each of the roots in a complete set of c-th roots of unity will result in zero unless n is a multiple of c; if $c|n$, then

$$\sum_{j=0}^{c-1} (\mathrm{e}^{2\pi \mathrm{i} j/c})^n = c \ . \tag{3.1.33}$$

If $c \not| n$, let $\zeta = \mathrm{e}^{2\pi \mathrm{i} n/c}$, and the sum of the n-th power of each of the c-th roots of unity can be written

$$Q = \sum_{j=0}^{c-1} \zeta^j \ . \tag{3.1.34}$$

Note that,

$$\zeta Q = \sum_{j=0}^{c-1} \zeta^{j+1} = \sum_{j=0}^{c-1} \zeta^j \ , \tag{3.1.35}$$

as $\zeta^c = \zeta^0 = 1$. Thus, $\zeta Q = Q$ and so $Q(\zeta - 1) = 0$. If $c \not| n$, then $\zeta \neq 1$ and the sum of the n-th powers of the roots of unity is zero.

As a result, we obtain the following corollary to lemmas 3.1.1 and 3.1.2.

Corollary 3.1.1. For a q-nary graph with $V = p \cdot q^r$ vertices, let $\beta_{p,q}(c)$ count the number of cycles of length $c > 1$ associated to $\tilde{A}_p$. Let $\beta_{p,q}(1) + 1$ be the number of 1-cycles associated to $\tilde{A}_p$ so that $\beta_{p,q}(1)$ counts the number of 1-cycles, excluding the 1-cycle that yields the eigenvalue q. Then

$$\mathrm{Tr}((A_V)^n) = q^n + \sum_{d|n} d \cdot \beta_{p,q}(d) \ . \tag{3.1.36}$$

Proof. The trace of the n-th power of A_V is the sum of the n-th powers of the eigenvalues of A_V. As previously stated, the sum of the n-th powers of a complete set of d-th roots of unity is d if $d|n$ and zero otherwise. Thus, if $\beta_{p,q}(d) \neq 0$ and $d|n$, then there are $\beta_{p,q}(d)$ complete sets of d-th roots of unity, and we get a contribution of $d \cdot \beta_{p,q}(d)$ to the sum. □

In order to count the number of primitive periodic orbits of length n, we consider powers of the adjacency matrix A_V and notice that the trace of $(A_V)^n$ counts the number of closed paths of length n on the graph, both primitive and non-primitive. In particular, letting $\mathrm{PO}_{p,q}(n)$ denote the number of primitive periodic orbits of length n,

$$\mathrm{Tr}((A_V)^n) = \sum_{d|n} d \cdot \mathrm{PO}_{p,q}(d) = \underbrace{\sum_{\substack{d|n \\ d \neq n}} d \cdot \mathrm{PO}_{p,q}(d)}_{\substack{\text{number of non-primitive} \\ \text{closed paths}}} + \underbrace{n \cdot \mathrm{PO}_{p,q}(n)}_{\substack{\text{number of primitive} \\ \text{closed paths}}} \ , \tag{3.1.37}$$

where the factors of d and n account for each of the distinct vertices that a closed path could begin on within each periodic orbit equivalence class.

Extending the results in [6] for q-nary de Bruijn graphs with $V = q^r$ vertices, we will use the previous results to relate the number of primitive periodic orbits of length n on a q-nary graph with $V = p \cdot q^r$ vertices to the number of q-nary Lyndon words of length n. To do so, we first notice that there are a total of q^n words of length n over a q-nary alphabet. Words of length n can be Lyndon words, rotations of Lyndon words, repetitions of shorter Lyndon words, or rotations of repetitions of shorter Lyndon words. If a word of length n is not a repetition of a shorter word, i.e., a Lyndon word or a rotation of a Lyndon word, then there are n members of its equivalence class by rotation. If a word of length n is a repetition of a shorter word of length d, where $d|n$, then there are d members of its equivalence class by rotation. Thus, we have the following classic result on counting words [93], which is similar in form to corollary 3.1.1 and equation (3.1.37).

Lemma 3.1.3.

$$\sum_{d|n} d \cdot L_q(d) = q^n \tag{3.1.38}$$

Now we can put these results together to obtain a theorem that precisely counts the number of primitive periodic orbits of length n in terms of Lyndon words of length n and the numbers of cycles of length n associated to $\tilde{A}_p$.

Theorem 3.1.1. For a q-nary graph with $V = p \cdot q^r$ vertices, the number of primitive periodic orbits of length n is $\mathrm{PO}_{p,q}(n) = \mathrm{L}_q(n) + \beta_{p,q}(n)$. Hence, for $n \geq p$, we have $\mathrm{PO}_{p,q}(n) = \mathrm{L}_q(n)$.

Proof. First, note that for $\beta_{p,q}(1) \geq 0$,

$$\mathrm{PO}_{p,q}(1) = \mathrm{Tr}(A_V) = q + \beta_{p,q}(1) = L_q(1) + \beta_{p,q}(1). \tag{3.1.39}$$

Let n be a prime. Then by corollary 3.1.1 and lemma 3.1.3, with (3.1.37) and (3.1.39) applied,

$$\mathrm{PO}_{p,q}(1) + n\mathrm{PO}_{p,q}(n) = \mathrm{Tr}((A_V)^n) \tag{3.1.40}$$

$$= q^n + \beta_{p,q}(1) + n\beta_{p,q}(n) \tag{3.1.41}$$

$$= L_q(1) + n\mathrm{L}_q(n) + \beta_{p,q}(1) + n\beta_{p,q}(n) \ , \tag{3.1.42}$$

so $\mathrm{PO}_{p,q}(n) = \mathrm{L}_q(n)$.

Now let n be a product of $m \geq 2$ primes and assume that the result holds for all divisors d of n that are a product of less than m primes. Then by (3.1.37), corollary 3.1.1, and lemma 3.1.3,

$$\sum_{d|n} d \cdot \mathrm{PO}_{p,q}(d) = \mathrm{Tr}((A_V)^n) = \sum_{d|n} d \cdot [L_q(d) + \beta_{p,q}(d)] \ , \tag{3.1.43}$$

and the result follows by induction on m. □

It is important to note that the theorem agrees with the previously known result [6] that when $p = 1$, $\mathrm{PO}_q(n) = \mathrm{L}_q(n)$, which was easy to see when we looked at labeling periodic orbits with words as in section 3.1.1. If $p = 1$, then $A_1 = [q]$ and $\mathrm{Tr}((A_{q^r})^n) = q^n$, so

$$\sum_{d|n} d \cdot \mathrm{PO}_{p,q}(d) = \sum_{d|n} d \cdot L_q(d) \ , \tag{3.1.44}$$

and by induction on the number of divisors of n, the result follows.

Now that we can count primitive periodic orbits, we wish to count primitive pseudo orbits. Once we know the numbers of primitive pseudo orbits of each length, we will be able to calculate the diagonal contribution to the variance in (2.5.12) for q-nary graphs with $V = p \cdot q^r$ vertices. When $p = 1$, we have a de Bruijn graph, and counting the numbers of primitive pseudo orbits of a particular length is equivalent to counting the number of strictly decreasing standard Lyndon word decompositions of words of the same length, which was accomplished with a generating function argument by Band, Harrison, and Sepanski in [6]. As we will use similar arguments to extend the result when $p > 1$, we will first examine their argument.

3.2.1 Primitive Pseudo Orbits on q-nary de Bruijn Graphs

Recall first the Chen-Fox-Lyndon theorem [34, 93] from section 2.4.

Theorem 3.2.1. Every non-empty word w can be uniquely formed by concatenating a non-increasing sequence of Lyndon words in lexicographic order. So

$$w = l_1 l_2 \dots l_k \ , \tag{3.2.1}$$

where $l_1, \dots, l_k \in \mathcal{L}$ and $l_i \trianglerighteq l_{i+1}$, for $i = 1, \dots, k-1$, using the lexicographic order.

For de Bruijn graphs, the decomposition of any q-nary word of length n corresponds to a pseudo orbit on the graph, as each Lyndon word in the decomposition corresponds uniquely to a primitive periodic orbit. As a primitive pseudo orbit does not contain any repeated periodic orbits, primitive pseudo orbits correspond

to words with strictly decreasing Lyndon word decompositions, where $w_i \triangleright w_{i+1}$ for $i = 1, \ldots, n-1$, as then no Lyndon words are repeated in the decomposition.

For example, the standard decomposition of the binary words of length four are shown below, with parentheses indicating the decomposition. The words with strictly decreasing decomposition are marked in bold font.

(0)(0)(0)(0)	**(0001)**	**(001)(0)**	**(0011)**
(01)(0)(0)	(01)(01)	**(011)(0)**	**(0111)**
(1)(0)(0)(0)	**(1)(001)**	**(1)(01)(0)**	**(1)(011)**
(1)(1)(0)(0)	(1)(1)(01)	(1)(1)(1)(0)	(1)(1)(1)(1)

In [6], it is shown that the number of strictly decreasing decompositions of q-nary words of length n where $n \geq 2$ is given by

$$\mathrm{Str}_q(n) = (q-1)q^{n-1} \ . \tag{3.2.2}$$

In the preceding example, it is clear that $\mathrm{Str}_2(4) = 8$. To obtain (3.2.2), a generating function is defined for the number of strictly decreasing standard decompositions,

$$P(x) = \sum_{n=0}^{\infty} \mathrm{Str}_q(n) \cdot x^n \ , \tag{3.2.3}$$

where $\mathrm{Str}_q(0) = 1$ and $\mathrm{Str}_q(1) = q$. This generating function is equivalently

$$P(x) = \prod_{l=1}^{\infty} (1 + x^l)^{L_q(l)} \ , \tag{3.2.4}$$

as the set of all words with strictly decreasing decompositions is in bijection with the set of all subsets of Lyndon words (without repetition). It is clear that any collection of unique Lyndon words can be ordered lexicographically and will correspond to a

word with strictly decreasing decomposition. The Chen-Fox-Lyndon theorem shows that any word with a strictly decreasing decomposition will correspond uniquely to a subset of Lyndon words without repetition.

To obtain (3.2.2), it is enough to show that $P = F$ on some interval, where

$$F(x) = \frac{qx^2 - 1}{qx - 1} = 1 + qx + \sum_{n=2}^{\infty} (q-1)q^{n-1}x^n \ . \tag{3.2.5}$$

This is accomplished in [6] by noting that $P(0) = F(0) = 1$ and showing that

$$\frac{\mathrm{d}}{\mathrm{d}x} \log P = \frac{\mathrm{d}}{\mathrm{d}x} \log F \tag{3.2.6}$$

on the interval $(-1, 1)$.

3.2.2 Primitive Pseudo Orbits on General q-nary Graphs

When $V = p \cdot q^r$ with $p > 1$ and n is sufficiently large, we will show that the number of primitive pseudo orbits on the graph, $\mathrm{PPO}_{p,q}(n)$, is a constant multiple of the $p = 1$ result for de Bruijn graphs, $\mathrm{PPO}_q(n) = (q-1)q^{n-1}$. We will also derive this p, q-dependent constant from the cycles of the permutation associated to $\tilde{A}_p$.

We define a generating function for the numbers of primitive pseudo orbits of length n,

$$P(x) = \sum_{n=0}^{\infty} \mathrm{PPO}_{p,q}(n) \cdot x^n \ , \tag{3.2.7}$$

where $\mathrm{PPO}_{p,q}(0) = 1$ and $\mathrm{PPO}_{p,q}(1) = q$. Then we note that we can use an equivalent form of $P(x)$,

$$P(x) = \prod_{l=1}^{\infty} (1 + x^l)^{\mathrm{PO}_{p,q}(l)} \ , \tag{3.2.8}$$

as the set of primitive pseudo orbits of length n is precisely the set of subsets of primitive periodic orbits without repetition. But we know from theorem 3.1.1 how $\mathrm{PO}_{p,q}(n)$ relates to $\mathrm{L}_q(n)$; precisely, for any $\beta_{p,q}(n) \neq 0$ associated to $\tilde{A}_p$, there are $\beta_{p,q}(n)$ additional primitive periodic orbits (beyond the number of Lyndon words) of length n on the graph. Therefore, we can write

$$P(x) = (1 + x^{c_1}) \cdots (1 + x^{c_\alpha}) \prod_{l=1}^{\infty} (1 + x^l)^{L_q(l)} \ , \tag{3.2.9}$$

where each c_j is the length of a cycle of $\tilde{A}_p$ (excluding the cycle of length one corresponding to $\lambda_0 = q$), α is the total number of these cycles, and

$$\sum_{j=1}^{\alpha} c_j = p - 1 \ . \tag{3.2.10}$$

Note that these c_j need not differ from one another.

Theorem 3.2.2. For a q-nary graph with $V = p \cdot q^r$ vertices, the number of primitive pseudo orbits of length $n > p$ is

$$\mathrm{PPO}_{p,q}(n) = C_{p,q} \cdot (q-1) q^{n-1} \ , \tag{3.2.11}$$

where

$$C_{p,q} = \begin{cases} 1 & \text{when } p = 1 \ , \\ \displaystyle\prod_{j=1}^{\alpha} (1 + q^{-c_j}) & \text{when } p > 1 \ . \end{cases} \tag{3.2.12}$$

Furthermore, $C_{p,q}$ is bounded above by a constant that grows at most linearly in p,

$$1 \leq C_{p,q} \leq \left(1 + \frac{1}{q}\right)(p-1) \ . \tag{3.2.13}$$

Proof. First we note that

$$\begin{aligned}(1+x^c)F(x) &= (1+x^c)\left[1 + qx + \sum_{n=2}^{\infty}(q-1)q^{n-1}x^n\right] \qquad (3.2.14)\\ &= \left[1 + qx + \sum_{n=2}^{\infty}(q-1)q^{n-1}x^n\right] + \left[x^c + qx^{c+1} + \sum_{n=2}^{\infty}(q-1)q^{n-1}x^{n+c}\right] \ .\end{aligned}$$

Changing variables with $m = n + c$, we then have

$$\begin{aligned}(1+x^c)F(x) &= 1 + qx + \cdots + [(q-1)q^{c-1}+1]x^c + [(q-1)q^c + q]x^{c+1} \qquad (3.2.15)\\ &\quad + \sum_{m=c+2}[(q-1)q^{m-1} + (q-1)q^{m-c-1}]x^m\\ &= 1 + qx + \cdots + [(q-1)q^{c-1}+1]x^c + [(q-1)q^c + q]x^{c+1} \qquad (3.2.16)\\ &\quad + (1+q^{-c})\sum_{n=c+2}(q-1)q^{n-1}x^n \ .\end{aligned}$$

Assume there is a single cycle associated to $\tilde{A}_p$; note that its length must be $p-1$. Then

$$\begin{aligned}P(x) &= (1+x^{p-1})F(x) \qquad (3.2.17)\\ &= 1 + qx + \cdots + [(q-1)q^{p-2}+1]x^{p-1} + [(q-1)q^{p-1} + q]x^p \qquad (3.2.18)\\ &\quad + (1+q^{-(p-1)})\sum_{n=p+1}^{\infty}(q-1)q^{n-1}x^n \ .\end{aligned}$$

Thus, for $n > p$, $C_{p,q} = (1 + q^{-(p-1)})$ and the number of primitive pseudo orbits of length n is $\mathrm{PPO}_{p,q}(n) = (1+q^{-(p-1)})(q-1)q^{n-1}$.

Now let us assume that the cycle lengths associated to $\tilde{A}_p$ are $c_1, c_2, \ldots, c_\alpha$ and, using (3.2.10),

$$2 + \sum_{j=1}^{\alpha-1} c_j = 2 + [(p-1) - c_\alpha] = p - c_\alpha + 1 \ , \tag{3.2.19}$$

we have the following inductive hypothesis,

$$\prod_{j=1}^{\alpha-1}(1+x^{c_j})F(x) = \sum_{n=0}^{p-c_\alpha} C_n x^n + \prod_{j=1}^{\alpha-1}(1+q^{-c_j})\left[\sum_{n=p-c_\alpha+1}^{\infty}(q-1)q^{n-1}x^n\right] \ , \tag{3.2.20}$$

where C_n are the coefficients of x_n for $n = 0, 1, \ldots, p - c_\alpha$. Multiplying both sides by $(1 + x^{c_\alpha})$, we find that powers of x that are at least $p + 1$ are given by

$$\prod_{j=1}^{\alpha-1}(1+q^{-c_j})\left[\sum_{n=p+1}^{\infty}(q-1)q^{n-1}x^n + \sum_{n=p-c_\alpha+1}^{\infty}(q-1)q^{n-1}x^{n+c_\alpha}\right] \ , \tag{3.2.21}$$

where a change of variables in the second sum, $m = n + c_\alpha$, results in powers of x that are at least $p + 1$ being given by

$$\prod_{j=1}^{\alpha-1}(1+q^{-c_j})\left[\sum_{n=p+1}^{\infty}(q-1)q^{n-1}(1+q^{-c_\alpha})x^n\right] \ , \tag{3.2.22}$$

which demonstrates the result in (3.2.12).

To see that $C_{p,q}$ is bounded as in (3.2.13), note that the lower bound is obtained when $p = 1$. As all the cycle lengths add to $p - 1$ (3.2.10), the greatest number of cycles that could be associated to $\tilde{A}_p$ would be $p-1$, and then each would have length $c = 1$, yielding the upper bound for $C_{p,q}$. □

3.3 The Diagonal Contribution to the Variance of the Coefficients of a q-nary Quantum Graph's Characteristic Polynomial

The previous result for the number of primitive pseudo orbits now enables us to find the diagonal contribution to $\langle |a_n|^2 \rangle_k$ for any q-nary graph with $V = p \cdot q^r$ vertices.

Recall that the variance of the coefficients of the graph's characteristic polynomial (2.2.47) is given by a sum over pairs of primitive pseudo orbits of the same topological and metric lengths. The primary contribution to the variance will be the diagonal contribution, which pairs each primitive pseudo orbit with itself.

Corollary 3.3.1. For a q-nary graph with $V = p \cdot q^r$ vertices, the diagonal contribution to the variance of the coefficients of $F_\zeta(k)$ over k is

$$\langle |a_n|^2 \rangle_{\text{diag}} = C_{p,q} \cdot \left(\frac{q-1}{q} \right), \tag{3.3.1}$$

for $p < n < B - p$ with $C_{p,q}$ as defined in (3.2.12).

Proof. As in (2.5.12), the diagonal contribution is given by

$$\langle |a_n|^2 \rangle_{\text{diag}} = \left(\frac{1}{q} \right)^n \cdot \text{PPO}_{p,q}(n) \ , \tag{3.3.2}$$

so we need only know the number of primitive pseudo orbits of length n. By theorem 3.2.2,

$$\langle |a_n|^2 \rangle_{\text{diag}} = \left(\frac{1}{q} \right)^n C_{p,q} \cdot (q-1) q^{n-1} \ , \tag{3.3.3}$$

which produces the result. □

We have now used the results on counting primitive periodic and primitive pseudo orbits on q-nary graphs to obtain the diagonal contribution to (2.2.47). As in [6], when $V = q^r$, $C_{p,q} = 1$ and

$$\langle |a_n|^2 \rangle_{\text{diag}} = \frac{q-1}{q} \ . \tag{3.3.4}$$

3.4 Examples

Here we consider examples of graphs for which the diagonal contribution to the variance of the graph's characteristic polynomial's coefficients (2.2.47) is computed.

Example 3.4.1. If we consider a binary graph with $V = 3 \cdot 2^r$ vertices, the permutation π associated to $\tilde{A}_3$ has the expected fixed point associated to $\lambda = 2$ and a 2-cycle associated to the primitive roots of unity 1, -1. Thus, $\mathrm{PO}_{3,2}(n) = \mathrm{L}_2(n)$ when $n \neq 2$ and $\mathrm{PO}_{3,2}(2) = \mathrm{L}_2(2) + 1$. As a result, $C_{3,2} = 1 + 2^{-2} = 5/4$ and $\langle |a_n|^2 \rangle_{\mathrm{diag}} = 5/8$. $\diamond$

Example 3.4.2. As a second example, let a binary graph have $V = 5 \cdot 2^r$ vertices. Then the permutation π associated to $\tilde{A}_5$ has the fixed point associated with the eigenvalue $\lambda = 2$ and a 4-cycle associated to the primitive fourth roots of unity. Then $\mathrm{PO}_{5,2}(n) = \mathrm{L}_2(n)$ when $n \neq 4$ and $\mathrm{PO}_{5,2}(4) = \mathrm{L}_2(4)+1$. Thus, $C_{5,2} = 1+2^{-4} = 17/16$ and $\langle |a_n|^2 \rangle_{\mathrm{diag}} = 17/32$. $\diamond$

Example 3.4.3. Now consider a ternary graph with $V = 2 \cdot 3^r$ vertices. The permutation π associated to $\tilde{A}_2$ has the fixed point associated with $\lambda = 3$ and an additional fixed point associated with $\lambda = 1$. Therefore, $\mathrm{PO}_{2,3}(n) = \mathrm{L}_3(n)$ for $n \geq 2$ and $\mathrm{PO}_{2,3}(1) = \mathrm{L}_3(1) + 1$. As a result, $C_{2,3} = 1 + 3^{-1} = 4/3$ and $\langle |a_n|^2 \rangle_{\mathrm{diag}} = 8/9$. $\diamond$

Example 3.4.4. As a final example, consider a ternary graph with $V = 5 \cdot 3^r$ vertices. The permutation π associated to $\tilde{A}_5$ has the fixed point corresponding to $\lambda = 3$ and 4-cycle associated to the primitive fourth roots of unity. Therefore,

$\mathrm{PO}_{5,3}(n) = \mathrm{L}_3(n)$ for $n \neq 4$ and $\mathrm{PO}_{5,3}(4) = \mathrm{L}_3(4) + 1$. As a result, $C_{5,3} = 1 + 3^{-4} = 82/81$ and $\langle |a_n|^2 \rangle_{\mathrm{diag}} = 164/243$. ◇

3.5 Conclusions

In [126], Tanner investigates the autocorrelation function of a quantum graph's spectral determinant after averaging the function over an ensemble of quantum graphs that preserves the underlying classical dynamics. This autocorrelation function can be written in terms of the generating function of the square moduli of the secular equation's coefficients. The square moduli of the secular equation's coefficients is precisely the $\langle |a_n|^2 \rangle_k$ (2.2.47), as $F_1(k)$ (2.2.19) corresponds to the secular equation (2.2.18). Obtaining this generating function is split into determining the permanent of a matrix and then considering non-diagonal contributions. The permanent can be replaced by a similar formula that corresponds to periodic orbits on the graph. He shows for which coefficients the diagonal contribution (approximated by this periodic orbit formula) is expected to be the variance of those coefficients and gives a closed form for the diagonal contribution. As an example, he numerically computes the square moduli of the secular equation's coefficients for the family of binary graphs with $V = 3 \cdot 2^r$ vertices for several values of r, comparing his results for the diagonal contribution of 0.625 from both the matrix permanent and the periodic orbit formula. He finds that, as predicted, the variance of these coefficients numerically approaches the diagonal contribution for all but the first two coefficients (and the last two, due to symmetry) in the semiclassical limit of an increasing sequence of graphs.

Our diagonal contribution computation for the family of binary graphs with $V = 3 \cdot 2^r$ matches Tanner's diagonal and numerical results. As our calculations for the number of primitive pseudo orbits are valid for $n > p$, we expect that $\langle |a_n|^2 \rangle_k$ approaches $\langle |a_n|^2 \rangle_{\text{diag}}$ for large n and r, with increasing r corresponding to the semi-classical limit for quantum graphs. This will be shown for binary graphs in Chapter Four and investigated for general q-nary graphs in Chapter Five. However, the way in which this is approached is new.

In standard calculations of spectral statistics such as the form factor, pairs of orbits of the same length are shown to contribute to different orders of a series expansion of the form factor. In [19, 20], Berkolaiko, Schanz, and Whitney show that both second- and third-order approximations of a series expansion of the form factor for a time-reversal invariant quantum graph are zero. As we expect that in the semiclassical limit, the variance of the graph's characteristic polynomial's coefficients will approach the diagonal contribution, it is reasonable to expect that the off-diagonal contributions will be zero. While we do show that $\langle |a_n|^2 \rangle_k$ approaches $\langle |a_n|^2 \rangle_{\text{diag}}$ for large n and r for families of binary graphs with $V = p \cdot 2^r$ vertices and fixed p in Chapter Four, summing the off-diagonal contributions alone will not be the manner in which we carry out the calculation. Rather, we will consider for every individual primitive pseudo orbit its set of possible partners with the same topological and metric lengths and sum the contributions of all these pairs. For most types of primitive pseudo orbits, we will find that these contributions to the variance (2.2.47) are collectively zero; it is important to note that each of these contributions will contain a diagonal pair.

Preliminary results for calculating the variance (2.2.47) for general q-nary graphs will be addressed in Chapter Five.

CHAPTER FOUR

Computing the Variance of the Coefficients for a Binary Quantum Graph's Characteristic Polynomial

In this chapter, we evaluate the entire double sum for the variance of the coefficients of the characteristic polynomial (2.2.47) for binary graphs, for which we previously obtained the diagonal contribution (3.3.1). In order to evaluate the sum (2.2.47), we must produce all primitive pseudo orbit pairs that have the same topological and metric lengths. To do so, we consider primitive pseudo orbits that contain repeated sequences of vertices and/or bonds and reorder the bonds to generate partners of the same length.

We will show that for a family of binary graphs with the number of vertices $V = p \cdot 2^r$, in the limit $r \to \infty$ the variance agrees with the result obtained by evaluating the diagonal contribution. Thus, we may think of the off-diagonal contributions as vanishing in the limit of large graphs. However, to compute the variance we will not separate the diagonal and off-diagonal contributions, but rather consider the contribution to (2.2.47) from each primitive pseudo orbit along with all its potential partners.

4.1 Self-Intersections in Pseudo Orbits on Binary Graphs

As the set of bond lengths of the graph is assumed to be incommensurate, the only way in which to construct primitive pseudo orbit pairs with the same topological and metric lengths is to use the same bonds in each pseudo orbit. The most obvious

way to do this is to take diagonal pairs in which $\bar{\gamma}' = \bar{\gamma}$, as in Chapter Three. To construct pairs of primitive pseudo orbits with the same topological and metric lengths such that $\bar{\gamma}' \neq \bar{\gamma}$, we consider primitive pseudo orbits with a self-intersection (or encounter). Here we will define what it means for a primitive pseudo orbit to have a single self-intersection; multiple self-intersections will be defined in section 4.1.4.

Consider a primitive pseudo orbit $\bar{\gamma} = \{\gamma_1, \gamma_2, \ldots, \gamma_{m_{\bar{\gamma}}}\}$. For $1 \leq j \leq m_{\bar{\gamma}}$, each γ_j is a primitive periodic orbit and can be written as a sequence of vertices and bonds. A *self-intersection*, or an *ℓ-encounter*, is a subsequence of repeated vertices and/or bonds $v_0, v_1, \ldots, v_{\tilde{n}-1}, v_{\tilde{n}}$ that appears exactly ℓ times in the primitive periodic orbit sequences of $\bar{\gamma}$ such that the vertices $s_1, s_2, \ldots s_\ell$ immediately preceding v_0 and the vertices $f_1, f_2, \ldots, f_\ell$ immediately following $v_{\tilde{n}}$ are distinct for some pair, i.e., $s_i \neq s_j$ for some $1 \leq i < j \leq \ell$ and $f_{i'} \neq f_{j'}$ for some $1 \leq i' < j' \leq \ell$. Note that if $\ell \geq 3$, there will only be two distinct choices of incoming vertices labeled $s_1, s_2, \ldots, s_\ell$ and only two distinct choices of outgoing vertices labeled $f_1, f_2, \ldots, f_\ell$, due to the structure of a binary graph. The subsequence $v_0, v_1, \ldots, v_{\tilde{n}-1}, v_{\tilde{n}}$ is referred to as an ℓ-encounter as it is repeated ℓ times in $\bar{\gamma}$. It is unnecessary that all repetitions of the encounter sequence are contained in a single periodic orbit of $\bar{\gamma}$. For $\bar{\gamma}$ to contain a single self-intersection, however, the periodic orbits not containing the encounter sequence cannot collectively contain any vertex more than once or intersect the orbits containing the encounter sequence; otherwise, there would be more than one self-intersection. The *encounter length* is the number of bonds $\tilde{n}$ in the self-intersection; if $\tilde{n} = 0$, then the ℓ-encounter is a single vertex. We call the sequences of vertices and bonds that begin at $v_{\tilde{n}}$ and end at v_0 *links*.

In the following sections, we classify primitive pseudo orbits based on their number of self-intersections, the number of times each self-intersection is repeated, and whether the intersections are of length zero, as pairs generated from primitive pseudo orbits with only short 2-encounters contribute differently to the variance (2.2.47).

4.1.1 A Single 2-Encounter

Consider the simplest self-intersection, a single 2-encounter. Denote a primitive pseudo orbit by $\bar{\gamma} = \{\gamma_1, \gamma_2, \ldots, \gamma_{m_{\bar{\gamma}}}\}$. Each primitive periodic orbit $\gamma_j \in \bar{\gamma}$ for $1 \leq j \leq m_{\bar{\gamma}}$ can be written as a sequence of vertices. The subsequence of vertices $v_0, v_1, \ldots, v_{\tilde{n}-1}, v_{\tilde{n}}$ is a 2-encounter if it appears exactly twice in the primitive periodic orbit sequences of $\bar{\gamma}$ such that the two vertices s_1 and s_2 immediately preceding v_0 are distinct, $s_1 \neq s_2$, and such that the two vertices f_1 and f_2 immediately following $v_{\tilde{n}}$ are distinct, $f_1 \neq f_2$; moreover, no subsequence of the 2-encounter is repeated three or more times. Note that, it is possible that $\tilde{n} = 0$ so that the 2-encounter is a single vertex. The two sequences of vertices that begin at $v_{\tilde{n}}$ and end at v_0 are the called *links*, and must not be identical, else the pseudo orbit is not primitive. If $\bar{\gamma}$ contains a single 2-encounter, then no vertices except those on the encounter will be repeated in the collection of primitive pseudo orbits.

Example 4.1.1. In figure 4.1, portions of graphs are shown, from which we will construct examples of primitive pseudo orbits that have a single 2-encounter. Let $\bar{\gamma} = \{\gamma_1, \gamma_2, \ldots, \gamma_{m_{\bar{\gamma}}}\}$ be a primitive pseudo orbit where γ_1 is a sequence of vertices and bonds shown in figure 4.1(a) such that

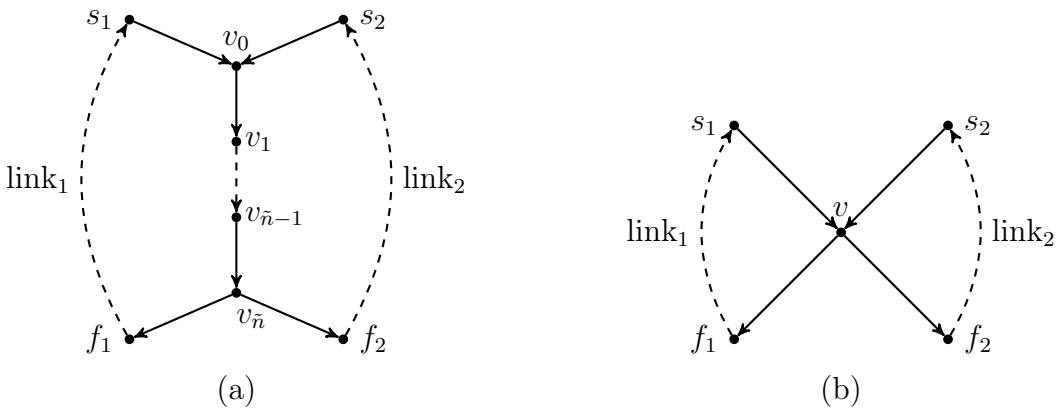

Figure 4.1. Portions of graphs from which a primitive pseudo orbit containing a figure eight orbit can be constructed. Primitive pseudo orbits will contain self-intersections (a) along $\tilde{n} > 0$ bonds or (b) where the intersection is a single vertex v, so $\tilde{n} = 0$.

$$\gamma_1 = (s_1, v_0, v_1, \ldots, v_{\tilde{n}-1}, v_{\tilde{n}}, f_2, \ldots, s_2, v_0, v_1, \ldots, v_{\tilde{n}-1}, v_{\tilde{n}}, f_1, \ldots, s_1) \ . \tag{4.1.1}$$

The primitive periodic orbits $\gamma_2, \ldots, \gamma_{m_{\tilde{\gamma}}}$ do not contain any of the vertices in γ_1, and they collectively contain no vertex more than once. Note here that γ_1 is a figure eight orbit as described in [19, 121]. Then the vertex sequence $v_0, v_1, \ldots, v_{\tilde{n}-1}, v_{\tilde{n}}$, which includes the bonds (v_0, v_1), $(v_1, v_2), \ldots,$ $(v_{\tilde{n}-1}, v_{\tilde{n}})$ is a 2-encounter; the *encounter length* is the number of bonds $\tilde{n}$. The self-intersection is entered from each of the two distinct vertices s_1, s_2; after entering from s_1 (or s_2) the orbit exits the self-intersection to vertex f_2 (or f_1, respectively) with each exit vertex f_1, f_2 distinct. We refer to the remaining sequences as *links*; in 4.1(a)

$$\text{link}_1 = (v_{\tilde{n}}, f_1, \ldots, s_1, v_0) \ , \tag{4.1.2}$$

and

$$\text{link}_2 = (v_{\tilde{n}}, f_2, \ldots, s_2, v_0) \ . \tag{4.1.3}$$

Then the primitive pseudo orbit $\bar{\gamma}' = \{\gamma', \gamma'', \gamma_2, \ldots, \gamma_{m_{\bar{\gamma}}}\}$ where

$$\gamma' = (s_1, v_0, v_1, \ldots, v_{\tilde{n}-1}, v_{\tilde{n}}, f_1, \ldots, s_1) \ , \tag{4.1.4}$$

and

$$\gamma'' = (s_2, v_0, v_1, \ldots, v_{\tilde{n}-1}, v_{\tilde{n}}, f_2, \ldots, s_2) \ , \tag{4.1.5}$$

has the same topological and metric lengths as $\bar{\gamma}$, as each of γ' and γ'' contains one link of the figure eight in γ_1 and one traversal of the encounter sequence. Thus in both $\bar{\gamma}$ and $\bar{\gamma}'$ all bonds are used the same number of times and the encounter sequence is used twice in total. Note that, this is the only way to reorder the sequence in such a way as to pair $\bar{\gamma}$ with a partner $\bar{\gamma}' \neq \bar{\gamma}$ of the same topological and metric lengths, and that $m_{\bar{\gamma}'} = m_{\bar{\gamma}} + 1$, as we have split one orbit in $\bar{\gamma}$ into two orbits in $\bar{\gamma}'$. $\diamond$

Example 4.1.2. We also note a similar example, in which the primitive pseudo orbit $\bar{\gamma} = \{\gamma_1, \gamma_2, \ldots, \gamma_{m_{\bar{\gamma}}}\}$ contains the vertex sequence $v_0, v_1, \ldots, v_{\tilde{n}-1}, v_{\tilde{n}}$ as a 2-encounter with

$$\gamma_1 = (s_1, v_0, v_1, \ldots, v_{\tilde{n}-1}, v_{\tilde{n}}, f_1, \ldots, s_1) \ , \tag{4.1.6}$$

and

$$\gamma_2 = (s_2, v_0, v_1, \ldots, v_{\tilde{n}-1}, v_{\tilde{n}}, f_2, \ldots, s_2) \ , \tag{4.1.7}$$

such that the primitive periodic orbits $\gamma_3, \ldots, \gamma_{m_{\bar{\gamma}}}$ do not contain any of the vertices in γ_1 or γ_2, and they collectively contain no vertex more than once. Then the only way to pair $\bar{\gamma}$ with a primitive pseudo orbit $\bar{\gamma}' \neq \bar{\gamma}$ such that $B_{\bar{\gamma}'} = B_{\bar{\gamma}}$ and $L_{\bar{\gamma}'} = L_{\bar{\gamma}}$ is to join γ_1, γ_2 at the self-intersection and obtain

$$\gamma = (s_1, v_0, v_1, \ldots, v_{\tilde{n}-1}, v_{\tilde{n}}, f_2, \ldots, s_2, v_0, v_1, \ldots, v_{\tilde{n}-1}, v_{\tilde{n}}, f_1, \ldots, s_1) \ , \qquad (4.1.8)$$

with $\bar{\gamma}' = \{\gamma, \gamma_3, \ldots, \gamma_{m_{\bar{\gamma}}}\}$. Note $m_{\bar{\gamma}'} = m_{\bar{\gamma}} - 1$. $\diamond$

Both of the previous examples also make sense in the context that the encounter occurs at a single vertex, i.e., $\tilde{n} = 0$. If we replace the encounter sequence of vertices, $v_0, v_1, \ldots, v_{\tilde{n}-1}, v_{\tilde{n}}$, with the single vertex v and use the previous orbit sequences as they appear in figure 4.1(b), then these are examples of 2-encounters of length zero.

4.1.2 A Single ℓ-Encounter with Distinct Links

Now we consider a single ℓ-encounter contained in a primitive pseudo orbit with distinct links on a binary graph when $\ell \geq 2$. Let $\bar{\gamma} = \{\gamma_1, \gamma_2, \ldots, \gamma_{m_{\bar{\gamma}}}\}$ be a primitive pseudo orbit. Each primitive periodic orbit $\gamma_j \in \bar{\gamma}$ for $1 \leq j \leq m_{\bar{\gamma}}$ can be written as a sequence of vertices. The subsequence of vertices $v_0, v_1, \ldots, v_{\tilde{n}-1}, v_{\tilde{n}}$ is an *ℓ-encounter* if it appears exactly ℓ times in the primitive periodic orbit sequences of $\bar{\gamma}$ such that the vertices $s_1, s_2, \ldots s_\ell$ immediately preceding v_0 and the vertices $f_1, f_2, \ldots, f_\ell$ immediately following $v_{\tilde{n}}$ are distinct for some pair, i.e., $s_i \neq s_j$ for some $1 \leq i < j \leq \ell$ and $f_{i'} \neq f_{j'}$ for some $1 \leq i' < j' \leq \ell$; moreover, no subsequence of the ℓ-encounter is repeated $\ell + 1$ or more times. Here we note that for a binary graph there are only two incoming and two outgoing bonds at each vertex, so there will necessarily be repeated vertices adjacent to the self-intersection when $\ell \geq 3$; we do not include these as part of the self-intersection as they are not repeated the maximum number of times ℓ. However, the collection of primitive periodic orbits that do not contain the encounter sequence contains no vertex more than once. Note that it is possible that $\tilde{n} = 0$ so

that the ℓ-encounter is a single vertex. Each of the ℓ sequences of vertices that begin at $v_{\tilde{n}}$ and end at v_0 is a *link*; here we require that no two link sequences are the same.

Example 4.1.3. Let $\bar{\gamma} = \{\gamma_1, \gamma_2, \ldots, \gamma_{m_{\bar{\gamma}}}\}$ be a primitive pseudo orbit where, letting enc $= (v_0, v_1, \ldots, v_{\tilde{n}-1}, v_{\tilde{n}})$ be the encounter sequence, the primitive periodic orbit γ_1 is given by

$$\gamma_1 = (s_2, \text{enc}, f_1, \ldots, s_1, \text{enc}, f_2, f_2' \ldots, s_2', s_2, \text{enc}, f_2, f_2'', \ldots, s_2'', s_2) \ , \tag{4.1.9}$$

a sequence of vertices and bonds corresponding to figure 4.2 such that none of these vertices are repeated in $\gamma_2, \ldots, \gamma_{m_{\bar{\gamma}}}$ and they collectively contain no vertex more than once. Twice the bond (s_2, v_0) appears at the beginning of the encounter sequence and twice the bond $(v_{\tilde{n}}, f_2)$ appears at the end of the encounter sequence. This is simply necessitated by the structure of a binary graph, and we do not count either bond as part of the 3-encounter along enc $= (v_0, v_1, \ldots, v_{\tilde{n}-1}, v_{\tilde{n}})$, as neither is repeated thrice. It follows that the links in this example are given by

$$\text{link}_1 = (v_{\tilde{n}}, f_1, \ldots, s_1, v_0) \ , \tag{4.1.10}$$

$$\text{link}_2 = (v_{\tilde{n}}, f_2, f_2', \ldots, s_2', s_2, v_0) \ , \tag{4.1.11}$$

$$\text{link}_3 = (v_{\tilde{n}}, f_2, f_2'', \ldots, s_2'', s_2, v_0) \ . \tag{4.1.12}$$

In generating partner pseudo orbits for $\bar{\gamma}$ that have the same topological and metric lengths, there are exactly six partner orbits; these correspond to the elements of the permutation group S_3. To see this, we note that a traversal of the encounter sequence is always followed by traversal of a link and vice versa. Thus, we will notate a periodic orbit as simply a sequence of links and assume that the encounter sequence follows

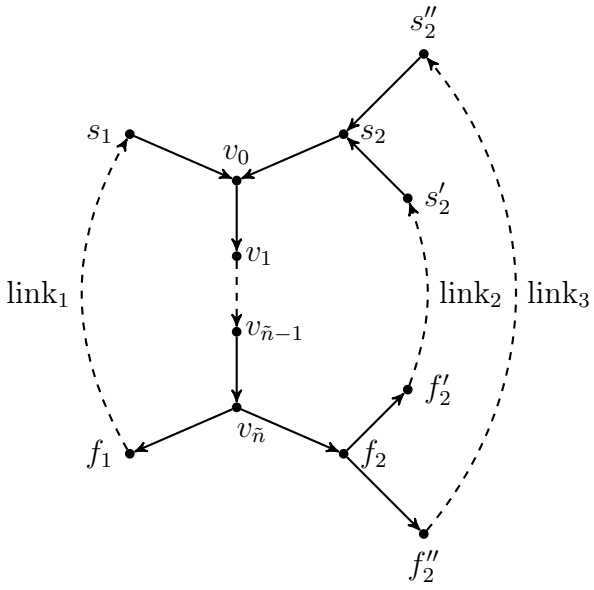

Figure 4.2. A portion of a graph from which a primitive pseudo orbit with an 3-encounter with three distinct links can be constructed.

each link. Then γ_1, as stated in (4.1.9), is equivalent to $\gamma_1 = (\text{link}_1, \text{link}_2, \text{link}_3)$ and corresponds to the permutation of links (1 2 3). The possible partner pseudo orbits of $\bar{\gamma}$ are listed in table 4.1. ◇

Table 4.1. All of the primitive periodic orbits that could replace $\gamma_1 = (\text{link}_1, \text{link}_2, \text{link}_3)$ to produce a partner pseudo orbit $\bar{\gamma}'$ in example 4.1.3.

Orbit(s) replacing γ_1 in $\bar{\gamma}'$	Permutation	$m_{\bar{\gamma}'}$
None	(1 2 3)	$m_{\bar{\gamma}'} = m_{\bar{\gamma}}$
$\gamma = (\text{link}_1, \text{link}_3, \text{link}_2)$	(1 3 2)	$m_{\bar{\gamma}'} = m_{\bar{\gamma}}$
$\gamma' = (\text{link}_1, \text{link}_2), \gamma'' = (\text{link}_3)$	(1 2)	$m_{\bar{\gamma}'} = m_{\bar{\gamma}} + 1$
$\gamma' = (\text{link}_1, \text{link}_3), \gamma'' = (\text{link}_2)$	(1 3)	$m_{\bar{\gamma}'} = m_{\bar{\gamma}} + 1$
$\gamma' = (\text{link}_2, \text{link}_3), \gamma'' = (\text{link}_1)$	(2 3)	$m_{\bar{\gamma}'} = m_{\bar{\gamma}} + 1$
$\gamma' = (\text{link}_1), \gamma'' = (\text{link}_2), \gamma''' = (\text{link}_3)$	e	$m_{\bar{\gamma}'} = m_{\bar{\gamma}} + 2$

Note that, this notation can also be applied to the single 2-encounter case in examples 4.1.1 and 4.1.2 using elements of S_2. In example 4.1.1, the permutation (1 2) corresponds to $\gamma_1 \in \bar{\gamma}$ and the only partners of $\bar{\gamma}$ are $\bar{\gamma}' = \bar{\gamma}$ and $\bar{\gamma}'$ such that

γ_1 is replaced with γ', γ'' corresponding to the identity permutation e. In example 4.1.2, the permutations are reversed; $\bar{\gamma}$ corresponds to the identity permutation, and the only partners of $\bar{\gamma}$ are itself and the primitive pseudo orbit $\bar{\gamma}'$ such that γ_1 and γ_2 are replaced by γ with corresponding permutation (1 2). In general, a primitive pseudo orbit $\bar{\gamma}$ on a binary graph with a single ℓ-encounter and ℓ distinct links can be represented by a member of the permutation group S_ℓ. Thus, all the possible partner orbits $\bar{\gamma}'$ correspond to elements of S_ℓ.

4.1.3 A Single ℓ-Encounter with Repeated Links, $\ell \geq 3$

Now we consider primitive pseudo orbits $\bar{\gamma}$ containing a single ℓ-encounter, $\ell \geq 3$, where one or more links are repeated in $\bar{\gamma}$. The partner pseudo orbits are no longer in bijection with the elements of S_ℓ, as permuting sets of repeated links does not produce unique pseudo orbits. To deal with this, we will consider a generalization of permutations of a set of link indices to Lyndon tuples over a multiset of link indices. To see the necessity of this, consider the following example.

Example 4.1.4. Consider the portion of a graph shown in figure 4.1(b) and let $\bar{\gamma} = \{\gamma_1, \gamma_2, \ldots, \gamma_{m_{\bar{\gamma}}}\}$ be such that

$$\gamma_1 = (s_2, v, f_1, \ldots, s_1, v, f_1, \ldots, s_1, v, f_2, \ldots, s_2) \ , \tag{4.1.13}$$

or in link notation, $\gamma_1 = (\text{link}_1, \text{link}_1, \text{link}_2)$. The primitive periodic orbits that do not contain the encounter sequence collectively contain no vertex more than once. While this pseudo orbit contains three links, the partner primitive pseudo orbits no longer correspond to the elements of S_3, as permuting the first two links leaves the orbit

unchanged. In fact, the only partners of $\bar{\gamma}$ are $\bar{\gamma}' = \bar{\gamma}$ and $\bar{\gamma}' = \{\gamma', \gamma'', \gamma_2, \ldots, \gamma_{m_{\bar{\gamma}}}\}$ where $\gamma' = (\text{link}_1)$ and $\gamma'' = (\text{link}_1, \text{link}_2)$. $\diamond$

Proposition 2.4.2 of Faal [54] regarding Lyndon tuples over a multiset allows us to conclude that the numbers of primitive pseudo orbits with odd and even numbers of periodic orbits are the same. For background and the setup of multisets, Lyndon tuples, and even/odd ℓ-words, see section 2.4. This will be important in the remainder of the chapter where we compute the variance of the coefficients of a binary graph's characteristic polynomial via a sum over pairs of primitive pseudo orbits.

We will reserve the proof of proposition 2.4.2 until we can prove a weighted version, theorem 4.1.1, that implies proposition 2.4.2. The proof of the weighted sum theorem will involve a map that will be useful to us later in computing contributions of orbit pairs to (2.2.47). It is interesting to note that proposition 2.4.2 was originally stated as a coin arrangements lemma and proven by Sherman [119]. If we have a fixed collection of ℓ objects of which m_1 are of the first kind, m_2 are of a second kind, up through m_μ of the μ-th kind, and $b_{\ell,k}$ is the number of "exhaustive unordered arrangements of these symbols into k disjoint, nonempty, circularly ordered sets such that no two circular orders are the same and none are periodic" [54, 119], then we have the identity

$$\sum_{k=1}^{\ell} (-1)^k b_{\ell,k} = 0 \tag{4.1.14}$$

when $\ell > 1$. In the case that the multiplicity of each object is one, $b_{\ell,k}$ counts the number of elements of S_ℓ with k disjoint cycles (these are *Stirling numbers*), and

implies that the number of permutations with an even number of cycles is the same as the number of permutations with an odd number of cycles, as noted in section 4.1.2.

Example 4.1.5. Let $M = [1^2, 2^2, 3]$. Note that there are $\frac{5!}{2! \cdot 2!} = 30$ words over this multiset. The words that have a strictly decreasing Lyndon factorization are shown with their corresponding Lyndon tuple in table 4.2. Note that there are six

Table 4.2. The 5-words over the multiset $M = [1^2, 2^2, 3]$ that have strictly decreasing Lyndon factorizations with their corresponding Lyndon tuples.

Even 5-words	Lyndon tuples	Odd 5-words	Lyndon tuples
11223	(11223)	12231	(1, 1223)
11232	(11232)	12321	(1, 1232)
11322	(11322)	13221	(1, 1322)
12123	(12123)	12312	(12, 123)
12132	(12132)	13212	(12, 132)
12213	(12213)	13122	(122, 13)
21231	(1, 123, 2)	21123	(1123, 2)
21312	(12, 13, 2)	21213	(1213, 2)
21321	(1, 132, 2)	21132	(1132, 2)
23121	(1, 12, 23)	23112	(112, 23)
31221	(1, 122, 3)	31122	(1122, 3)
32112	(112, 2, 3)	32121	(1, 12, 2, 3)

words not included here. The words 22113, 22131, 22311, 23211, 31212, and 32211 have decreasing Lyndon decompositions that are not strictly decreasing. Moreover, we note that 22131 and 23211 have decompositions with an even number of Lyndon words - (1, 13, 2, 2) and (1, 1, 2, 23) - while the remainder have decompositions with odd numbers of Lyndon words. It is interesting to note that the parity result in proposition 2.4.2 is only stating that the subset of words with an associated Lyndon

tuple, in which Lyndon words are not repeated, has equal numbers of words with odd and even Lyndon index. $\diamond$

In order to prove proposition 2.4.2, we first recall some well-known properties of Lyndon words; for preliminary details, see section 2.4. Recall from section 2.4 that a Lyndon word w is by definition strictly smaller lexicographically than any of its rotations, so for any factorization $w = uv$ with u, v non-empty, $uv \lhd vu$. A *suffix* of the non-empty word w is any word v such that $w = uv$. If u, v are both non-empty, then v is a *proper suffix* of w. If $w \in \mathcal{L}\backslash\mathcal{A}$, a Lyndon word that is not a single letter, and $w = rs$ such that s is of maximal length with $r, s \in \mathcal{L}$, then the pair (r, s) is the *standard factorization* of w.

The following lemma comes from Faal [54].

Lemma 4.1.1. If $w = rs$ is a Lyndon word with $r, s \in \mathcal{L}$ and $r \lhd s$ with

a) $r \in \mathcal{A}$, then (r, s) is the standard factorization of w.

b) r not a single letter, then let the standard factorization of r be (r_1, s_1). If $s \lhd s_1$, then (r, s) is the standard factorization of w.

Proof.

a) If $r \in \mathcal{A}$ and $s \in \mathcal{L}$, then s is clearly of maximal length.

b) Let the standard factorization of r be given by (r_1, s_1) and $s \lhd s_1$. Suppose, for the sake of contradiction, that s is not of maximal length. Then $r = r'_1 s'_1$ such that $r'_1 \in \mathcal{L}$ and $s'_1 s \in \mathcal{L}$. By proposition 2.4.1, $s'_1 \lhd s$. If $s_1 \trianglelefteq s'_1$, then

$s_1 \triangleleft s$, a contradiction. So let $s_1 \triangleright s_1'$. We know that $r = r_1 s_1 = r_1' s_1'$ where s_1 is the proper suffix of maximum length such that both $r_1, s_1 \in \mathcal{L}$; therefore, s_1' is a proper suffix of s_1. But as s_1 is a Lyndon word, $s_1 \triangleleft s_1'$ by proposition 2.4.1, a contradiction. Thus, s is of maximal length and (r, s) is the standard factorization of w.

□

As in [54], we now prove proposition 2.4.2 by proving a weighted generalization. In particular, we note that the definition of splittable Lyndon words and the mapping between odd and even Lyndon words that is involved in this proof will be used in subsequent proofs to compute contributions of pseudo orbit pairs to (2.2.47).

For a word w with an associated Lyndon tuple, $\text{tup}(w) = (l_1, l_2, \ldots, l_k)$ such that $l_1 \triangleleft l_2 \triangleleft \cdots \triangleleft l_k$, the first Lyndon word l_1 in $\text{tup}(w)$ is *splittable* if it is not a single letter and its standard factorization (r_1, s_1) satisfies $s_1 \triangleleft l_2$. We define the *weight* of a letter $a \in \mathcal{A}$ to be a formal variable x_a. For any Lyndon word $l = a_1 a_2 \cdots a_\ell$, the *weight* $\text{wt}(l) = x_{a_1} x_{a_2} \cdots x_{a_\ell}$ is the product of the weights of its letters. Further, the *weight* of the Lyndon tuple $\text{tup}(w) = (l_1, l_2, \ldots, l_k)$ associated to a word w is the product of the weights of its Lyndon words,

$$\text{wt}(w) = \prod_{i=1}^{k} \text{wt}(l_i) \ . \tag{4.1.15}$$

Denote the set of all odd ℓ-words over M by O and the set of even ℓ-words over M by E. The following theorem generalizes proposition 2.4.2.

Theorem 4.1.1. Let $\mathcal{A} = \{1, 2, \ldots, \mu\}$ be a finite ordered alphabet and

$$M = [1^{m_1}, 2^{m_2}, \ldots, \mu^{m_\mu}] \tag{4.1.16}$$

be a multiset over $\mathcal{A}$ of cardinality $\ell > 1$. The weighted sum of even ℓ-words over M is the same as the weighted sum of odd ℓ-words over M,

$$\sum_{w \in E} \mathrm{wt}(w) = \sum_{w \in O} \mathrm{wt}(w) \ . \tag{4.1.17}$$

Proof. Let w be an ℓ-word with Lyndon tuple $\mathrm{tup}(w) = (l_1, l_2, \ldots, l_k)$. We consider two cases depending on whether l_1 is splittable.

If l_1 is splittable, let the standard factorization of l_1 be the pair (r_1, s_1). Then there is a mapping $f_1(w) \mapsto w'$ such that

$$\mathrm{tup}(w') = (r_1, s_1, l_2, \ldots, l_k) \ . \tag{4.1.18}$$

Note that $\mathrm{tup}(w')$ is in fact a Lyndon tuple as l_1 splittable implies $s_1 \lhd l_2$. Moreover, this map is well-defined, weight-preserving, and parity-changing, since $\mathrm{wt}(l_1) = \mathrm{wt}(r_1) \cdot \mathrm{wt}(s_1)$ and $i_{\mathcal{L}}(w') = i_{\mathcal{L}}(w) - 1$.

If $\mathrm{tup}(w)$ is such that l_1 is not splittable, then there is a mapping $f_2(w) \mapsto w'$ such that

$$\mathrm{tup}(w') = (l_0, l_3, \ldots, l_k) \ , \tag{4.1.19}$$

where $l_0 = l_1 l_2$. Note that by proposition 2.4.1, l_0 is a Lyndon word, and $l_0 \lhd l_2 \lhd l_3$ so $\mathrm{tup}(w')$ is a Lyndon tuple. Moreover, this map is well-defined, weight-preserving, and parity-changing, since $\mathrm{wt}(l_0) = \mathrm{wt}(l_1) \cdot \mathrm{wt}(l_2)$ and $i_{\mathcal{L}}(w') = i_{\mathcal{L}}(w) + 1$.

Thus, every Lyndon tuple associated to an even ℓ-word maps to a unique Lyndon tuple associated to an odd ℓ-word, and these partial mappings are invertible. There-

fore, there is a total mapping that is a weight-preserving bijection from E to O, where for w such that $\text{tup}(w) = (l_1, l_2, \ldots, l_k)$,

$$f(w) = \begin{cases} w_1 & \text{if } \text{tup}(w_1) = f_1(\text{tup}(w)) \text{ when } l_1 \text{ is splittable,} \\ w_2 & \text{if } \text{tup}(w_2) = f_2(\text{tup}(w)) \text{ when } l_1 \text{ is not splittable.} \end{cases} \tag{4.1.20}$$

Thus, the weighted sums over E and O are equal. □

Of course, if the formal weight associated to each letter is one, this is proposition 2.4.2. We use this result to show that the set of primitive pseudo orbit partners of $\bar{\gamma}$ with an associated link set given by multiset M is balanced in terms of the odd/even parity of the number of primitive periodic orbits contained in each pseudo orbit in section 4.3.2.

4.1.4 Multiple Encounters

We now consider primitive pseudo orbits with multiple self-intersections. Let $\bar{\gamma} = \{\gamma_1, \gamma_2, \ldots, \gamma_{m_{\bar{\gamma}}}\}$ be a primitive pseudo orbit; each primitive periodic orbit $\gamma_j \in \bar{\gamma}$ for $1 \leq j \leq m_{\bar{\gamma}}$ can be written as a sequence of vertices. The subsequence of vertices $v_{0i}, v_{1i}, \ldots, v_{\tilde{n}-1_i}, v_{\tilde{n}i}$ is a *self-intersection* or an ℓ_i*-encounter* if it appears exactly ℓ_i times in the primitive periodic orbit sequences of $\bar{\gamma}$ such that the vertices $s_{1i}, s_{2i}, \ldots s_{\ell i}$ immediately preceding v_{0i} and the vertices $f_{1i}, f_{2i}, \ldots, f_{\ell i}$ immediately following $v_{\tilde{n}i}$ are distinct for some pair, i.e., $s_{hi} \neq s_{j_i}$ for some $1 \leq h_i < j_i \leq \ell_i$ and $f_{h'_i} \neq f_{j'_i}$ for some $1 \leq h'_i < j'_i \leq \ell_i$, for all $i = 1, \ldots, N$. Note that it is possible that $\tilde{n}_i = 0$ so that the ℓ_i-encounter is a single vertex. Then $\bar{\gamma}$ has N self-intersections of types

$\vec{\ell} = (\ell_1, \ell_2, \ldots, \ell_N)$. The collection of primitive periodic orbits that do not contain the encounter sequence contains no vertex more than once.

At the i-th encounter there are ℓ_i sequences of vertices that begin at $v_{\tilde{n}i}$ and each of these ends at v_{0j} for some $j = 1, \ldots, N$; there are also ℓ_i sequences of vertices at that end at v_{0i} and began at $v_{\tilde{n}j}$ for some $j = 1, \ldots, N$. These sequences do not contain encounter sequences, and we refer to them as *outgoing* and *incoming links* at the encounter, respectively. In the previous cases of having a single encounter, each link was necessarily both incoming and outgoing to the single encounter (and thus we did not distinguish them); in the case of multiple encounters, a link sequence need not necessarily be both at the i-th encounter. As in section 4.1.1, if $\ell_i = 2$ for some encounter, then the two incoming links must be distinct (similarly for the outgoing links), else the encounter is not of maximum length. However, if $\ell_i \geq 3$ for some encounter, then there will be at least two distinct incoming links and at least two distinct outgoing links, but links may be used more than once.

In order to obtain a primitive pseudo orbit with multiple self-intersections, it may be that $\bar{\gamma}$ contains multiple periodic orbits such as those described in examples 4.1.1, 4.1.2, or 4.1.3 that do not overlap one another. It is also possible to construct primitive pseudo orbits with multiple self-intersections from the portions of graphs drawn in figure 4.3, as in the following examples.

Example 4.1.6. Let $\bar{\gamma} = \{\gamma_1, \gamma_2, \ldots, \gamma_{m_{\bar{\gamma}}}\}$ where $\gamma_1 = (\text{link}_1, \text{link}_2, \text{link}_3, \text{link}_4)$ is an orbit on the portion of the graph pictured in figure 4.3(a), and no other orbit in $\bar{\gamma}$ repeats vertices contained in γ_1 or has encounters. Then $\bar{\gamma}$ has two 2-encounters of

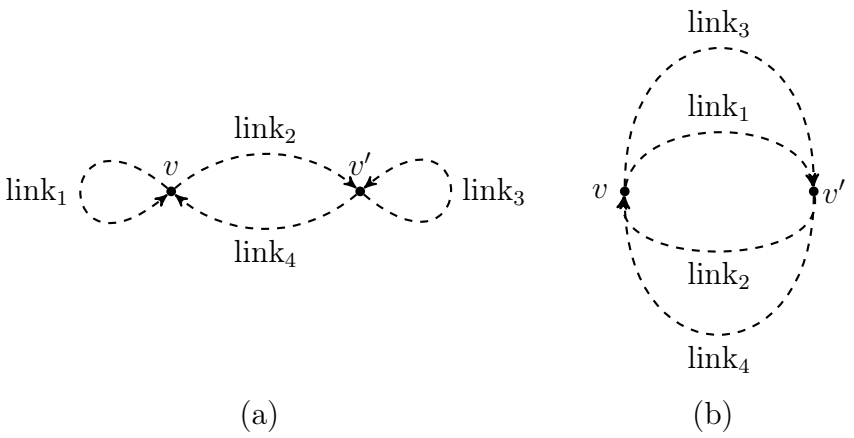

Figure 4.3. Portions of graphs from which primitive pseudo orbits with multiple encounters can be constructed.

length zero at the vertices v and v'. Note that link_1 is both incoming and outgoing at the 2-encounter v, while link_2 is outgoing at v and incoming at the 2-encounter v'; link_4 is outgoing at v' and incoming at v while link_3 is incoming and outgoing at v'. ◇

Example 4.1.7. Let $\bar{\gamma} = \{\gamma_1, \gamma_2, \ldots, \gamma_{m_{\bar{\gamma}}}\}$ where $\gamma_1 = (\text{link}_1, \text{link}_2, \text{link}_3, \text{link}_4)$ is an orbit on the portion of the graph pictured in figure 4.3(b), and no other orbit in $\bar{\gamma}$ repeats vertices contained in γ_1 or has encounters. Then $\bar{\gamma}$ has two 2-encounters of length zero at the vertices v and v'. Note that link_1 and link_3 are outgoing at the 2-encounter v and incoming at the 2-encounter v', while link_2 and link_4 are outgoing at v' and incoming at v. ◇

Example 4.1.8. Let $\bar{\gamma} = \{\gamma_1, \gamma_2, \ldots, \gamma_{m_{\bar{\gamma}}}\}$ where $\gamma_1 = (\text{link}_1, \text{link}_2, \text{link}_3, \text{link}_3, \text{link}_4)$ is an orbit on the portion of the graph pictured in figure 4.3(a), and no other orbit

in $\bar{\gamma}$ repeats vertices contained in γ_1 or has encounters. Then $\bar{\gamma}$ has a 2-encounter of length zero at the vertex v and a 3-encounter of length zero at the vertex v'. $\diamond$

When a primitive pseudo orbit contained a single encounter, we generated its partner pseudo orbits by reordering links. We will do something similar here; however, we need to rearrange the order in which outgoing links are traversed following incoming links at each self-intersection in order to generate all partner orbits. To do so, we will use what we call connection diagrams at each encounter.

We will denote each of the incoming links by a point on the left-hand side of the diagram and each of the outgoing links by a point on the right-hand side of the diagram. Each primitive pseudo orbit $\bar{\gamma}$ has a unique arrangement of which outgoing links follow which incoming links at each of the $i = 1, \ldots, N$ encounters. In the case where each of the ℓ_i incoming links and each of the ℓ_i outgoing links are distinct, this arrangement is given by a permutation $\rho_i \in S_{\ell_i}$,

$$\rho_i = \begin{pmatrix} 1 & 2 & \ldots & \ell_i \\ \rho_i(1) & \rho_i(2) & \ldots & \rho_i(\ell_i) \end{pmatrix} . \tag{4.1.21}$$

In the case of a single encounter with distinct links, this permutation also denotes the order in which $\text{link}_1, \text{link}_2, \ldots, \text{link}_{\ell_i}$ are traversed, as before, since there are no other encounters at which the ordering of vertex sequences can change. For multiple encounters, this permutation will only tell us the ordering of incoming and outgoing links at a particular encounter; in particular, the incoming j-th link is followed by the outgoing $\rho_i(j)$-th link, for $j = 1, \ldots, \ell_i$. See figure 4.4 for an example of how, at a 3-encounter, each possible connection diagram corresponds to a member of the symmetric group S_3.

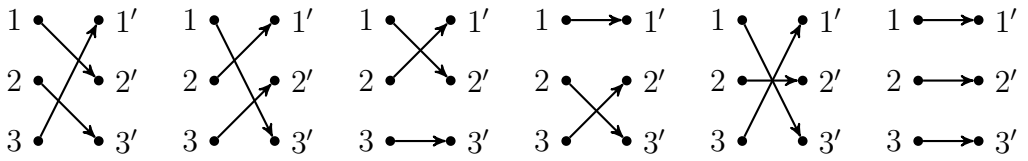

Figure 4.4. All the possible connection diagrams at a 3-encounter with distinct incoming links 1, 2, 3, and distinct outgoing links 1', 2', 3'.

Now consider the case of the i-th encounter of type ℓ_i where some of the incoming and/or outgoing links are repeated. We consider two multisets at the i-th encounter, $M_i^{in} = [1^{m_1^{in}}, 2^{m_2^{in}}, \ldots, \mu^{m_\mu^{in}}]$ and $M_i^{out} = [(1')^{m_1^{out}}, (2')^{m_2^{out}}, \ldots, (\mu')^{m_{\mu'}^{out}}]$. Then we consider connection diagrams $\hat{\rho}_i$ at each encounter from the set $\hat{S}_{\ell_i}$ of ways to uniquely rearrange connections between M_i^{in} and M_i^{out},

$$\hat{\rho}_i = \begin{pmatrix} 1 & \ldots & 1 & 2 & \ldots & 2 & \mu & \ldots & \mu \\ \hat{\rho}_i(1) & \ldots & \hat{\rho}_i(1) & \hat{\rho}_i(2) & \ldots & \hat{\rho}_i(2) & \hat{\rho}_i(\mu) & \ldots & \hat{\rho}_i(\mu) \end{pmatrix} , \tag{4.1.22}$$

where there are m_j^{in} copies of each incoming link index in the upper row for $j = 1, \ldots, \mu$. When $\mu = \mu' = \ell_i$, then $\hat{S}_{\ell_i}$ is the symmetric group S_{ℓ_i}. Otherwise, the size of the set is $|\hat{S}_{\ell_i}| < \ell_i!$. See figure 4.5 for an example of all the possible connection diagrams at a 4-encounter with repeated links such that $M_i^{in} = [1^2, 2, 3]$ and $M_i^{out} = [1^3, 2]$. To any pseudo orbit there is an associated vector $\vec{\ell} = (\ell_1, \ell_2, \ldots, \ell_N)$ of encounter types and a vector $\vec{\rho} = (\hat{\rho}_1, \hat{\rho}_2, \ldots, \hat{\rho}_N)$ of connection diagrams that determine the

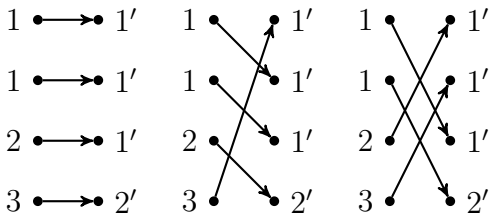

Figure 4.5. All the possible connection diagrams at a 4-encounter with one repeated incoming link in $M_i^{in} = [1^2, 2, 3]$ and one repeated outgoing link in $M_i^{out} = [1^3, 2]$.

connections between incoming and outgoing links at each encounter. Note that, as the vector $\vec{\rho}$ always depends on the vector $\vec{\ell}$, we will not explicitly denote this relationship. Given vectors $\vec{\ell}$ and $\vec{\rho}$ associated to a sequence of vertices and bonds, we let the unique primitive pseudo orbit determined by them be denoted $\bar{\gamma}(\vec{\rho})$. To generate all the partner orbits of a particular primitive pseudo orbit $\bar{\gamma}(\vec{\rho})$, we will need to consider all possible connection diagrams at each of the N encounters that result in primitive pseudo orbits $\bar{\gamma}'(\vec{\rho})$ as $\vec{\rho}$ ranges over all connection diagrams.

4.2 An Alternative Formulation of the Variance Sum

As derived in (2.2.47), the variance of the coefficients of the graph's characteristic polynomial can be written as a finite sum over primitive pseudo orbit pairs where both orbits in the pair have topological length n and the same metric length,

$$\langle |a_n|^2 \rangle_k = \sum_{\substack{\{\bar{\gamma},\bar{\gamma}'\}: \\ B_{\bar{\gamma}}=B_{\bar{\gamma}'}=n}} (-1)^{m_{\bar{\gamma}}+m_{\bar{\gamma}'}} A_{\bar{\gamma}} \bar{A}_{\bar{\gamma}'} \delta_{L_{\bar{\gamma}},L_{\bar{\gamma}'}} \ . \tag{4.2.1}$$

Given a primitive pseudo orbit $\bar{\gamma}$ of topological length n, this pseudo orbit $\bar{\gamma}$ has a well-defined number of self-intersections $0 \leq N \leq n$. If $N = n$, each vertex is a self-intersection, but no self-intersections contain bonds. While this type of orbit will appear infrequently, if ever, on q-nary graphs, it is an obvious upper bound on the number of self-intersections on a primitive pseudo orbit. We will denote the set of primitive pseudo orbits with topological length n and N self-intersections by $\mathcal{P}_N^n$.

Further, we let the set $\mathcal{P}_{\bar{\gamma}}$ be the set of all primitive pseudo orbits $\bar{\gamma}'$ such that $B_{\bar{\gamma}'} = B_{\bar{\gamma}}$ and $L_{\bar{\gamma}'} = L_{\bar{\gamma}}$. As we assume the bond lengths of our graph are incommensurate, a pseudo orbit $\bar{\gamma}'$ must traverse the same bonds as $\bar{\gamma}$ the same number of times

in order for $\bar{\gamma}'$ to belong to $\mathcal{P}_{\bar{\gamma}}$. This implies that for $\bar{\gamma} \in \mathcal{P}_N^n$, also $\mathcal{P}_{\bar{\gamma}} \subset \mathcal{P}_N^n$. We denote the contribution of pairs including a given primitive pseudo orbit $\bar{\gamma}$ to $\langle |a_n|^2 \rangle_k$ by

$$C_{\bar{\gamma}} = \sum_{\substack{\{\bar{\gamma},\bar{\gamma}'\} \\ \bar{\gamma}' \in \mathcal{P}_{\bar{\gamma}}}} (-1)^{m_{\bar{\gamma}}+m_{\bar{\gamma}'}} A_{\bar{\gamma}} \bar{A}_{\bar{\gamma}'} \ ; \tag{4.2.2}$$

then

$$\langle |a_n|^2 \rangle_k = \sum_{N=0}^{n} \sum_{\bar{\gamma} \in \mathcal{P}_N^n} C_{\bar{\gamma}} \ . \tag{4.2.3}$$

Note that, the sum (2.2.47) is a double sum over the primitive pseudo orbits $\bar{\gamma}$ and $\bar{\gamma}'$, where terms in the sum can only be non-zero if the topological and metric lengths of the two pseudo orbits are equal. Moreover, the sets $\mathcal{P}_N^n$ are disjoint for differing values of n and/or N. Thus, this alternative formulation of the sum accounts for each pair of primitive pseudo orbits with the same topological and metric lengths exactly once.

4.3 Computing $C_{\bar{\gamma}}$

It remains to find the contribution $C_{\bar{\gamma}}$ (4.2.2) defined in section 4.2 for each primitive pseudo orbit $\bar{\gamma}$. For a fixed length n, we classify primitive pseudo orbits based on the number of self-intersections N, the number of times $\vec{\ell} = (\ell_1, \ell_2, \ldots, \ell_N)$ that each self-intersection is repeated, and the number N_0 of these self-intersections of length zero. The vertex scattering matrix at each vertex of the graph is the 2×2 Discrete Fourier Transform matrix (2.5.11),

$$\sigma^{(v)} = \frac{1}{\sqrt{2}} \begin{pmatrix} 1 & 1 \\ 1 & -1 \end{pmatrix} \ ; \tag{4.3.1}$$

note that all entries of this matrix are real-valued. We will then proceed to show that for most types of primitive pseudo orbits, the contribution $C_{\bar{\gamma}}$ is zero. For the two cases with nonzero contribution, primitive pseudo orbits without self-intersections and primitive pseudo orbits with only 2-encounters of length zero, we will compute these contributions and asymptotically determine the size of the sets of pseudo orbits of these types to show that the variance of the binary graph's characteristic polynomial's coefficients agrees with the diagonal approximation of Chapter Three in the limit of large graphs.

4.3.1 A Single ℓ-Encounter with $\ell \geq 2$ of Positive Length and ℓ Distinct Links

First we consider the contribution $C_{\bar{\gamma}}$ of a primitive pseudo orbit which has $N = 1$ self-intersections, the encounter length $\tilde{n} > 0$ is positive, and where the links adjacent to the encounter are distinct. We have already shown that the primitive pseudo orbit $\bar{\gamma}$ with an ℓ-encounter corresponds uniquely to some permutation in S_ℓ, and that the partner pseudo orbits $\bar{\gamma}' \in \mathcal{P}_{\bar{\gamma}}$ are in bijection with the elements of S_ℓ. Moreover, recall from section 2.3 that the numbers of odd and even permutations in S_ℓ are equal. Here, we will show the sign of the permutation depends on the number of primitive periodic orbits in the primitive pseudo orbit, while the scattering amplitude product $A_{\bar{\gamma}}\bar{A}_{\bar{\gamma}'}$ is the same for all partners $\bar{\gamma}'$ of $\bar{\gamma}$, and consequently the contribution is $C_{\bar{\gamma}} = 0$.

Let $\tilde{n} > 0$, as in examples 4.1.1, 4.1.2, and 4.1.3, and consider the stability amplitudes $A_{\bar{\gamma}}$ and $A_{\bar{\gamma}'}$. We let A_{link_i} denote the product of scattering amplitudes at the vertices on link_i between $v_{\tilde{n}}$ and v_0, for $i = 1, 2, \ldots, \ell$. Let A_{enc} denote the product of scattering amplitudes at the vertices along the self-intersection between v_0 and $v_{\tilde{n}}$.

We note that $\bar{\gamma}$ will pick up a scattering coefficient from each of the incoming vertices $s_1, \ldots, s_\ell$ to v_1 at v_0 and a scattering coefficient from $v_{\tilde{n}-1}$ to each of the outgoing vertices $f_1, \ldots, f_\ell$ at $v_{\tilde{n}}$. Thus, the stability amplitude $A_{\bar{\gamma}}$ is

$$A_{\bar{\gamma}} = \left(\prod_{\substack{h=1 \\ \gamma_h \text{ has no encounter}}}^{m_{\bar{\gamma}}} A_{\gamma_h} \right) A_{\text{enc}}^{\ell} \left(\prod_{i=1}^{\ell} A_{\text{link}_i} \sigma_{v_1, s_i}^{(v_0)} \sigma_{f_i, v_{\tilde{n}-1}}^{(v_{\tilde{n}})} \right) . \tag{4.3.2}$$

Permuting the order in which links are traversed to obtain partner orbits $\bar{\gamma}'$ does not change any of these scattering coefficients, so $A_{\bar{\gamma}'} = A_{\bar{\gamma}}$. Then as the scattering amplitudes are given by the real-valued 2×2 Discrete Fourier Transform matrix (4.3.1),

$$A_{\bar{\gamma}} \bar{A}_{\bar{\gamma}'} = \left(\frac{1}{2} \right)^n . \tag{4.3.3}$$

Thus, the contribution (4.2.2) of all pairs associated to a fixed primitive pseudo orbit $\bar{\gamma}$ of this type is

$$C_{\bar{\gamma}} = \left(\frac{1}{2} \right)^n \sum_{\substack{\{\bar{\gamma}, \bar{\gamma}'\} \\ \bar{\gamma}' \in \mathcal{P}_{\bar{\gamma}}}} (-1)^{m_{\bar{\gamma}} + m_{\bar{\gamma}'}} . \tag{4.3.4}$$

We note that $(-1)^{m_{\bar{\gamma}}}$ is fixed, so we need only know the number of primitive periodic orbits in each possible partner of $\bar{\gamma}$.

In section 4.1.2, we saw that for a particular $\bar{\gamma}$ with an ℓ-encounter, each partner orbit $\bar{\gamma}' \in \mathcal{P}_{\bar{\gamma}}$ could be associated to a unique element of S_ℓ. We remind the reader that the sign of a permutation is related to the number of cycles in its disjoint cycle decomposition by proposition 2.3.1. The following corollary relates the sign of a permutation to the number of primitive periodic orbits in a primitive pseudo orbit.

Corollary 4.3.1. Let $\bar{\gamma}$ be a primitive pseudo orbit with an ℓ-encounter and ℓ distinct links, and $\sigma_{\bar{\gamma}} \in S_\ell$ its associated permutation. Then

$$(-1)^{m_{\bar{\gamma}}} = \operatorname{sgn}(\sigma_{\bar{\gamma}}) \cdot (-1)^{\ell} \ . \tag{4.3.5}$$

Proof. Note that the number of primitive periodic orbits $m_{\bar{\gamma}}$ in $\bar{\gamma}$ corresponds to the total number of cycles $T(\sigma_{\bar{\gamma}})$ in $\sigma_{\bar{\gamma}}$. So $\operatorname{sgn}(\sigma_{\bar{\gamma}}) = (-1)^{m_{\bar{\gamma}}+\ell}$ and the result follows. □

Thus, we have the following contribution to (4.2.3).

Lemma 4.3.1. For any primitive pseudo orbit $\bar{\gamma}$ containing a single ℓ-encounter of positive length for $\ell \geq 2$ with ℓ distinct links, $C_{\bar{\gamma}} = 0$.

Proof. From (4.3.4) and corollary 4.3.1,

$$C_{\bar{\gamma}} = \left(\frac{1}{2}\right)^n \operatorname{sgn}(\sigma_{\bar{\gamma}}) \sum_{\sigma_{\bar{\gamma}'} \in S_\ell} \operatorname{sgn}(\sigma_{\bar{\gamma}'}) \ ; \tag{4.3.6}$$

as the number of odd and even permutations in S_ℓ is the same, the result follows. □

4.3.2 A Single ℓ-Encounter with $\ell \geq 3$ of Positive Length with Repeated Links

As in section 4.3.1, we note that a primitive pseudo orbit with a single ℓ-encounter for $\ell \geq 3$ of positive length with repeated links also has $A_{\bar{\gamma}} = \bar{A}_{\bar{\gamma}'}$, and thus, $A_{\bar{\gamma}}\bar{A}_{\bar{\gamma}'} = 2^{-n}$. As in section 4.1.3, the set of links defines a multiset M. To each primitive pseudo orbit with repeated links, there is an associated Lyndon tuple $\operatorname{tup}(w) = (l_1, l_2, \ldots, l_k)$ over a word w of length ℓ from the set of Lyndon tuples $\mathcal{L}(M)$ over M. Each Lyndon word l_i in $\operatorname{tup}(w)$ uniquely corresponds to a primitive periodic orbit in $\bar{\gamma}$, so the number of periodic orbits in $\bar{\gamma}$ is the number of Lyndon words in $\operatorname{tup}(w)$. As the

Lyndon index $i_{\mathcal{L}}(w) = \ell - k$, we have

$$m_{\bar{\gamma}} = \ell - i_{\mathcal{L}}(w) \ . \tag{4.3.7}$$

Lemma 4.3.2. For any primitive pseudo orbit $\bar{\gamma}$ containing a single ℓ-encounter of positive length for $\ell \geq 3$ with repeated links, $C_{\bar{\gamma}} = 0$.

Proof. From proposition 2.4.2 and (4.3.7),

$$C_{\bar{\gamma}} = \left(\frac{1}{2}\right)^n (-1)^{2\ell + i_{\mathcal{L}}(w)} \sum_{\mathrm{tup}(w') \in \mathcal{L}(M)} (-1)^{i_{\mathcal{L}}(w')} = 0 \ . \tag{4.3.8}$$

□

4.3.3 A Single ℓ-Encounter with $\ell \geq 3$ of Length Zero

Now we consider a primitive pseudo orbit $\bar{\gamma}$ with a single ℓ-encounter where $\ell \geq 3$ and the length of the encounter is zero. We treat the cases when the links are distinct and when there are repeated links simultaneously by describing the contribution using the multiset notation. When all the links are distinct, each element of the multiset has multiplicity one. This case is treated separately from the case where the self-intersection has positive length, as here the product of stability amplitudes depends on how many times the single negative scattering coefficient at v (see (4.3.1)) appears in $A_{\bar{\gamma}}\bar{A}_{\bar{\gamma}'}$. To show that $C_{\bar{\gamma}} = 0$, we will show that any Lyndon tuple over M with even (odd) Lyndon index uniquely maps to a Lyndon tuple over M with odd (even) Lyndon index such that the corresponding pseudo orbits have the same number of negative scattering coefficients associated to them.

Consider figure 4.6, where we zoom in on the encounter vertex v and the adjacent vertices. We have previously labeled the adjacent vertices by $s_1, \ldots, s_\ell$ and $f_1, \ldots, f_\ell$, but noted that the incoming and outgoing sets of vertices can have only two distinct members on a binary graph; for simplicity, here we will label the incoming vertices by a and b and the outgoing vertices by c and d. In order for v to be traversed by $\bar{\gamma}$

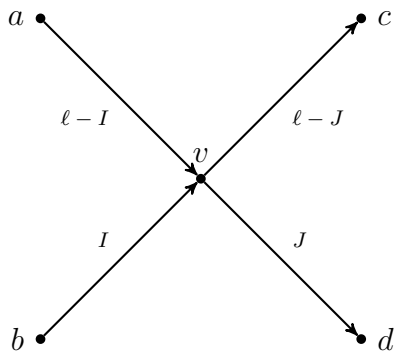

Figure 4.6. An ℓ-encounter at vertex v with the incoming and outgoing bonds at v. Links are not pictured, but each link begins at either vertex c or d and ends at either vertex a or b.

a total of ℓ times, $\bar{\gamma}$ must enter through bonds (a, v) and (b, v) a total of ℓ times, with each bond used at least once (otherwise the encounter is not of length zero). Without loss of generality, the diagram can be labeled so that the bond (b, v) is traversed I times and the bond (a, v) is traversed $\ell - I$ times. Similarly, we label the diagram such that bond (v, d) is used J times and the bond (v, c) is therefore used $\ell - J$ times. We will also assume that $\ell - J \geq 2$, as $\ell \geq 3$.

Without loss of generality, we will assign the scattering coefficient $\sigma_{c,b}^{(v)}$ to be the single negative scattering coefficient in (4.3.1). Thus, to compute $C_{\bar{\gamma}}$, we need to consider the number of times that a link ending with the bond (b, v) is followed by a

link beginning with the bond (v, c) in $\bar{\gamma}$ and each of its partner orbits. For a primitive pseudo orbit $\bar{\gamma}$, we assign the link labels such that the multiset $C \subset M$ of links ending at the bond (v, c) consists of the first ν labels for $\nu < \mu$,

$$C = [1^{m_1}, 2^{m_2}, \ldots, \nu^{m_\nu} : \text{link}_i \text{ begins with bond } (v, c) \text{ for } 1 \leq i \leq \nu] \ . \tag{4.3.9}$$

As $\ell - J \geq 2$, so also $|C| \geq 2$. Then let $B \subset M$ be the multiset such that

$$B = [i^{m_i} : \text{link}_i \text{ ends with bond } (b, v)] \ . \tag{4.3.10}$$

Note that if link_i is repeated m_i times in $\bar{\gamma}$, then i has multiplicity m_i in M, and thus has multiplicity m_i in the set B or C in which it is present. It is possible for the intersection of multisets B and C to be non-empty.

Here we will rely on the mapping f (4.1.20) between odd and even Lyndon tuples defined in the proof of theorem 4.1.1.

Proposition 4.3.1. Let $M = [1^{m_1}, 2^{m_2}, \ldots, \mu^{m_\mu}]$ be a multiset where $m_i > 0$ for all $i = 1, \ldots, \mu$, and let $B, C \subset M$ be defined as above. Let $T : \mathcal{L}(M) \to \mathbb{N}_0$ be a function that counts the number of times a label from the set B is followed by a label from the set C (cyclically) in the Lyndon words of some Lyndon tuple $\text{tup}(w)$. If $f(w) = w'$, then $T(\text{tup}(w)) = T(\text{tup}(w'))$.

Proof. Let M, B, and C be multisets as described and $\text{tup}(w) = (l_1, l_2, \ldots, l_k) \in \mathcal{L}(M)$ for $w = l_k \ldots l_2 l_1$ the strictly decreasing Lyndon decomposition, so $l_1 \lhd l_2 \lhd \cdots \lhd l_k$. Note that l_1 must begin with the letter one.

If l_1 is not a splittable Lyndon word, either l_1 is a single letter or its standard factorization (r_1, s_1) does not satisfy $s_1 \lhd l_2$. Suppose $l_1 \in \mathcal{A}$; then l_2 begins with an

element of C, as $|C| \geq 2$. Under the map f the first two words of the Lyndon tuple are combined into $l_0 = l_1 l_2$ and the letter l_1 is now followed by an element of C, the first letter of l_2, and the last letter of l_2 is now followed (cyclically) by the letter l_1, which is also an element of C. Then for Lyndon tuples $\text{tup}(w)$ and $\text{tup}(w') = (l_0, l_3, \ldots, l_k)$ such that $f(w) = w'$, also $T(\text{tup}(w)) = T(\text{tup}(w'))$.

Suppose $l_1 \notin \mathcal{A}$ does not split because it has standard factorization (r_1, s_1) with $s_1 \triangleright l_2$. We claim that $s_1 \triangleright l_2$ implies that l_2 must begin with an element of C. If l_1 contains a single element of C, then as $|C| \geq 2$ and $l_1 \triangleleft l_2 \triangleleft \cdots \triangleleft l_k$ with each a Lyndon word, l_2 begins with an element of C. Otherwise, l_1 contains multiple elements of C; as s_1 is the minimum proper suffix lexicographically of l_1 by proposition 2.4.2, it must also begin with an element of C. As $l_2 \triangleleft s_1$ by assumption, l_2 must also begin with an element of C. As l_1 is not splittable, the map f combines l_1 and l_2 into $l_0 = l_1 l_2$; so $f(w) = w'$ for $\text{tup}(w)$ and $\text{tup}(w') = (l_0, l_3, \ldots, l_k)$ and also $T(\text{tup}(w)) = T(\text{tup}(w'))$.

If l_1 is splittable, then $|l_1| \geq 2$ and l_1 has standard factorization (r_1, s_1) such that $s_1 \triangleleft l_2$. We claim that in order for l_1 to split, it must contain at least two elements of C. For the sake of contradiction, assume that l_1 has only one element of C, which must be the leading one. Then the least proper suffix s_1 of l_1 begins with an element that is greater than all elements of C. But as $|C| \geq 2$, l_2 must begin with an element of C, and $s_1 \triangleright l_2$, a contradiction. As l_1 contains at least two elements of C, consider its standard factorization (r_1, s_1); as s_1 is the least proper suffix of l_1 lexicographically by proposition 2.4.2, both r_1 and s_1 begin with elements of C. Then for Lyndon tuples $\text{tup}(w)$ and $\text{tup}(w') = (r_1, s_1, l_2, \ldots, l_k)$ such that $f(w) = w'$, also $T(\text{tup}(w)) = T(\text{tup}(w'))$. $\square$

If a primitive pseudo orbit $\bar{\gamma}$ corresponds to the Lyndon tuple $\mathrm{tup}(w)$, then $T(\mathrm{tup}(w))$ is the number of times that the scattering coefficient $\sigma_{c,b}^{(v)}$ appears in $A_{\bar{\gamma}}$. We have shown that the partner orbits of a primitive pseudo orbit $\bar{\gamma}$ are given by all the Lyndon tuples in $\mathcal{L}(M)$. As a result of the labeling of links in proposition 4.3.1, the map f between odd and even Lyndon tuples does not change the number of times any letter in a Lyndon tuple (in particular, any letter in the multiset B) is followed (cyclically) by a letter in the multiset C. Thus, for any even (odd) Lyndon tuple $\mathrm{tup}(w)$ associated to a partner orbit $\bar{\gamma}' \in \mathcal{P}_{\bar{\gamma}}$, the map f produces an odd (even) Lyndon tuple $\mathrm{tup}(w')$ such that $T(\mathrm{tup}(w)) = T(\mathrm{tup}(w'))$. Therefore, the number of times that $\sigma_{c,b}^{(v)}$ appears in $\bar{A}_{\bar{\gamma}'}$ is associated to the same number of primitive pseudo orbits $\bar{\gamma}'$ with $m_{\bar{\gamma}'}$ even as with $m_{\bar{\gamma}'}$ odd. As a result, we have the following contribution to (4.2.3).

Lemma 4.3.3. For any primitive pseudo orbit $\bar{\gamma}$ containing a single ℓ-encounter of length zero for $\ell \geq 3$, $C_{\bar{\gamma}} = 0$.

Proof. Let $\bar{\gamma}$ be a primitive pseudo orbit containing a single ℓ-encounter of length zero for $\ell \geq 3$, where $\bar{\gamma}$ corresponds to some Lyndon tuple $\mathrm{tup}(w) \in \mathcal{L}(M)$. The partner pseudo orbits $\bar{\gamma}' \in \mathcal{P}_{\bar{\gamma}}$ correspond to all the Lyndon tuples $\mathrm{tup}(w') \in \mathcal{L}(M)$. Consider the number of times $T(\mathrm{tup}(w'))$ that a tuple $\mathrm{tup}(w')$ has a letter from the set B followed (cyclically) by a letter from the set C in its Lyndon words. The value of $T(\mathrm{tup}(w'))$ must be from the set $\{I - \min\{I, J\}, I - \min\{I, J\} + 1, \ldots, \min\{I, \ell - J\}\}$. We let the index α range over this set, and consider the elements of $\mathcal{L}(M)$ by subsets with the same value α. Then by proposition 4.3.1 and the correspondence between

a Lyndon tuple's Lyndon index and the number of periodic orbits in a pseudo orbit (4.3.7),

$$C_{\bar{\gamma}} = \left(\frac{1}{2}\right)^n (-1)^{2\ell+T(\mathrm{tup}(w))+i_{\mathcal{L}}(w)} \sum_{\alpha=I-\min\{I,J\}}^{\min\{I,\ell-J\}} (-1)^{\alpha} \sum_{\substack{\mathrm{tup}(w')\in\mathcal{L}(M):\\ T(\mathrm{tup}(w'))=\alpha}} (-1)^{i_{\mathcal{L}}(w')} = 0 \ . \tag{4.3.11}$$

□

4.3.4 Pairs of Primitive Pseudo Orbits with Multiple Encounters

As in section 4.1.4, a primitive pseudo orbit $\bar{\gamma}$ contains a finite number of encounters N of types $\vec{\ell} = (\ell_1, \ell_2, \ldots, \ell_N)$ with a connection vector $\vec{\rho} = (\rho_1, \rho_2, \ldots, \rho_N)$ that shows the order in which the incoming links are followed by outgoing links at each of the N encounters in $\bar{\gamma}$. Here we show that if *any* of these self-intersections is of positive length, or of length zero at an ℓ_i-encounter for $\ell_i \geq 3$, then the total contribution of $\bar{\gamma}$ paired with all its possible partners is zero. Here we assume that at least one encounter is of either of these types; the case where all N encounters are 2-encounters of length zero will be covered in section 4.3.5.

To see this, consider the contribution $C_{\bar{\gamma}}$ (4.2.2) to the variance of the coefficients of the graph's characteristic polynomial (4.2.3). For a particular primitive pseudo orbit $\bar{\gamma}$, we wish to generate all the partner primitive pseudo orbits $\bar{\gamma}' \in \mathcal{P}_{\bar{\gamma}}$. Here we will do so by considering each $\bar{\gamma}'(\vec{\rho})$ that is primitive as the elements of $\vec{\rho}$ range over all the connection diagrams at each encounter, $\hat{\rho}_i \in \hat{S}_{\ell_i}$ for $i = 1, \ldots, N$. Then the contribution $C_{\bar{\gamma}}$ is given by

$$C_{\bar{\gamma}} = \sum_{\hat{\rho}_N \in \hat{S}_{\ell_N}} \cdots \sum_{\hat{\rho}_1 \in \hat{S}_{\ell_1}} (-1)^{m_{\bar{\gamma}}+m_{\bar{\gamma}'(\vec{\rho})}} A_{\bar{\gamma}} \bar{A}_{\bar{\gamma}'(\vec{\rho})} \ . \tag{4.3.12}$$

Lemma 4.3.4. For any primitive pseudo orbit $\bar{\gamma}$ containing N self-intersections of types $\vec{\ell} = (\ell_1, \ell_2, \ldots, \ell_N)$ such that at least one self-intersection is either of positive length or is an ℓ_i-encounter of length zero with $\ell_i \geq 3$, $C_{\bar{\gamma}} = 0$.

Proof. As there are a finite number of self-intersections, possible connection diagrams at each encounter can be summed over in any order. Without loss of generality, let the first encounter be of either positive length or of type $\ell_1 \geq 3$ with length zero. We wish to first compute the innermost sum,

$$\sum_{\hat{\rho}_1 \in \hat{S}_{\ell_1}} (-1)^{m_{\bar{\gamma}} + m_{\bar{\gamma}'(\vec{\rho})}} A_{\bar{\gamma}} \bar{A}_{\bar{\gamma}'(\vec{\rho})} \ , \tag{4.3.13}$$

when all other connection diagrams $\hat{\rho}_i \in \hat{S}_{\ell_i}$ are fixed for $i = 2, \ldots, N$ in the partner pseudo orbit $\bar{\gamma}'(\vec{\rho})$.

However, this is precisely a sum that we have computed in lemma 4.3.1, 4.3.2, or 4.3.3. Having fixed the internal connection diagrams at all but the first encounter, reconnecting incoming and outgoing links at the first encounter is equivalent to considering all orderings of links that both begin and end at that first encounter, as in sections 4.3.1, 4.3.2, and 4.3.3. So to sum over the primitive pseudo orbit partners of $\bar{\gamma}$ in (4.3.13), we consider permutations or Lyndon tuples (as appropriate) of links (rather than connection diagrams) that intersect at the first encounter. Hence, the sum in (4.3.13) is zero and $C_{\bar{\gamma}} = 0$. □

4.3.5 Pairs of Primitive Pseudo Orbits with One or More 2-Encounters of Length Zero

Lastly, we consider the contribution $C_{\bar{\gamma}}$ to (4.2.3) from pairs of primitive pseudo orbits that have any number N of 2-encounters all of length zero, so $N = N_0$. These are the only types of pseudo orbits with encounters that contribute nonzero terms $C_{\bar{\gamma}}$ to (4.2.3). We have already covered the contributions of 2-encounters of positive length in section 4.3.1; however, in computing the contributions of 2-encounters of any length simultaneously, we obtain a Vandermonde-type identity that we have not been able to find in the literature. See Appendix A for details.

Let us consider the stability amplitude associated to each primitive pseudo orbit in a pair with a single 2-encounter at a vertex in the pseudo orbit $\bar{\gamma}$. The only two examples of a pseudo orbit with such a single 2-encounter are those described in examples 4.1.1 and 4.1.2, letting $\tilde{n} = 0$. First, we will show that the product of stability amplitudes is the same for each example.

We let A_{link_i} denote the product of scattering amplitudes at the vertices on link_i where each link begins and ends at the encounter vertex v, for $i = 1, 2$. If we let $\bar{\gamma}$ and $\bar{\gamma}'$ be as in example 4.1.1, then

$$A_{\gamma_1} = A_{\text{link}_1} A_{\text{link}_2} \sigma^{(v)}_{f_1,s_1} \sigma^{(v)}_{f_2,s_2} \ . \tag{4.3.14}$$

However, for $\bar{\gamma}'$, the reordering of the links at v necessarily changes the scattering coefficients, and

$$A_{\gamma'} A_{\gamma''} = A_{\text{link}_1} A_{\text{link}_2} \sigma^{(v)}_{f_1,s_2} \sigma^{(v)}_{f_2,s_1} \ . \tag{4.3.15}$$

Considering a single self-intersection in $\{\bar{\gamma}, \bar{\gamma}'\}$, all other orbits in $\bar{\gamma}$ are unchanged in $\bar{\gamma}'$, and therefore have identical stability amplitudes. So,

$$A_{\bar{\gamma}}\bar{A}_{\bar{\gamma}'} = \left(\prod_{h=2}^{m_{\bar{\gamma}}} |A_{\gamma_h}|^2\right) |A_{\text{link}_1}|^2 |A_{\text{link}_2}|^2 \sigma^{(v)}_{f_1,s_1}\sigma^{(v)}_{f_2,s_2}\bar{\sigma}^{(v)}_{f_1,s_2}\bar{\sigma}^{(v)}_{f_2,s_1} \ . \tag{4.3.16}$$

Note that if we consider a pseudo orbit $\bar{\gamma}$ with a single 2-encounter as in example 4.1.2, then

$$A_{\gamma_1}A_{\gamma_2} = A_{\text{link}_1}A_{\text{link}_2}\sigma^{(v)}_{f_1,s_2}\sigma^{(v)}_{f_2,s_1} \ , \tag{4.3.17}$$

and

$$A_{\gamma} = A_{\text{link}_1}A_{\text{link}_2}\sigma^{(v)}_{f_1,s_1}\sigma^{(v)}_{f_2,s_2} \ , \tag{4.3.18}$$

so $A_{\bar{\gamma}}A_{\bar{\gamma}'}$ is the same for examples 4.1.1 and 4.1.2.

Now, as $s_1 \neq s_2$ and $f_1 \neq f_2$, all four entries of the binary scattering matrix (4.3.1) appear in the product of the scattering amplitudes,

$$\sigma^{(v)}_{f_1,s_1}\sigma^{(v)}_{f_2,s_2}\bar{\sigma}^{(v)}_{f_1,s_2}\bar{\sigma}^{(v)}_{f_2,s_1} = -\left(\frac{1}{2}\right)^2 . \tag{4.3.19}$$

Note that all scattering amplitudes are real-valued when $q = 2$, and that $\tilde{n} = 0$ implies

$$A_{\bar{\gamma}}\bar{A}_{\bar{\gamma}'} = -\left(\frac{1}{2}\right)^n \ . \tag{4.3.20}$$

Now consider primitive pseudo orbits with N 2-encounters of length zero and $N = N_0$. There is an associated vector $\vec{\rho}$ of connection diagrams (permutations $\rho_i \in S_2$ for $i = 1, \ldots, N$) that determine how the two incoming links are followed by the two outgoing links at the i-th encounter in $\bar{\gamma}$, as in section 4.3.4. We then consider the partner pseudo orbits $\bar{\gamma}'(\vec{\rho})$ generated by considering all possible vectors

$\vec{\rho}$ with $\rho_i \in S_2$ for $i = 1, \ldots, N$. For any self-intersection v at which the permutation from S_2 is the same in both $\bar{\gamma}$ and $\bar{\gamma}'(\vec{\rho})$, the scattering coefficients from (4.3.1) at the self-intersection v are the same in each of the pseudo orbits and the product is $1/4$. However, at the i-th self-intersection v for which $\rho_i = (1\ 2)$ in $\bar{\gamma}$ but $\rho_i = (1)(2)$ in $\bar{\gamma}'(\vec{\rho})$ (or vice versa), each of the scattering coefficients in $\sigma^{(v)}$ appears exactly once in $A_{\bar{\gamma}}\bar{A}_{\bar{\gamma}'(\vec{\rho})}$. Thus, if j is the number of 2-encounters of length zero in $\bar{\gamma}$ at which the connection diagram is changed in $\bar{\gamma}'$, then

$$A_{\bar{\gamma}}\bar{A}_{\bar{\gamma}'} = (-1)^j \left(\frac{1}{2}\right)^n \ . \tag{4.3.21}$$

To understand the factor $(-1)^{m_{\bar{\gamma}}+m_{\bar{\gamma}'}}$ in (4.2.2) for any general pair $\{\bar{\gamma}, \bar{\gamma}'\}$ with $N = N_0$ 2-encounters, consider first the particular type of pseudo orbit with $N = N_0 = 1$ self-intersection. If the self-intersection is contained in a periodic orbit $\gamma \in \bar{\gamma}$, then reordering links at this self-intersection will result in two orbits $\gamma', \gamma'' \in \bar{\gamma}'$, thereby increasing the number of periodic orbits in $\bar{\gamma}'$ relative to $\bar{\gamma}$; so $m_{\bar{\gamma}'} = m_{\bar{\gamma}} + 1$. If the self-intersection comes from a repeated sequence of vertices where one traversal is in some $\gamma' \in \bar{\gamma}$ and the second traversal is in $\gamma'' \in \bar{\gamma}$ for $\gamma' \neq \gamma''$, then reordering links at this self-intersection will join the two orbits and decrease the number of periodic orbits in $\bar{\gamma}'$ relative to $\bar{\gamma}$; so $m_{\bar{\gamma}'} = m_{\bar{\gamma}} - 1$. As there is only one 2-cycle permutation of the exit vertices, a reordering at a single self-intersection must either increase or decrease the number of orbits in a pseudo orbit by one, and the value of $m_{\bar{\gamma}} + m_{\bar{\gamma}'}$ depends on the orbit structure. However, as it suffices to know the parity of -1 for any structure with j reordered self-intersections, it is enough to recognize that the

parity of $(-1)^m_{\bar{\gamma}'}$ is the same as $(-1)^m_{\bar{\gamma}}$ if $\bar{\gamma}'$ was obtained from $\bar{\gamma}$ by reordering at an even number of self-intersections, and the parity of $m_{\bar{\gamma}'}$ differs from that of $m_{\bar{\gamma}}$ if $\bar{\gamma}'$ was obtained from $\bar{\gamma}$ by reordering at an odd number of self-intersections. So if j is the number of 2-encounters at which links are reordered to obtain $\bar{\gamma}'$, then

$$(-1)^{m_{\bar{\gamma}}+m_{\bar{\gamma}'}} = (-1)^j \ . \tag{4.3.22}$$

Let $\hat{\mathcal{P}}^n_N \subset \mathcal{P}^n_N$ be the set of all primitive pseudo orbits of length n with N self-intersections such that $\vec{\ell} = (2, \ldots, 2)$. Moreover, let $\hat{\mathcal{P}}^n_{N=N_0}$ be the subset of $\hat{\mathcal{P}}^n_N$ such that each 2-encounter has length zero.

Lemma 4.3.5. For any primitive pseudo orbit $\bar{\gamma} \in \hat{\mathcal{P}}^n_{N=N_0}$ for $N > 0$, the contribution of all primitive pseudo orbit pairs $\{\bar{\gamma}, \bar{\gamma}'\}$ to (4.2.3) is

$$C_{\bar{\gamma}} = 2^N \cdot \left(\frac{1}{2}\right)^n \ . \tag{4.3.23}$$

Proof. Let $\bar{\gamma} \in \hat{\mathcal{P}}^n_{N=N_0}$ and consider partner orbits $\bar{\gamma}' \in \mathcal{P}_{\bar{\gamma}}$. We let the number of self-intersections at which link connections are rearranged be indexed by j; then

$$C_{\bar{\gamma}} = \sum_{\substack{\{\bar{\gamma},\bar{\gamma}'\} \\ \bar{\gamma}' \in \mathcal{P}_{\bar{\gamma}}}} (-1)^{m_{\bar{\gamma}}+m_{\bar{\gamma}'}} A_{\bar{\gamma}} \bar{A}_{\bar{\gamma}'} = \left(\frac{1}{2}\right)^n \sum_{j=0}^{N} (-1)^{2j} \binom{N}{j} \ , \tag{4.3.24}$$

by equations (4.3.21) and (4.3.22), and as there are $\binom{N}{j}$ ways of choosing j self-intersections to rearrange at a time. Noting the well-known identity [111],

$$\sum_{j=0}^{N} \binom{N}{j} = 2^N \ , \tag{4.3.25}$$

the result follows. □

Note that for any pseudo orbit, if the partner pseudo orbit is generated by rearranging at no self-intersections ($j = 0$), then that particular term belongs also to the diagonal contribution.

We have now seen that a primitive pseudo orbit containing only 2-encounters of length zero is the only type of pseudo orbit with self-intersection(s) with a non-zero contribution $C_{\bar{\gamma}}$ to (4.2.3). Thus, we have the following theorem.

Theorem 4.3.1. The variance of the n-th coefficient of a binary quantum graph's characteristic polynomial (4.2.3) is given by the number of primitive pseudo orbits of length n without self-intersections, and the number of primitive pseudo orbits of length n with $N = N_0 > 0$ self-intersections that are 2-encounters of length zero,

$$\langle |a_n|^2 \rangle_k = \frac{1}{2^n} \left(|\mathcal{P}_0^n| + \sum_{N=1}^{n} 2^N \cdot |\hat{\mathcal{P}}_{N=N_0}^n| \right) \ . \tag{4.3.26}$$

Proof. Combining lemmas 4.3.1, 4.3.2, 4.3.3, 4.3.4, and 4.3.5, the result follows. □

Theorem 4.3.2. In the limit of long pseudo orbits, the variance $\langle |a_n|^2 \rangle_k$ of a binary graph's characteristic polynomial is

$$\lim_{n\to\infty} \langle |a_n|^2 \rangle_k = \frac{C_{p,q}}{2} \ , \tag{4.3.27}$$

where $C_{p,q}$ is as defined in (3.2.12).

Proof. We seek to asymptotically determine the sizes of the relevant sets $\hat{\mathcal{P}}_{N=N_0}^n$ in (4.3.26). To have a 2-encounter of length zero, a periodic orbit must pass through some vertex v twice and subsequently exit on a different bond the second time. The

probability that the orbit leaves v on a different bond the second time it visits v than it did the first time is $1/2$ and thus, the probability is $(1/2)^N$ that a pseudo orbit with N self-intersections has $N = N_0$. So for n sufficiently large,

$$|\hat{\mathcal{P}}^n_{N=N_0}| \approx \left(\frac{1}{2}\right)^N \cdot |\hat{\mathcal{P}}^n_N| \ . \tag{4.3.28}$$

Let $(\hat{\mathcal{P}}^n_N)^c = \mathcal{P}^n_N \backslash \hat{\mathcal{P}}^n_N$ be the set of all primitive pseudo orbits of topological length n with N self-intersections that have $\vec{\ell} = (\ell_1, \ell_2, \ldots, \ell_N)$ repetitions, such that at least one $\ell_i \geq 3$. In order to have an ℓ-encounter with $\ell \geq 3$, after a 2-encounter the pseudo orbit must return to the first vertex of the encounter sequence v_0 for a third time. There are many ways to make an encounter in a pseudo orbit, as there are n possible points of intersection, but only one way to make a 2-encounter into a 3-encounter (or $\ell > 3$ encounter) by intersecting at the encounter vertex.

As binary graphs are mixing [124], the probability to land on any vertex after a large number of steps is B^{-1}. Hence, the number of orbits in $(\hat{\mathcal{P}}^n_N)^c$ scales with the size of $\mathcal{P}^n_N$ asymptotically like $1/B$. Thus, for large enough n,

$$|\hat{\mathcal{P}}^n_N| \approx |\mathcal{P}^n_N| \ . \tag{4.3.29}$$

Substituting (4.3.28) and (4.3.29) in (4.3.26), for n large enough,

$$\langle |a_n|^2 \rangle_k \approx \left(\frac{1}{2}\right)^n \sum_{N=0}^{n} |\mathcal{P}^n_N| \ . \tag{4.3.30}$$

Noting that the sets $\mathcal{P}^n_N$ are pairwise disjoint for differing values of $0 \leq N \leq n$, and that the union of them is the set of all primitive pseudo orbits $\mathrm{PPO}_{p,2}(n)$ of length n, we have that, for large n,

$$\langle |a_n|^2 \rangle_k \approx \left(\frac{1}{2}\right)^n \cdot \mathrm{PPO}_{p,2}(n) = C_{p,q} \cdot 2^{n-1} \left(\frac{1}{2}\right)^n \ , \tag{4.3.31}$$

as the number of primitive pseudo orbits $\mathrm{PPO}_{p,2}(n)$ is given by (3.2.11). □

The characteristic polynomial $F_\zeta(k)$ has $B+1$ coefficients where $a_n = \bar{a}_{B-n}$ (2.2.29), so $\langle |a_n|^2 \rangle_k = \langle |a_{B-n}|^2 \rangle_k$. The limit $n \to \infty$ is thus understood in the context of simultaneously increasing the number of coefficients. This amounts to increasing the size of the graph within a particular family by fixing the ratio n/B and letting $r \to \infty$ in the number of bonds $B = p \cdot 2^{r+1}$. Moreover, this limit of large graphs corresponds to the semiclassical limit of increasing eigenvalue density in the quantum graph setting.

4.4 Examples

To demonstrate our result numerically, we generate a q-nary graph in MatLab of the appropriate dimensions with each of the B bond lengths uniformly distributed random numbers in the interval $[0.9, 1.1]$. We expect the mean spacing of the square roots of the graph's eigenvalues k to be approximately the ratio of pi to the total length of the graph by the Weyl law in lemma 2.2.1. Then we generate the characteristic polynomial of $U(k) = S\mathrm{e}^{\mathrm{i}kL}$ as in (2.2.28) for each value of k. For the numerics plotted in figures 4.7, 4.8, and 4.9, the characteristic polynomial was typically evaluated for 50 million mean spacings; for the larger values of B, MatLab was run on Baylor's Kodiak high performance computing cluster. However, for $B = 160$, the simulation appeared to have converged quickly, so we ended the simulation at 26.5 million mean spacings;

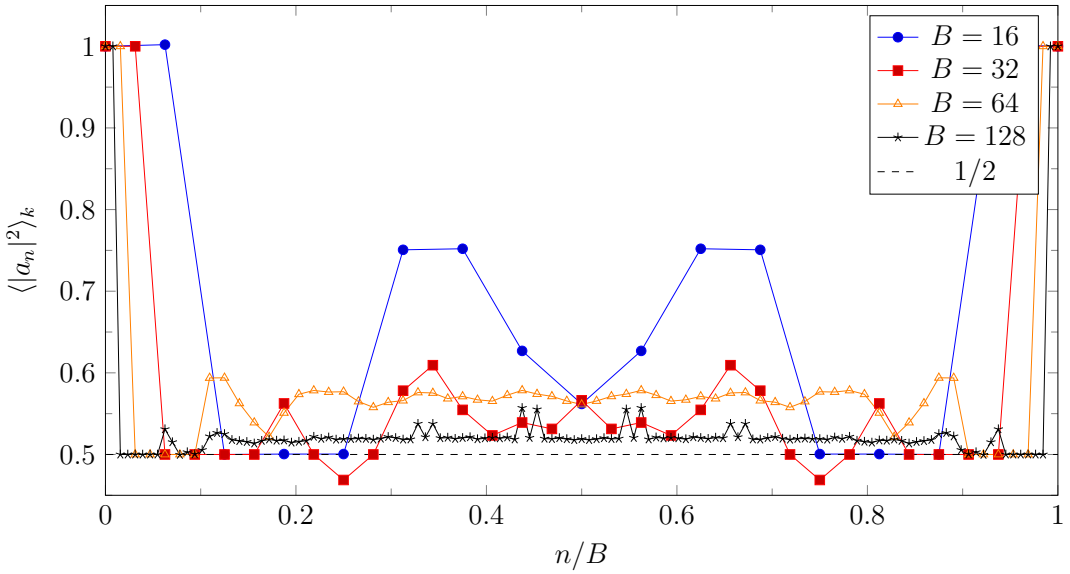

Figure 4.7. Variance of coefficients of the characteristic polynomial for a family of binary graphs with $p = 1$ averaged over a window of 50,000,000 mean spacings. The plot shows the convergence to the diagonal contribution $\langle |a_n|^2 \rangle_{\text{diag}} = 1/2$.

for $B = 192$, the simulation ended at 20.9 million mean spacings. For $B = 320$, the simulation met the maximum run time on Kodiak after 23.9 million mean spacings.

The variance of the coefficients for the binary family of graphs with $V = 2^r$ vertices and $B = 2^{r+1}$ bonds is shown in figure 4.7 for $r = 3, 4, 5, 6$; it approaches $1/2$, as r increases. This value was given by theorem 4.3.2 where $C_{1,2} = 1$. To see that these numerics agree with our formula, consider the following example.

Example 4.4.1. Consider the binary graph with $V = 8$ vertices and $B = 16$ bonds, as in figure 1.9. As $p = 1$, the number of primitive periodic orbits of length n is exactly the number of binary Lyndon words, $\text{PO}_2(n) = \text{L}_2(n)$. Moreover, the number of primitive pseudo orbits of topological length n is $\text{PPO}_2(n) = 2^{n-1}$. These primitive pseudo orbits can be sorted into sets of those without self-intersections, and those with only 2-encounters of length zero. Table 4.3 shows the sizes of these

sets for all applicable numbers of self-intersections for $0 \leq n \leq 8$. For a detailed description of how these set sizes are determined using Lyndon words, see Appendix B. For $9 \leq n \leq 16$, the Rieman-Siegel formula (2.2.29) applies to the variance. The formula for the variance (4.3.26) is applied to obtain the variance in the fifth column. The values of the variance $\langle |a_n|^2 \rangle_k$ for a random matrix of bond lengths are averaged over 50 million mean spacings, as in figure 4.7 for $B = 16$ and are given in the penultimate column. The error between our formula and the numerics is shown in the last column. $\diamond$

Table 4.3. For a binary graph with $V = 8$ vertices and $B = 16$ bonds, the sizes of the sets of primitive pseudo orbits for which $C_{\bar{\gamma}} \neq 0$ and the resulting variance for the first half of the characteristic polynomial's coefficients are given. The last two columns give the numerical values of the variance shown in figure 4.7 and the error between our formula and the numerics.

n	$\lvert\mathcal{P}_0^n\rvert$	$\lvert\hat{\mathcal{P}}_{N=N_0=1}^n\rvert$	$\lvert\hat{\mathcal{P}}_{N=N_0=2}^n\rvert$	$\langle \lvert a_n\rvert^2 \rangle_k$	Numerics	Error
0	1	0	0	1	1.000000	0.000000
1	2	0	0	1	0.999991	0.000009
2	2	0	0	1/2	0.499999	0.000001
3	4	0	0	1/2	0.499999	0.000001
4	8	0	0	1/2	0.499999	0.000001
5	8	8	0	3/4	0.749998	0.000002
6	8	20	0	3/4	0.749986	0.000014
7	16	16	8	5/8	0.624989	0.000011
8	16	16	24	9/16	0.562501	-0.000001

The variance of the coefficients for the binary family of graphs with $V = 3 \cdot 2^r$ vertices and $B = 3 \cdot 2^{r+1}$ bonds is shown in figure 4.8 for $r = 1, 2, 3, 4, 5$; it approaches $5/8$, as r increases. This value was given by theorem 4.3.2 where $C_{3,2} = 5/4$, as calculated in example 3.4.1. To see that these numerics agree with our formula, consider the following example.

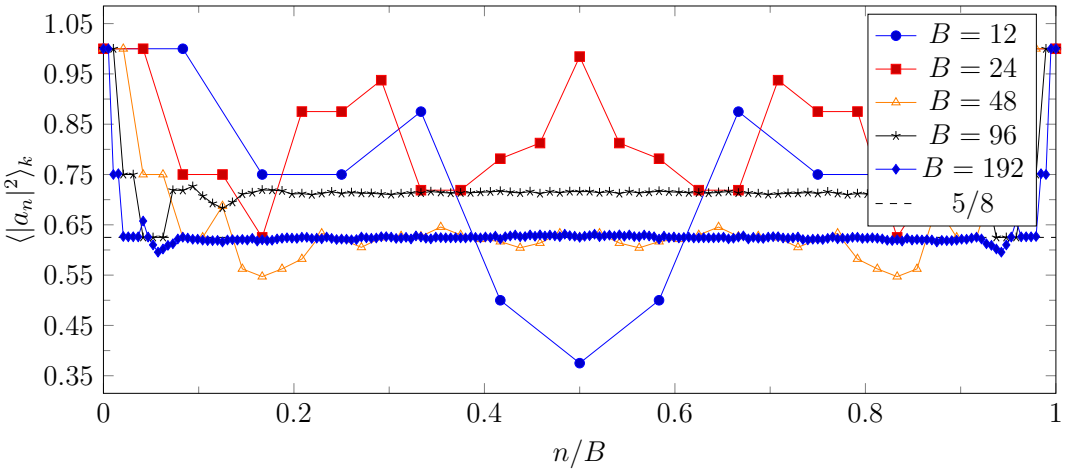

Figure 4.8. Variance of coefficients of the characteristic polynomial for a family of binary graphs with $p = 3$ averaged over a window of 50,000,000 mean spacings. The plot shows the convergence to the diagonal contribution $\langle |a_n|^2 \rangle_{\text{diag}} = 5/8$.

Example 4.4.2. Consider the binary graph with $V = 6$ vertices and $B = 12$ bonds. As $p = 3$, the number of primitive periodic orbits of length n is exactly the number of binary Lyndon words, $\text{PO}_{3,2}(n) = \text{L}_2(n)$ for $n \neq 2$, and $\text{PO}_{3,2}(2) = \text{L}_2(2) + 1$. Moreover, the number of primitive pseudo orbits of topological length n is $\text{PPO}_{3,2}(n) = 5 \cdot 2^{n-3}$ for $n > 3$. These primitive pseudo orbits can be sorted into sets of those without self-intersections, and those with only 2-encounters of length zero. Table 4.3 shows the sizes of these sets for all applicable numbers of self-intersections for $0 \leq n \leq 6$. For a detailed description of how these set sizes are determined using Lyndon words, see Appendix C. For $7 \leq n \leq 12$, the Rieman-Siegel formula (2.2.29) applies to the variance. The formula for the variance (4.3.26) is applied to obtain the variance in the fifth column. The values of the variance $\langle |a_n|^2 \rangle_k$ for a random matrix of bond lengths are averaged over 50 million mean spacings, as in figure 4.8

for $B = 12$ and are given in the penultimate column. The error between our formula and the numerics is shown in the last column. $\diamond$

Table 4.4. For a binary graph with $V = 6$ vertices and $B = 12$ bonds, the sizes of the sets of primitive pseudo orbits for which $C_{\bar{\gamma}} \neq 0$ and the resulting variance for the first half of the characteristic polynomial's coefficients are given. The last two columns give the numerical values of the variance shown in figure 4.8 and the error between our formula and the numerics.

n	$\lvert\mathcal{P}_0^n\rvert$	$\lvert\hat{\mathcal{P}}_{N=N_0=1}^n\rvert$	$\langle\lvert a_n\rvert^2\rangle_k$	Numerics	Error
0	1	0	1	1.000000	0.000000
1	2	0	1	1.000000	0.000000
2	3	0	3/4	0.750001	-0.000001
3	6	0	3/4	0.750003	-0.000003
4	10	4	7/8	0.874999	0.000001
5	8	4	1/2	0.499998	0.000002
6	8	8	3/8	0.374999	0.000001

The variance of the coefficients for the binary family of graphs with $V = 5 \cdot 2^r$ vertices and $B = 5 \cdot 2^{r+1}$ bonds is shown in figure 4.9 for $r = 2, 3, 4, 5$; it approaches 17/32, as r increases. This value was given by theorem 4.3.2 where $C_{5,2} = 17/16$, as calculated in example 3.4.2.

4.5 Conclusions

We have evaluated the entire sum (2.2.47) over all pairs of primitive pseudo orbits of the same topological and metric lengths on quantum binary graphs. This was done by formulating the pseudo orbit sum (4.2.3) so that each primitive pseudo orbit is paired with every possible partner. Once we evaluated this sum, we then applied asymptotic arguments regarding the number of primitive pseudo orbits of particular types on binary graphs and found that our results agree with both the previous results of Band-Harrison-Sepanski and Tanner [6, 126], as well as with numerical simulations.

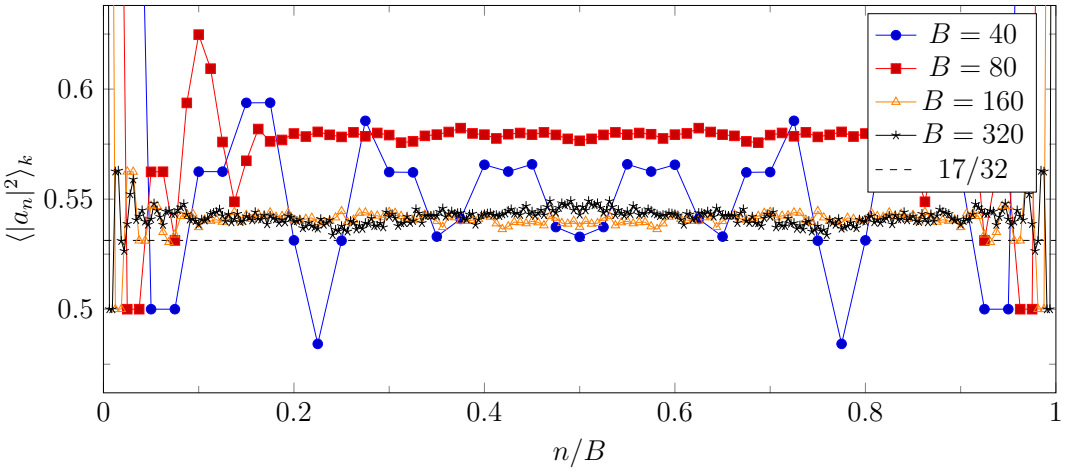

Figure 4.9. Variance of coefficients of the characteristic polynomial for a family of binary graphs with $p = 5$ averaged over a window of 50,000,000 mean spacings. The plot shows the convergence to the diagonal contribution $\langle |a_n|^2 \rangle_{\text{diag}} = 17/32$.

Our result is very specific, in that the spectral statistic considered is the variance of the coefficients of a quantum binary graph's characteristic polynomial, the graph structure makes the formulation of the variance a finite sum over pseudo orbits, and that counting all the primitive pseudo orbits is possible on a binary graph. However, this is the first case in the literature where similar sums over orbit pairs have been completely evaluated. Typically, after doing partial sums over particular types of orbits, heuristic arguments justify neglecting the other orbits. Here, the only asymptotic argument involves determining the relative sizes of sets of contributing orbits in the large graph limit, after having evaluated the entire sum for any graph size.

We also point out that as the spectral statistic we evaluated did not involve a series expansion in some semi-classical parameter, and thus every pair of pseudo orbits contributed in the same way, we used a cancellation mechanism that is not found elsewhere in the literature either. This involved considering diagonal and off-diagonal

pairs together, in order to get contributions of zero from most sets of related pseudo orbit pairs. Of course, this is not possible for evaluation of all spectral statistics, but it offers a new approach, when applicable.

As binary graphs lack time-reversal invariance, the appropriate random matrix statistic to compare to is the variance of the coefficients of the characteristic polynomial over the Gaussian Unitary Ensemble of random matrices, $\langle |a_n|^2 \rangle = 1$. Our asymptotic result, whilst constant, does not agree with the random matrix result. Rather it should be seen as a case where the universal random matrix result is multiplied by a system-specific constant. One can also see that if the result that $\lim_{n\to\infty} \langle |a_n|^2 \rangle_k = C_{p,q} \cdot \dfrac{q-1}{q}$ holds for q-nary graphs generally, then at least for de Bruijn graphs (where $p = 1$), a sequence of graphs with increasing connectivity q and increasing size $r \to \infty$ does approach the random matrix result. Preliminary investigation of the variance (2.2.47) for general q-nary graphs is the focus of Chapter Five.

CHAPTER FIVE

Computing the Variance of the Coefficients for a q-nary Quantum Graph's Characteristic Polynomial

In this chapter, we formulate preliminary results for the variance $\langle |a_n|^2 \rangle_k$ (2.2.47) of the coefficients of the characteristic polynomial for q-nary quantum graphs, for which we previously obtained the diagonal contribution (3.3.1). As in Chapter Four, to evaluate the whole sum (2.2.47), we must produce primitive pseudo orbit pairs with distinct members that have the same topological and metric lengths. To do so, we again consider orbits that contain repeated sequences of vertices and bonds.

We formulate the variance of the coefficients of a quantum q-nary graph's characteristic polynomial as in (4.2.3), summing contributions of all the partners of a given primitive pseudo orbit. In the case of binary graphs, the stability amplitude product $A_{\bar{\gamma}}\bar{A}_{\bar{\gamma}'} = \pm 2^{-n}$ was real-valued, and we could factor 2^{-n} out of the contribution (4.2.2) from a primitive pseudo orbit and each of its partners and deal with only the corresponding sign for each partner. For q-nary graphs, there is a corresponding factor of q^{-n} in $A_{\bar{\gamma}}\bar{A}_{\bar{\gamma}'}$ for any primitive pseudo orbit pair $\{\bar{\gamma}, \bar{\gamma}'\}$ of the same topological and metric lengths. Thus, the contribution of a primitive pseudo orbit with an encounter of positive length paired with each of its partners of the same length will be zero, as in Chapter Four. However, here we must deal with complex scattering coefficients and we will need to average over the ways to assign these coefficients to

each of the incoming and outgoing vertices when considering primitive pseudo orbits with a self-intersection of length zero.

5.1 Self-Intersections in Pseudo Orbits on q-nary Graphs

Again, we wish to construct primitive pseudo orbit pairs $\{\bar{\gamma}, \bar{\gamma}'\}$ with the same topological and metric lengths such that $\bar{\gamma}' \neq \bar{\gamma}$. We let self-intersections, ℓ-encounters, encounter length, and links be defined in the same way as in Chapter Four. We first consider primitive pseudo orbits with a single encounter.

In Chapter Four we examined contributions to the variance $\langle |a_n|^2 \rangle_k$ for binary graphs from pseudo orbit pairs with at least one self-intersection. To extend the approach to q-nary graphs we must consider multiple distinct incoming and outgoing bonds at the ends of the encounter, see figure 5.1. Thus, for q-nary graphs with $q \geq 3$, scattering coefficients from the Discrete Fourier Transform matrix (2.5.11) will typically be complex. Because the pairs of primitive pseudo orbits with the same

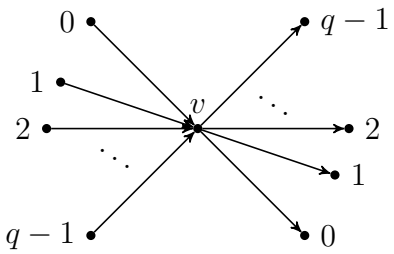

Figure 5.1. On a q-nary graph, at self-intersection v, there are q possible choices of incoming bonds and q possible choices of outgoing bonds.

topological and metric lengths traverse the same bonds the same numbers of times, the only scattering coefficients that differ between the two pseudo orbits are those picked up at an encounter of length zero. There are q^2 possible scattering coefficients

at any given vertex; we can use up to ℓ^2 of these in the partner pseudo orbits associated with an ℓ-encounter of length zero. The results in Chapter Four simplify, as $q^2 = \ell^2$ for a single 2-encounter on a binary graph. Additionally, the stipulation that not all incoming and outgoing bonds are the same at an encounter means that for a 2-encounter both must be different, and so $A_{\bar{\gamma}}\bar{A}_{\bar{\gamma}'}$ includes all $\ell^2 = q^2 = 4$ possible scattering coefficients at the encounter vertex precisely once for $\bar{\gamma}' \neq \bar{\gamma}$. For an ℓ-encounter on a q-nary graph, this will not typically be the case.

5.1.1 A Single Encounter of Positive Length

For a pseudo orbit with a single encounter, rearranging the order that links are taken following the encounter produces pseudo orbit partners with the same length, such that primitive pairs contribute to (4.2.3). As in sections 4.1.2 and 4.1.3, primitive pseudo orbits with a single ℓ-encounter can be represented by either permutations from the symmetric group S_ℓ if all ℓ links are distinct, or by Lyndon tuples over a multiset with size ℓ if any of the links are repeated. Some examples of primitive pseudo orbit pairs on a ternary graph follow.

Example 5.1.1. Let $\bar{\gamma} = \{\gamma_1, \gamma_2, \ldots, \gamma_{m_{\bar{\gamma}}}\}$ be a primitive pseudo orbit where, letting $\text{enc} = (v_0, v_1, \ldots, v_{\tilde{n}-1}, v_{\tilde{n}})$ be the 3-encounter sequence, the primitive periodic orbit γ_1 is given by

$$\gamma_1 = (s_3, \text{enc}, f_1, \ldots, s_1, \text{enc}, f_2, \ldots, s_2, \text{enc}, f_3, \ldots, s_3) \ , \tag{5.1.1}$$

a sequence of vertices and bonds corresponding to the portion of a ternary graph in figure 5.2 such that none of these vertices are repeated in $\gamma_2, \ldots, \gamma_{m_{\bar{\gamma}}}$ and no vertex

in $\gamma_2, \ldots, \gamma_{m_{\bar{\gamma}}}$ is used collectively more than once. It follows that the links in this

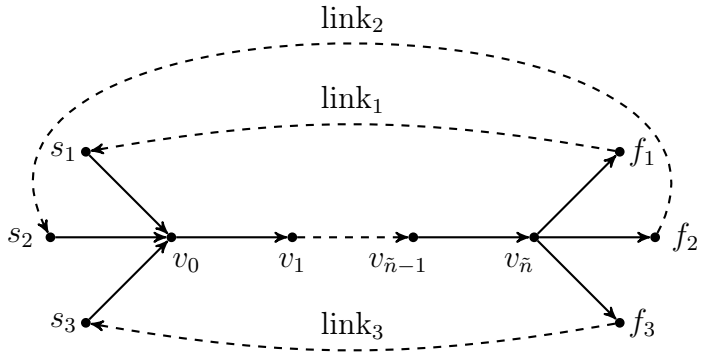

Figure 5.2. A portion of a graph from which a primitive pseudo orbit containing a 3-encounter with distinct links can be constructed.

example are given by

$$\text{link}_1 = (v_{\tilde{n}}, f_1, \ldots, s_1, v_0) \ , \tag{5.1.2}$$

$$\text{link}_2 = (v_{\tilde{n}}, f_2, \ldots, s_2, v_0) \ , \tag{5.1.3}$$

$$\text{link}_3 = (v_{\tilde{n}}, f_3, \ldots, s_3, v_0) \ . \tag{5.1.4}$$

There are exactly six partner pseudo orbits for $\bar{\gamma}$ that have the same topological and metric lengths; these correspond to the elements of the permutation group S_3. We see this by associating to each primitive partner orbit of $\bar{\gamma}$ a permutation from S_3, where $\gamma_1 = (\text{link}_1, \text{link}_2, \text{link}_3)$ corresponds to the link permutation (1 2 3), as in section 4.1.2. Then the possible partner pseudo orbits of $\bar{\gamma}$ are the same as those in table 4.1. ◇

Example 5.1.2. Let $\bar{\gamma} = \{\gamma_1, \gamma_2, \ldots, \gamma_{m_{\bar{\gamma}}}\}$ be a primitive pseudo orbit where, letting enc $= (v_0, v_1, \ldots, v_{\tilde{n}-1}, v_{\tilde{n}})$ be the 4-encounter sequence, the primitive periodic orbit γ_1 is given by

$$\gamma_1 = (s_3, \mathrm{enc}, f_1, \ldots, s_1, \mathrm{enc}, f_2, \ldots, s_2, \mathrm{enc}, f_3, \ldots, s_3) \ , \tag{5.1.5}$$

and the primitive periodic orbit γ_2 is given by

$$\gamma_2 = (s_1, \mathrm{enc}, f_1, \ldots, s_1) \ , \tag{5.1.6}$$

sequences of vertices and bonds corresponding to the portion of a ternary graph in figure 5.2 such that none of these vertices are repeated in $\gamma_3, \ldots, \gamma_{m_{\bar{\gamma}}}$ and no vertex in $\gamma_3, \ldots, \gamma_{m_{\bar{\gamma}}}$ is used collectively more than once. It follows that the links in this example are the same as the links in example 5.1.1, but that here the first link is used twice.

In generating partner pseudo orbits for $\bar{\gamma}$ that have the same topological and metric lengths, there are exactly ten partner orbits; these correspond to the Lyndon tuples of the link index multiset $M = [1^2, 2, 3]$ as shown in table 5.1. The two

Table 5.1. The 4-words over the multiset $M = [1^2, 2, 3]$ that have strictly decreasing Lyndon factorizations with their corresponding Lyndon tuples.

Even 4-words	Lyndon tuples	Odd 4-words	Lyndon tuples
1123	(1123)	1231	(1, 123)
1132	(1132)	1312	(12, 13)
1213	(1213)	1321	(1, 132)
2131	(1, 13, 2)	2113	(113, 2)
3121	(1, 12, 3)	3112	(112, 3)

4-words 2311 and 3211 over M are not included, as neither corresponds to a Lyndon tuple. ◇

As a result, we have the following lemma concerning contributions of primitive pseudo orbits with a single encounter of positive length and their partner orbits. The proof is the same as the proofs of lemmas 4.3.1 and 4.3.2.

Lemma 5.1.1. For any primitive pseudo orbit $\bar{\gamma}$ containing a single ℓ-encounter of positive length, $C_{\bar{\gamma}} = 0$.

Proof. As the stability amplitudes of $\bar{\gamma}$ and $\bar{\gamma}'$ are the same when the encounter length $\tilde{n} > 0$, the product $A_{\bar{\gamma}}\bar{A}_{\bar{\gamma}'}$ is q^{-n}. Thus, if $\bar{\gamma}$ has a single ℓ-encounter with ℓ distinct links, and corresponds to the permutation $\sigma_{\bar{\gamma}} \in S_\ell$, then the partners $\bar{\gamma}' \in \mathcal{P}_{\bar{\gamma}}$ correspond to the elements of S_ℓ, and

$$C_{\bar{\gamma}} = \left(\frac{1}{q}\right)^n \operatorname{sgn}(\sigma_{\bar{\gamma}}) \sum_{\sigma_{\bar{\gamma}'} \in S_\ell} \operatorname{sgn}(\sigma_{\bar{\gamma}'}) = 0 \ . \tag{5.1.7}$$

If $\bar{\gamma}$ has an ℓ-encounter with at least one repeated link for $\ell \geq 3$, and it corresponds to the Lyndon tuple $\operatorname{tup}(w) \in \mathcal{L}(M)$, then the partners $\bar{\gamma}' \in \mathcal{P}_{\bar{\gamma}}$ are the elements of $\mathcal{L}(M)$, and

$$C_{\bar{\gamma}} = \left(\frac{1}{q}\right)^n (-1)^{i_{\mathcal{L}}(w)} \sum_{\operatorname{tup}(w') \in \mathcal{L}(M)} (-1)^{i_{\mathcal{L}}(w')} = 0 \ . \tag{5.1.8}$$

□

5.1.2 One or More 2-Encounters with Length Zero

In the binary graph case, we picked a particular primitive pseudo orbit $\bar{\gamma}$ with a single 2-encounter of length zero, assigned a scattering matrix at the encounter vertex, and found that the way in which we assigned scattering coefficients did not affect the contribution $C_{\bar{\gamma}}$. This was because $q^2 = \ell^2$ and every bond used adjacent to the 2-encounter had to be distinct, so all scattering coefficients at the encounter appeared exactly once in $A_{\bar{\gamma}}\bar{A}_{\bar{\gamma}'}$ when pairing $\bar{\gamma}$ with the partner $\bar{\gamma}' \neq \bar{\gamma}$ of the same length. Here, the argument of $A_{\bar{\gamma}}\bar{A}_{\bar{\gamma}'}$ depends on the way in which we assign the

scattering vertex $\sigma^{(v)}$ at the encounter vertex v. So for any choice of primitive pseudo orbit $\bar{\gamma}$, we will average over the possible ways of assigning scattering coefficients at v. Since the sum over primitive pseudo orbit pairs (2.2.47) is finite, we can average over the ways of assigning scattering coefficients at any vertex, then evaluate the sum using the average value of $A_{\bar{\gamma}}\bar{A}_{\bar{\gamma}'}$ for each primitive pseudo orbit pair. Moreover, this result would then be evaluated asymptotically in the limit of large coefficients on large graphs, analogously to theorem 4.3.2. Given an orbit with an encounter of length zero on a large graph, there will be many other orbits with the same structure at different locations on the graph, but with different assignments of the scattering matrix at the encounter. Averaging over the assignments of the scattering matrix at the encounter vertex will therefore not affect the large graph asymptotics, even for a single realization of the scattering matrix assignments on that large graph.

We begin by considering a single 2-encounter of length zero on a q-nary graph. Though there are q choices of incoming and q choices of outgoing bonds at the encounter vertex (see figure 5.1), only two of each of these will be used in the 2-encounter. If we zoom in on the encounter vertex and the adjacent bonds that appear in a primitive pseudo orbit, the structure is the same as in figure 4.6 with $I = J = 1$. In order to enforce the structure of a 2-encounter of length zero, we place constraints on the choices of vertices a, b, c, and d, namely,

$$a \neq b \text{ and } c \neq d. \tag{5.1.9}$$

The product of stability amplitudes for the primitive pseudo orbit pair in example 4.1.1 with a single 2-encounter of length zero, where a figure eight primitive periodic

orbit is broken into two orbits, is given in (4.3.16). Without loss of generality, the index begins at $h = 3$ if $\{\bar{\gamma}, \bar{\gamma}'\}$ is as in example 4.1.2, where two primitive periodic orbits are joined to make a figure eight orbit. Using the scattering matrix (2.2.20),

$$A_{\bar{\gamma}}\bar{A}_{\bar{\gamma}'} = \left(\frac{1}{q}\right)^n \sigma^{(v)}_{d,a}\sigma^{(v)}_{c,b}\bar{\sigma}^{(v)}_{c,a}\bar{\sigma}^{(v)}_{d,b} \tag{5.1.10}$$

$$= \left(\frac{1}{q}\right)^n \mathrm{e}^{2\pi\mathrm{i}(ad+bc-ac-bd)/q} \tag{5.1.11}$$

$$= \left(\frac{1}{q}\right)^n \mathrm{e}^{2\pi\mathrm{i}(a-b)(d-c)/q} \ . \tag{5.1.12}$$

In the other pair of different pseudo orbits considered in the case of a 2-encounter of length zero, example 4.1.2, where two orbits in the pseudo orbit are joined at the encounter vertex to obtain the partner orbit, we saw that the product of stability amplitudes was the same and so will also be given by (5.1.12). For both examples, as in the case of binary graphs, $m_{\bar{\gamma}'} = m_{\bar{\gamma}} \pm 1$, and so $m_{\bar{\gamma}} + m_{\bar{\gamma}'} = 2m_{\bar{\gamma}} \pm 1$, depending on whether the figure eight is in $\bar{\gamma}$ or $\bar{\gamma}'$. Then for a single 2-encounter of length zero on a q-nary graph, we obtain the following average.

Lemma 5.1.2. For a single 2-encounter of length zero on a q-nary graph, the average value of $A_{\bar{\gamma}}\bar{A}_{\bar{\gamma}'}$ for $\bar{\gamma}' \neq \bar{\gamma}$ is

$$\langle A_{\bar{\gamma}}\bar{A}_{\bar{\gamma}'}\rangle = -\frac{1}{q-1}\left(\frac{1}{q}\right)^n \ . \tag{5.1.13}$$

For a diagonal pair $\bar{\gamma}' = \bar{\gamma}$, $|A_{\bar{\gamma}}|^2 = q^{-n}$.

Proof. Using (5.1.12),

$$\langle A_{\bar{\gamma}} \bar{A}_{\bar{\gamma}'} \rangle = \left(\frac{1}{q}\right)^n \frac{\displaystyle\sum_{a,b,c,d=0}^{q-1} \mathrm{e}^{2\pi \mathrm{i}(a-b)(d-c)/q}(1-\delta_{a,b})(1-\delta_{c,d})}{\displaystyle\sum_{a,b,c,d=0}^{q-1}(1-\delta_{a,b})(1-\delta_{c,d})} \tag{5.1.14}$$

$$= \left(\frac{1}{q}\right)^n \frac{-q^3+q^2}{q^4-2q^3+q^2} \tag{5.1.15}$$

$$= -\frac{1}{q-1}\left(\frac{1}{q}\right)^n , \tag{5.1.16}$$

where we enforce the conditions (5.1.9). □

Again, let the set $\hat{\mathcal{P}}^n_{N=N_0}$ denote the set of primitive pseudo orbits of topological length n having N self-intersections, all of which are 2-encounters of length zero.

Lemma 5.1.3. For any primitive pseudo orbit $\bar{\gamma} \in \hat{\mathcal{P}}^n_{N=N_0}$ for $N > 0$, the average contribution of all primitive pseudo orbit pairs $\{\bar{\gamma}, \bar{\gamma}'\}$ to (4.2.3) is

$$C_{\bar{\gamma}} = \left(\frac{q}{q-1}\right)^N \cdot \left(\frac{1}{q}\right)^n . \tag{5.1.17}$$

Proof. As $\bar{\gamma}$ contains N 2-encounters of length zero, index the number of 2-encounters at which $\bar{\gamma}$ is rearranged to obtain a partner pseudo orbit $\bar{\gamma}' \in \mathcal{P}_{\bar{\gamma}}$ by j. Then

$$C_{\bar{\gamma}} = \left(\frac{1}{q}\right)^n \sum_{j=0}^{N} (-1)^{2j} \left(\frac{1}{q-1}\right)^j \binom{N}{j} . \tag{5.1.18}$$

Using the binomial expansion,

$$\sum_{j=0}^{N} \binom{N}{j} x^j = (x+1)^N . \tag{5.1.19}$$

the result follows. □

Note that, in the case of binary graphs where $q = 2$, this result is equivalent to lemma 4.3.5.

5.1.3 A Single ℓ-Encounter of Length Zero with ℓ Distinct Links

Now we consider a single ℓ-encounter in a primitive pseudo orbit pair with distinct links on a q-nary graph; thus, each of the incoming (and outgoing) bonds at the encounter vertex is distinct and the connection diagram can be described as a permutation of the exit vertices from S_ℓ. Given an ℓ-encounter, we find the average of $A_{\bar{\gamma}}\bar{A}_{\bar{\gamma}'}$ when the connection diagram at the encounter is an ℓ-cycle. We claim that this is sufficient to describe partner orbits having connection diagrams associated to any permutation in S_ℓ. For a 3-encounter, if the connection diagram is a 2-cycle, then the pairs of pseudo orbits have the structure already considered for a 2-encounter, and the average was already evaluated in lemma 5.1.2. By induction on the length of the cycles considered, we obtain an average for pairs described by any connection diagram that is a single cycle. We use the disjoint cycle factorization of a permutation in S_ℓ to evaluate the average for pairs with the partner pseudo orbit generated by any permutation $\rho \in S_\ell$.

At an encounter of length zero, the stability amplitude product $A_{\bar{\gamma}}\bar{A}_{\bar{\gamma}'}$ is given in general by

$$A_{\bar{\gamma}}\bar{A}_{\bar{\gamma}'} = \left(\frac{1}{q}\right)^n \left[\omega^{s_1 f_1 + s_2 f_2 + \cdots + s_\ell f_\ell} \overline{\omega}^{s_1 f_{\rho(1)} + s_2 f_{\rho(2)} + \cdots + s_\ell f_{\rho(\ell)}}\right] , \tag{5.1.20}$$

where ρ is a permutation that describes which exit vertices from the encounter follow which entrance vertices to the encounter, as in the connection diagrams introduced

in section 4.1.4. We use the identity permutation e to describe the ordering of exit vertices in $\bar{\gamma}$. We will consider the average when the permutation ρ is a single ℓ-cycle. The scattering coefficients come from the Discrete Fourier Transform matrix (2.5.11), and the value of $A_{\bar{\gamma}}\bar{A}_{\bar{\gamma}'}$ depends on the way that the scattering coefficients are assigned at the encounter vertex. At an ℓ-encounter of length zero the entry vertices $s_1, \ldots, s_\ell$ cannot all be the same (and neither can the exit vertices $f_1, \ldots, f_\ell$); otherwise, the encounter is not of length zero.

Here we derive the average value of the stability amplitude product for primitive pseudo orbit pairs containing a single ℓ-encounter of length zero, where the permutation ρ generating $\bar{\gamma}'$ is an ℓ-cycle.

Lemma 5.1.4. For a single ℓ-encounter of length zero on a q-nary graph and the partners $\bar{\gamma}' \in \mathcal{P}_{\bar{\gamma}}$ of $\bar{\gamma}$ such that $\bar{\gamma}' \neq \bar{\gamma}$, where the permutation ρ generating $\bar{\gamma}'$ is an ℓ-cycle, the average value of $A_{\bar{\gamma}}\bar{A}_{\bar{\gamma}'}$ is

$$\langle A_{\bar{\gamma}}\bar{A}_{\bar{\gamma}'}\rangle = -\frac{1}{q^{\ell-1}-1}\left(\frac{1}{q}\right)^n . \tag{5.1.21}$$

Proof. We find the average value of $A_{\bar{\gamma}}\bar{A}_{\bar{\gamma}'}$ by evaluating

$$\frac{\displaystyle\sum_{j=1}^{\ell}\sum_{s_j,f_j=0}^{q-1}\prod_{j=1}^{\ell}\omega^{s_j(f_j-f_{\rho(j)})}\left(1-\prod_{i=2}^{\ell}\delta_{s_1,s_i}\right)\left(1-\prod_{i=2}^{\ell}\delta_{f_1,f_i}\right)}{\displaystyle\sum_{j=1}^{\ell}\sum_{s_j,f_j=0}^{q-1}\left(1-\prod_{i=2}^{\ell}\delta_{s_1,s_i}\right)\left(1-\prod_{i=2}^{\ell}\delta_{f_1,f_i}\right)} . \tag{5.1.22}$$

The individual sums are

$$\sum_{j=1}^{\ell}\sum_{s_j,f_j=0}^{q-1}\left(1-\prod_{i=2}^{\ell}\delta_{s_1,s_i}\right)\left(1-\prod_{i=2}^{\ell}\delta_{f_1,f_i}\right) = q^2(q^{\ell-1}-1)^2 , \tag{5.1.23}$$

and

$$\sum_{j=1}^{\ell}\sum_{s_j,f_j=0}^{q-1}\prod_{j=1}^{\ell}\omega^{s_j(f_j-f_{\rho(j)})}\left(1-\prod_{i=2}^{\ell}\delta_{s_1,s_i}\right)\left(1-\prod_{i=2}^{\ell}\delta_{f_1,f_i}\right) \tag{5.1.24}$$

$$=\sum_{j=1}^{\ell}\sum_{f_j=0}^{q-1}\left(1-\prod_{i=2}^{\ell}\delta_{f_1,f_i}\right)\left[q^{\ell}\prod_{i=1}^{\ell}\delta_{f_i,f_{\rho(i)}}-q\right] \tag{5.1.25}$$

$$=\sum_{j=1}^{\ell}\sum_{f_j=0}^{q-1}-q\left(1-\prod_{i=2}^{\ell}\delta_{f_1,f_i}\right) \tag{5.1.26}$$

$$=-q^2(q^{\ell-1}-1)\ . \tag{5.1.27}$$

To evaluate the second sum, we note that, as ρ has a single cycle, $\prod_{i=1}^{\ell}\delta_{f_i,f_{\rho(i)}}$ is zero unless all the f_i are equal. As this is not possible, the result follows. □

We now use the disjoint cycle factorization of a permutation to describe the average value of $A_{\bar\gamma}\bar{A}_{\bar\gamma'}$ for any combination of rearrangements of the exit vertices at an ℓ-encounter.

Corollary 5.1.1. For a single ℓ-encounter of length zero on a q-nary graph and the partners $\bar\gamma'\in\mathcal{P}_{\bar\gamma}$ of $\bar\gamma$ such that $\bar\gamma'\neq\bar\gamma$, let ρ be the permutation of the exit vertices that generates $\bar\gamma'$. Let $\rho=\rho_1\rho_2\cdots\rho_m$ be the disjoint cycle decomposition of ρ, where ρ_i is a k_i-cycle and $k_i>1$; we ignore fixed points in the decomposition, as they do not generate any rearrangements at the encounter. Then the average value of $A_{\bar\gamma}\bar{A}_{\bar\gamma'}$ is

$$\langle A_{\bar\gamma}\bar{A}_{\bar\gamma'}\rangle=(-1)^m\left(\frac{1}{q}\right)^n\prod_{i=1}^{m}\frac{1}{q^{k_i-1}-1}\ , \tag{5.1.28}$$

and $|A_{\bar\gamma}|^2=q^{-n}$.

As in Chapter Four, we numerically determined $\langle |a_n|^2 \rangle_k$ by averaging coefficients of the characteristic polynomial over a window of values of k with typically 50 million mean spacings. For $B = 162$, we ended the simulation's run on Baylor's Kodiak high performance computing cluster at 23.75 million mean spacings, as it appeared to have converged very quickly. For $B = 486$, the simulation met its maximum run time on Kodiak at 9.6 million mean spacings.

The variance of the coefficients for the ternary family of graphs with $V = 2 \cdot 3^r$ vertices and $B = 2 \cdot 3^{r+1}$ bonds is shown in figure 5.3 for $r = 1, 2, 3, 4$; it approaches

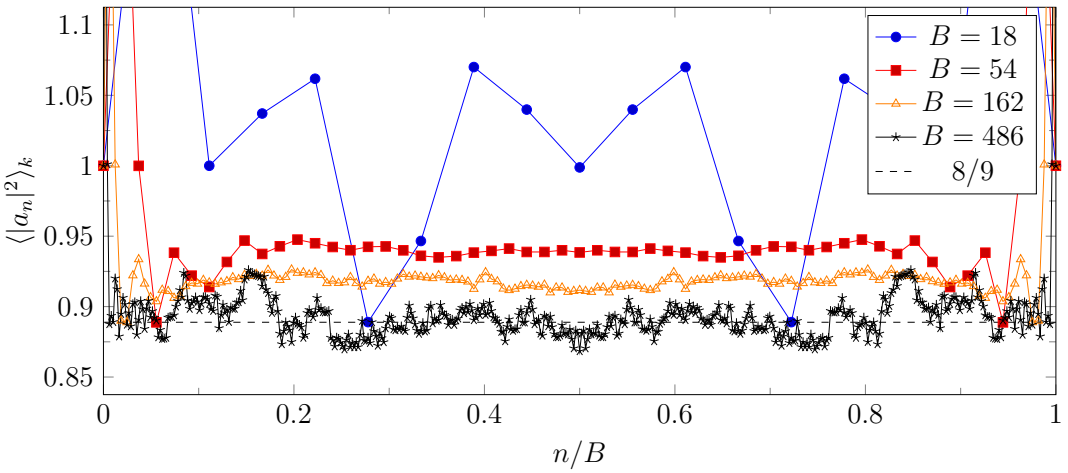

Figure 5.3. Variance of coefficients of the characteristic polynomial for a family of ternary graphs with $p = 2$ averaged over a window of 50,000,000 mean spacings. The plot shows the convergence to the diagonal contribution $\langle |a_n|^2 \rangle_{\text{diag}} = 8/9$.

the diagonal contribution of $8/9$, as r increases. This value is determined by theorem 4.3.2 with $C_{2,3} = 4/3$, as evaluated in example 3.4.3. The variance of the coefficients for the ternary family of graphs with $V = 5 \cdot 3^r$ vertices and $B = 5 \cdot 3^{r+1}$ bonds is

shown in figure 5.4 for $r = 0, 1, 2$; it approaches the diagonal contribution of 164/243, as r increases. This value is determined by theorem 4.3.2 with $C_{5,3} = 82/81$, as evaluated in example 3.4.4.

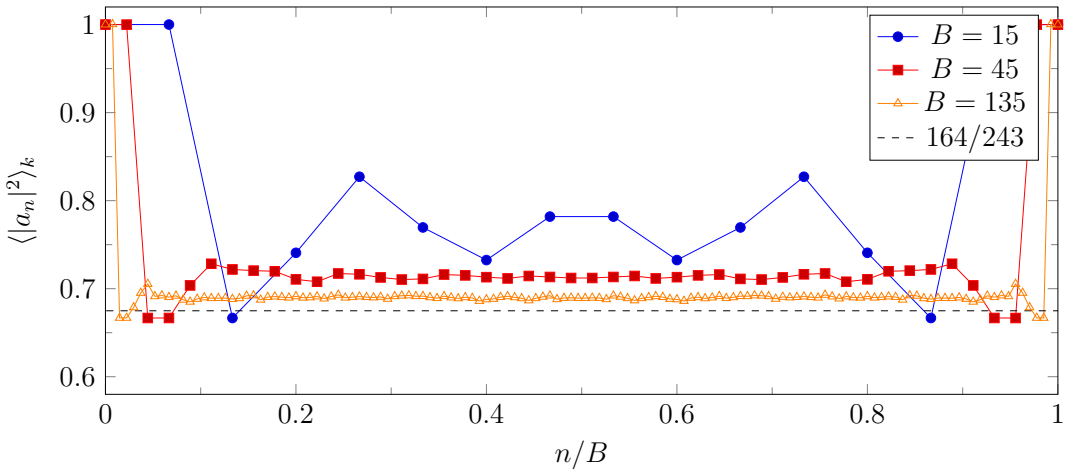

Figure 5.4. Variance of coefficients of the characteristic polynomial for a family of ternary graphs with $p = 5$ averaged over a window of 50,000,000 mean spacings. The plot shows the convergence to the diagonal contribution $\langle |a_n|^2 \rangle_{\text{diag}} = 164/243$.

5.3 Conclusions and Future Work

It seems that we should be able to obtain the full range of results for q-nary graphs that mirror those for binary graphs. However, these results will be for the variance of the coefficients averaged over the assignment of the vertex scattering matrices. As discussed, this additional averaging will not effect the asymptotics of the variance of the coefficients in the large coefficient (equivalently long pseudo orbit) and large graph limit.

We can already show that a primitive pseudo orbit $\bar{\gamma}$ with a single self-intersection of positive length and its partners have a net zero contribution. Moreover, we can

determine the contribution $C_{\bar{\gamma}}$ for a primitive pseudo orbit $\bar{\gamma}$ with multiple self-intersections, so long as each is a 2-encounter of length zero; this result agrees with the similar result for binary graphs. We know how to evaluate the average of the product of stability amplitudes for a primitive pseudo orbit containing a single ℓ-encounter. After all types of multiple encounter scenarios are evaluated, we believe the variance formula for binary graphs (4.3.26) will generalize to a sum that requires determining the size of the set of primitive pseudo orbits without self-intersections, and the sizes of sets of primitive pseudo orbits containing only ℓ-encounters of length zero for $\ell \leq q$. Lastly, our analysis thus far and our numerics for ternary graphs point to an asymptotic result,

$$\lim_{n\to\infty} \langle |a_n|^2 \rangle_k = C_{p,q} \cdot \frac{q-1}{q} \ , \tag{5.3.1}$$

in the semiclassical limit of large graphs, which is the diagonal contribution.

APPENDICES

APPENDIX A

A New Vandermonde Identity

Here we consider an alternative calculation of $C_{\bar{\gamma}}$ for primitive pseudo orbits that have only 2-encounters of any length. The result relies on a Vandermonde-type identity that we have not been able to find elsewhere in the literature.

Consider a primitive pseudo orbit $\bar{\gamma}$. If j is the number of 2-encounters at which the connections between incoming and outgoing links are reordered in the partner $\bar{\gamma}'$, then $(-1)^{m_{\bar{\gamma}}+m_{\bar{\gamma}'}} = (-1)^j$ as in (4.3.22). We showed previously with (4.3.14), (4.3.15), (4.3.17), (4.3.18), that for a pair of primitive pseudo orbits $\{\bar{\gamma}, \bar{\gamma}'\}$ with a single 2-encounter of positive length, the product of scattering amplitudes along an encounter is the same for $\bar{\gamma}$ and $\bar{\gamma}'$. For a pair of primitive pseudo orbits $\{\bar{\gamma}, \bar{\gamma}'\}$ with a single 2-encounter of length zero, the product of scattering amplitudes at the encounter vertex v is $-1/4$, (4.3.19), when $\bar{\gamma}' \neq \bar{\gamma}$. Thus, for primitive pseudo orbit pairs with multiple 2-encounters, each self-intersection of length zero at which the links are reordered in $\bar{\gamma}'$ will contribute a factor of -1 to $A_{\bar{\gamma}}\bar{A}_{\bar{\gamma}'}$. Let the number of 2-encounters of length zero at which the connections between incoming and outgoing links are reordered in the partner $\bar{\gamma}'$ be k; then,

$$A_{\bar{\gamma}}\bar{A}_{\bar{\gamma}'} = (-1)^k \left(\frac{1}{2}\right)^n \quad . \tag{A.0.1}$$

Now we compute $C_{\bar{\gamma}}$ in the case that $\bar{\gamma}$ has $N > 0$ self-intersections, each of which is a 2-encounter, with N_0 of these of length zero. Note that N_0 can be zero and

at most N. We will index the number of self-intersections at which incoming and outgoing link connections are reordered in $\bar{\gamma}'$ by j, and index the number of these self-intersections of length zero by k; note $k \leq j$. So for a fixed $\bar{\gamma}$ with N 2-encounters and N_0 2-encounters of length zero, the contribution to (4.2.3) is

$$C_{\bar{\gamma}} = \sum_{\substack{\{\bar{\gamma},\bar{\gamma}'\} \\ \bar{\gamma}' \in \mathcal{P}_{\bar{\gamma}}}} (-1)^{m_{\bar{\gamma}}+m_{\bar{\gamma}'}} A_{\bar{\gamma}} \bar{A}_{\bar{\gamma}'} \tag{A.0.2}$$

$$= \left(\frac{1}{2}\right)^n \sum_{j=0}^{N} (-1)^j \sum_{k=0}^{j} (-1)^k \binom{N_0}{k} \binom{N-N_0}{j-k} \tag{A.0.3}$$

$$= \left(\frac{1}{2}\right)^n \cdot \begin{cases} 2^N & \text{when } N_0 = N \\ \\ 0 & \text{when } N_0 < N \ . \end{cases} \tag{A.0.4}$$

Note that the inner sum in (A.0.3) is an alternating Vandermonde sum. We prove (A.0.4) using the following lemma.

Lemma A.0.1.

$$\sum_{j=0}^{N} \sum_{k=0}^{j} (-1)^{j+k} \binom{N_0}{k} \binom{N-N_0}{j-k} = \begin{cases} 2^N & \text{when } N_0 = N \\ \\ 0 & \text{when } N_0 < N \end{cases} . \tag{A.0.5}$$

Proof. If $N_0 = N$, then by the identity (4.3.25),

$$\sum_{j=0}^{N} \sum_{k=0}^{j} (-1)^{j+k} \binom{N}{k} \delta_{j-k,0} = \sum_{j=0}^{N} \binom{N}{j} = 2^N \ . \tag{A.0.6}$$

If $N_0 < N$, then summing over the j,k-triangle horizontally rather than vertically, and re-indexing the inner sum where $i = j - k$, we obtain

$$\sum_{j=0}^{N}\sum_{k=0}^{j}(-1)^{j+k}\binom{N_0}{k}\binom{N-N_0}{j-k} = \sum_{k=0}^{N}\sum_{j=k}^{N}(-1)^{j+k}\binom{N_0}{k}\binom{N-N_0}{j-k} \tag{A.0.7}$$

$$= \sum_{k=0}^{N}\binom{N_0}{k}\sum_{i=0}^{N-k}(-1)^{i}\binom{N-N_0}{i}\,. \tag{A.0.8}$$

Notice that when $k > N_0$, $\binom{N_0}{k} = 0$, so we reduce the upper limit of k to N_0. Similarly, the summation over i should range from zero up to a fixed $N-k$ for fixed k, but $\binom{N-N_0}{i} = 0$ if $i > N-N_0$. Thus, the contribution to the inner sum is zero if $i > N-k$ where $k < N_0$. Hence,

$$\sum_{j=0}^{N}\sum_{k=0}^{j}(-1)^{j+k}\binom{N_0}{k}\binom{N-N_0}{j-k} = \sum_{k=0}^{N_0}\binom{N_0}{k}\sum_{i=0}^{N-N_0}(-1)^{i}\binom{N-N_0}{i}\,. \tag{A.0.9}$$

However, the sum over i is identically zero [111], and the lemma holds. □

APPENDIX B

The Primitive Pseudo Orbits for the Binary Graph with Eight Vertices

For the binary graph with $V = 8$ vertices and $B = 16$ bonds, shown in figure 1.9, the variance of the coefficients of the graph's characteristic polynomial were given in table 4.3. Here we explain how the sizes of the relevant sets were determined.

Recall that as the number of bonds is precisely a power of two (here $p = 1$), the primitive periodic orbits of length n correspond uniquely to binary Lyndon words of length n. Moreover, the primitive pseudo orbits of length n correspond uniquely to the binary words of length n that have a strictly decreasing Lyndon decomposition. Table B.1 lists the sizes of all sets of primitive pseudo orbits of the lengths corresponding to the first half of the characteristic polynomial's coefficients. Note that, $\mathcal{P}_0^0 = \{\bar{0}\}$, the empty pseudo orbit.

Table B.1. For a binary graph with $V = 8$ vertices and $B = 16$ bonds, the sizes of the sets of primitive pseudo orbits for $0 \leq n \leq 8$ are given.

n	$PPO_2(n)$	$\lvert\mathcal{P}_0^n\rvert$	$\lvert\hat{\mathcal{P}}^n_{N=N_0=1}\rvert$	$\lvert\hat{\mathcal{P}}^n_{N=N_0=2}\rvert$	$\lvert\{\bar{\gamma} : B_{\bar{\gamma}} = n, C_{\bar{\gamma}} = 0\}\rvert$
0	1	1	0	0	0
1	2	2	0	0	0
2	2	2	0	0	0
3	4	4	0	0	0
4	8	8	0	0	0
5	16	8	8	0	0
6	32	8	20	0	4
7	64	16	16	8	24
8	128	16	16	24	72

For the non-empty sets of orbits in table B.1, the words with strictly decreasing Lyndon decomposition corresponding to the primitive pseudo orbits are listed.

$$\mathcal{P}_0^1 = \{(0),\ (1)\} \tag{B.0.1}$$

$$\mathcal{P}_0^2 = \{(01),\ (1)(0)\} \tag{B.0.2}$$

$$\mathcal{P}_0^3 = \{(001),\ (01)(0),\ (011),\ (1)(01)\} \tag{B.0.3}$$

$$\mathcal{P}_0^4 = \{(0001),\ (001)(0),\ (0011),\ (011)(0),\ (0111),\ (1)(001),\ (1)(01)(0),\ (1)(011)\} \tag{B.0.4}$$

$$\mathcal{P}_0^5 = \{(00011),\ (0011)(0),\ (00111),\ (0111)(0),\ (1)(0001),\ (1)(001)(0),\ (1)(0011),\ (1)(011)(0)\} \tag{B.0.5}$$

$$\mathcal{P}_{N=N_0=1}^5 = \{(00001),\ (0001)(0),\ (00101),\ (01)(001)\ (01011),\ (011)(01),\ (01111),\ (1)(0111)\} \tag{B.0.6}$$

$$\mathcal{P}_0^6 = \{(000111),\ (001011),\ (001101),\ (1)(00011),\ (00111)(0),\ (01)(0011),\ (1)(0011)(0),\ (011)(001)\} \tag{B.0.7}$$

$$\mathcal{P}_{N=N_0=1}^6 = \{(000011),\ (000101),\ (001111),\ (010111),\ (1)(00001),\ (00011)(0),\ (00101)(0),\ (1)(00101),\ (1)(00111),\ (01011)(0),\ (1)(01011),\ (01111)(0),\ (01)(0001),\ (0111)(01),\ (1)(0001)(0),\ (1)(0111)(0),\ (01)(001)(0),\ (1)(01)(001),\ (011)(01)(0),\ (1)(011)(01)\} \tag{B.0.8}$$

$$\{\bar{\gamma} : B_{\bar{\gamma}} = 6, C_{\bar{\gamma}} = 0\} = \{(000001),\ (00001)(0),\ (011111),\ (1)(01111)\} \tag{B.0.9}$$

$$\mathcal{P}_0^7 = \{(0001011),\ (0001101),\ (001011)(0),\ (0010111),$$
$$(001101)(0),\ (0011101),\ (01)(00011),\ (01)(0011)(0),$$
$$(01)(00111),\ (011)(0001),\ (011)(001)(0),\ (0111)(001),$$
$$(1)(001011),\ (1)(001101),\ (1)(01)(0011),\ (1)(011)(001)\} \quad \text{(B.0.10)}$$

$$\mathcal{P}_{N=N_0=1}^7 = \{(0000111),\ (000111)(0),\ (0001111),\ (001111)(0),$$
$$(010111)(0),\ (0111)(01)(0),\ (1)(000011),\ (1)(000101),$$
$$(1)(00011)(0),\ (1)(000111),\ (1)(00101)(0),\ (1)(00111)(0),$$
$$(1)(01)(0001),\ (1)(01)(001)(0),\ (1)(01011)(0),$$
$$(1)(011)(01)(0)\} \quad \text{(B.0.11)}$$

$$\mathcal{P}_{N=N_0=2}^7 = \{(0000101), (000101)(0),\ (01)(00001),\ (01)(0001)(0),$$
$$(0101111),\ (01111)(01),\ (1)(010111),\ (1)(0111)(01)\} \quad \text{(B.0.12)}$$

$$\{\bar{\gamma} : B_{\bar{\gamma}} = 7, C_{\bar{\gamma}} = 0\} = \{(0000001),\ (000001)(0),\ (0000011),\ (000011)(0),$$
$$(0001001),\ (001)(0001),\ (001)(0011),\ (0010101),$$
$$(0011)(001),\ (0011011),\ (0011111),\ (01)(00101),$$
$$(0101011),\ (01011)(01),\ (011)(0011),\ (0110111),$$
$$(0111)(011),\ (011111)(0),\ (0111111),\ (1)(000001),$$
$$(1)(00001)(0),\ (1)(001111),\ (1)(01111)(0),$$
$$(1)(011111)\} \quad \text{(B.0.13)}$$

$$\mathcal{P}_0^8 = \{(00010111),\ (00011101),\ (0010111)(0),\ (0011101)(0),$$
$$(01)(000111),\ (01)(00111)(0),\ (0111)(0001),\ (0111)(001)(0),$$
$$(1)(0001011),\ (1)(0001101),\ (1)(001011)(0),\ (1)(001101)(0),$$
$$(1)(01)(00011),\ (1)(01)(0011)(0),\ (1)(011)(0001),$$
$$(1)(011)(001)(0)\} \tag{B.0.14}$$

$$\mathcal{P}_{N=N_0=1}^8 = \{(00001011),\ (00001101),\ (0001011)(0),\ (0001101)(0),$$
$$(00101111),\ (00111101),\ (01)(000011),\ (01)(00011)(0),$$
$$(01)(001111),\ (011)(00001),\ (011)(0001)(0),\ (01111)(001),$$
$$(1)(0010111),\ (1)(0011101),\ (1)(01)(00111),$$
$$(1)(0111)(001)\} \tag{B.0.15}$$

$$\mathcal{P}_{N=N_0=2}^8 = \{(00001111),\ (00010011),\ (00011001),\ (0001111)(0),$$
$$(001)(00011),\ (00101101),\ (0011)(0001),\ (00110111),$$
$$(00111011),\ (01011)(001),\ (0101111)(0),\ (011)(00101),$$
$$(011)(00111),\ (011)(01)(001),\ (0111)(0011),\ (01111)(01)(0),$$
$$(1)(0000101),\ (1)(0000111),\ (1)(000101)(0),\ (1)(000111)(0),$$
$$(1)(01)(00001),\ (1)(01)(0001)(0),\ (1)(010111)(0),$$
$$(1)(0111)(01)(0)\} \tag{B.0.16}$$

$$\{\bar{\gamma} : B_{\bar{\gamma}} = 8, C_{\bar{\gamma}} = 0\} = \{(00000001),\ (0000001)(0),\ (00000011),\ (00000101),$$
$$(0000011)(0),\ (00000111),\ (00001001),\ (0000101)(0),$$
$$(0000111)(0),\ (0001001)(0),\ (00010101),\ (00011011),$$
$$(00011111),\ (001)(00001),\ (001)(0001)(0),\ (00100101),$$
$$(0010011)(0),\ (00100111),\ (00101)(001),\ (0010101)(0),$$
$$(00101011),\ (0011)(001)(0),\ (00110101),\ (0011011)(0),$$
$$(00111)(001),\ (0011111)(0),\ (00111111),\ (01)(000001),$$
$$(01)(00001)(0),\ (01)(000101),\ (01)(00101)(0),$$
$$(01)(001011),\ (01)(001101),\ (0101011)(0),\ (01010111),$$
$$(01011)(01)(0),\ (01011011),\ (010111)(01),\ (01011111),$$
$$(011)(00011),\ (011)(0011)(0),\ (011)(01011),\ (0110111)(0),$$
$$(01101111),\ (0111)(011)(0),\ (01111)(011),\ (011111)(01),$$
$$(0111111)(0),\ (01111111),\ (1)(0000001),\ (1)(000001)(0),$$
$$(1)(0000011),\ (1)(000011)(0),\ (1)(0001001),\ (1)(0001111),$$
$$(1)(001)(0001),\ (1)(0010011),\ (1)(0010101),\ (1)(0011)(001),$$
$$(1)(0011011),\ (1)(001111)(0),\ (1)(0011111),\ (1)(01)(00101),$$
$$(1)(0101011),\ (1)(01011)(01),\ (1)(0101111),\ (1)(011)(0011),$$
$$(1)(0110111),\ (1)(0111)(011,\ (1)(01111)(01),$$
$$(1)(011111)(0),\ (1)(0111111)\} \qquad \text{(B.0.17)}$$

APPENDIX C

The Primitive Pseudo Orbits for the Binary Graph with Six Vertices

For the binary graph with $V = 6$ vertices and $B = 12$ bonds in figure C.1, the variance of the coefficients of the graph's characteristic polynomial were given in table 4.4. Here we explain how the sizes of the relevant sets were determined.

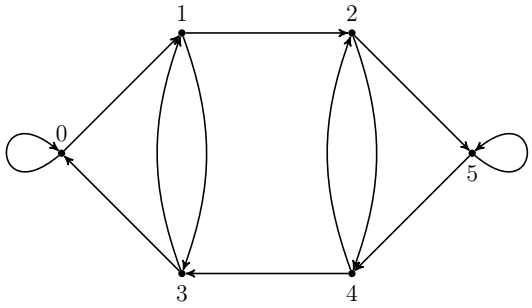

Figure C.1. The binary graph with $V = 3 \cdot 2$ vertices and $B = 3 \cdot 2^2$ bonds

As the number of bonds $B = 3 \cdot 2^2$ has a factor of three, the primitive periodic orbits of length n are not in bijection with the set of binary Lyndon words of length n. Here, we use words over the vertex label alphabet $\mathcal{V} = \{0, 1, 2, 3, 4, 5\}$ to represent a closed path and rotations of the word represent closed paths that belong to the same periodic orbit. A word of length n corresponds to a closed path of length n. For example, the word 013 labels the path of length of three that traverses vertices 0, 1, 3, and returns to 0. We use parentheses to mark differing periodic orbits in the primitive pseudo orbit. Table C.1 lists the sizes of all sets of primitive pseudo orbits of the lengths corresponding to the first half of the characteristic polynomial's

coefficients. As $C_{3,2} = 5/4$, the number of primitive pseudo orbits of length n is $PPO_{3,2}(n) = 5 \cdot 2^{n-3}$ for $n > 3$, by theorem 3.2.2. Note that, $\mathcal{P}_0^0 = \{\bar{0}\}$, the empty pseudo orbit.

Table C.1. For a binary graph with $V = 6$ vertices and $B = 12$ bonds, the sizes of the sets of primitive pseudo orbits for $0 \leq n \leq 6$ are given.

n	$PPO_2(n)$	$\lvert\mathcal{P}_0^n\rvert$	$\lvert\hat{\mathcal{P}}_{N=N_0=1}^n\rvert$	$\lvert\{\bar{\gamma} : B_{\bar{\gamma}} = n, C_{\bar{\gamma}} = 0\}\rvert$
0	1	1	0	0
1	2	2	0	0
2	3	3	0	0
3	6	6	0	0
4	10	6	4	0
5	20	8	4	8
6	40	8	8	24

For the non-empty sets of orbits in table C.1, the words corresponding to the primitive pseudo orbits are listed.

$$\mathcal{P}_0^1 = \{(0),\ (5)\} \tag{C.0.1}$$

$$\mathcal{P}_0^2 = \{(13),\ (24),\ (5)(0)\} \tag{C.0.2}$$

$$\mathcal{P}_0^3 = \{(013),\ (13)(0),\ (24)(0),\ (254),\ (5)(13),\ (5)(24)\} \tag{C.0.3}$$

$$\mathcal{P}_0^4 = \{(1243),\ (24)(13),\ (254)(0),\ (5)(013),\ (5)(13)(0),\ (5)(24)(0)\} \tag{C.0.4}$$

$$\{\bar{\gamma} : B_{\bar{\gamma}} = 4, C_{\bar{\gamma}} = 0\} = \{(0013),\ (013)(0),\ (2554),\ (5)(254)\} \tag{C.0.5}$$

$$\begin{aligned}\mathcal{P}_0^5 = \{&(01243),\ (12543),\ (1243)(0),\ (5)(1243),\\ &(24)(013),\ (254)(13),\ (24)(13)(0),\ (5)(24)(13)\}\end{aligned} \tag{C.0.6}$$

$$\mathcal{P}_{N=N_0=1}^5 = \{(5)(0013),\ (2554)(0),\ (5)(013)(0),\ (5)(254)(0)\} \tag{C.0.7}$$

$$\{\bar{\gamma} : B_{\bar{\gamma}} = 5, C_{\bar{\gamma}} = 0\} = \{(00013),\ (0013)(0),\ (01313),\ (13)(013),$$
$$(24254),\ (254)(24),\ (25554),\ (5)(2554)\} \tag{C.0.8}$$

$$\mathcal{P}_0^6 = \{(012543),\ (12543)(0),\ (254)(013),\ (254)(13)(0),$$
$$(5)(01243),\ (5)(1243)(0),\ (5)(24)(013),\ (5)(24)(13)(0)\} \tag{C.0.9}$$

$$\mathcal{P}_{N=N_0=1}^6 = \{(001243),\ (01243)(0),\ (24)(013)(0),\ (24)(0013),$$
$$(2554)(13),\ (5)(12543),\ (5)(254)(24),\ (554312),\} \tag{C.0.10}$$

$$\{\bar{\gamma} : B_{\bar{\gamma}} = 6, C_{\bar{\gamma}} = 0\} = \{(000013),\ (00013)(0),\ (001313),\ (01313)(0)$$
$$(124243),\ (124313),\ (13)(0013),\ (13)(013)(0)$$
$$(13)(1243),\ (24)(1243),\ (24254)(0),\ (254)(24)(0)$$
$$(2554)(24),\ (25554)(0),\ (5)(00013),\ (5)(0013)(0)$$
$$(5)(01313),\ (5)(13)(013),\ (5)(24254),\ (5)(254)(24)$$
$$(5)(2554)(0),\ (5)(25554),\ (554242),\ (555542)\} \tag{C.0.11}$$

BIBLIOGRAPHY

[1] Appel, K., & Haken, W. (1976). Every planar map is four colorable. *Bulletin of the American Mathematical Society*, *82*, 711–712.

[2] Aviram, A., & Ratner, M. A. (Eds.). (1998). Molecular electronics: Science and technology, Humacao, Puerto Rico: New York: New York Academy of Sciences, *852*.

[3] Avishai, Y., Hatsugai, Y., & Kohmoto, M. (1993). Localization problem of a two-dimensional lattice in a random magnetic-field. *Physical review. B, Condensed matter*, *47*, 9561–9565.

[4] Ball, W. W. R., & Coxeter, H. S. M. (1974). *Mathematical recreations & essays* (12th ed.). Buffalo: University of Toronto Press.

[5] Band, R., Harrison, J. M., & Joyner, C. H. (2012). Finite pseudo orbit expansions for spectral quantities of quantum graphs. *Journal of Physics A: Mathematical and Theoretical*, *45*, 325204.

[6] Band, R., Harrison, J. M., & Sepanski, M. (2019). Lyndon word decompositions and pseudo orbits on q-nary graphs. *Journal of Mathematical Analysis and Applications*, *470*, 135–144.

[7] Bandeira, N., Pham, V., Pevzner, P., Arnott, D., & Lill, J. (2008). Automated de novo protein sequencing of monoclonal antibodies. *Nature biotechnology*, *26*.

[8] Barba, J. C., Finkel, F., González-López, A., & Rodríguez, M. A. (2008). Polychronakos-Frahm spin chain of BC_N type and the Berry-Tabor conjecture. *Physical review. B, Condensed matter and materials physics*, *77*, 214422.

[9] Barra, F., & Gaspard, P. (2001). Classical dynamics on graphs. *Physical review. E, Statistical, nonlinear, and soft matter physics*, *63*, 066215.

[10] Berg, B. A., Markum, H., & Pullirsch, R. (1999). Quantum chaos in compact lattice QED. *Physical Review. D*, *59*, 097504.

[11] Berkolaiko, G. (2017). An elementary introduction to quantum graphs. *700*, 41–72.

[12] Berkolaiko, G., Bogomolny, E. B., & Keating, J. P. (2001). Star graphs and Šeba billiards. *Journal of Physics A: Mathematical and General*, *34*, 335.

[13] Berkolaiko, G., & Keating, J. P. (1999). Two-point spectral correlations for star graphs. *Journal of Physics A: Mathematical and General*, *32*, 7827–7841.

[14] Berkolaiko, G., Keating, J. P., & Smilansky, U. (2007). Quantum ergodicity for graphs related to interval maps. *Communications in Mathematical Physics*, *273*, 137–159.

[15] Berkolaiko, G., Keating, J. P., & Winn, B. (2003). Intermediate wave function statistics. *Physical Review Letters*, *91*, 134103.

[16] Berkolaiko, G., Keating, J. P., & Winn, B. (2004). No quantum ergodicity for star graphs. *Communications in Mathematical Physics*, *250*, 259–285.

[17] Berkolaiko, G., & Kuchment, P. (2012). Dependence of the spectrum of a quantum graph on vertex conditions and edge lengths. In A. H. Barnett, C. S. Gordon, P. A. Perry, & A. Uribe (Eds.), *Spectral Geometry: Proceedings of symposia in pure mathematics* (Vol. 84).

[18] Berkolaiko, G., & Kuchment, P. (2013). *Introduction to quantum graphs*. Mathematical Surveys and Monographs. Providence, RI: American Mathematical Society.

[19] Berkolaiko, G., Schanz, H., & Whitney, R. S. (2002). Leading off-diagonal correction to the form factor of large graphs. *Physical Review Letters*, *88*, 104101.

[20] Berkolaiko, G., Schanz, H., & Whitney, R. S. (2003). Form factor for a family of quantum graphs: An expansion to third order. *Journal of Physics A: Mathematical and General*, *36*, 8373–8392.

[21] Berry, M. V. (1985). Semiclassical theory of spectral rigidity. *Proceedings of the Royal Society of London. Series A, Mathematical and Physical Sciences*, *400*, 229–251.

[22] Berry, M. V., & Tabor, M. (1977). Level clustering in the regular spectrum. *Proceedings of the Royal Society of London. Series A, Mathematical and Physical Sciences*, *356*, 375–394.

[23] Bièvre, S. (2000). Quantum chaos: A brief first visit.

[24] Birkhoff, G. (1946). Tres observaciones sobre el algebra lineal. *Universidad Nacional de Tucumán: Revista Matemáticas y Física Teórica*, *5*, 147–151.

[25] Bohigas, O., Giannoni, M. J., Ozorio De Almeida, A. M., & Schmit, C. (1995). Chaotic dynamics and the GOE-GUE transition. *Nonlinearity*, *8*, 203–221.

[26] Bohigas, O., Giannoni, M. J., & Schmit, C. (1984). Characterization of chaotic quantum spectra and universality of level fluctuation laws. *Physical Review Letters*, *52*, 1–4.

[27] Bolte, J., & Harrison, J. (2003a). Spectral statistics for the Dirac operator on graphs. *Journal of Physics A: Mathematical and General*, *36*, 2747–2769.

[28] Bolte, J., & Harrison, J. (2003b). The spin contribution to the form factor of quantum graphs. *Journal of Physics A: Mathematical and General*, *36*, L433–L440.

[29] Braun, P., & Haake, F. (2010). Level statistics in arithmetical and pseudo-arithmetical chaos. *Journal of Physics A: Mathematical and Theoretical*, *43*, 262001.

[30] Carini, J., Londergan, J., & Murdock, D. (1997a). Bound states in waveguides and bent quantum wires. I. Applications to waveguide systems. *Physical review. B, Condensed matter and materials physics*, *55*, 9842–9851.

[31] Carini, J., Londergan, J., & Murdock, D. (1997b). Bound states in waveguides and bent quantum wires. II. electrons in quantum wires. *Physical review. B, Condensed matter and materials physics*, *55*, 9852–9859.

[32] Carlson, R. (1999). Inverse eigenvalue problems on directed graphs. *Transactions of the American Mathematical Society*, *351*, 4069–4088.

[33] Chakraborty, A., Dutta, T., Mondal, S., & Nath, A. (2018). Application of graph theory in social media. *International Journal of Computer Sciences and Engineering*, *6*, 722–729.

[34] Chen, K. T., Fox, R. H., & Lyndon, R. C. (1958). Free differential calculus, IV. The quotient groups of the lower central series. *Annals of Mathematics*, *68*, 81–95.

[35] Cheon, T., Exner, P., & Turek, O. (2010). Tripartite connection condition for a quantum graph vertex. *Physics Letters A*, *375*, 113–118.

[36] Clemente, F., Martins, F., & Mendes, R. (2016). *Social network analysis applied to team sports analysis*. Cham; New York: Springer.

[37] Compeau, P. E. C., Pevzner, P. A., & Tesler, G. (2011). Why are de Bruijn graphs useful for genome assembly? *Nature biotechnology*, *29*, 987–991.

[38] Datta, S. (1999). *Electronic transport in mesoscopic systems*. Cambridge: Cambridge University Press.

[39] Davis, P. J. (1979). *Circulant matrices*. New York, NY: Wiley.

[40] de Bruijn, N. G. (1946). A combinatorial problem. *Koninklijke Nederlandse Akademie V. Wetenschappen*, *49*, 758–764.

[41] Deo, N. (2016). *Graph theory with applications to engineering & computer science*. Mineola, New York: Dover Publications, Inc.

[42] Diestel, R. (2017). *Graph theory*. Berlin, Germany: Springer.

[43] Duval, J. P. (1983). Factorizing words over an ordered alphabet. *Journal of Algorithms*, *4*, 363–381.

[44] Dyson, F. (1962a). A Brownian-motion model for the eigenvalues of a random matrix. *Journal of Mathematical Physics*, *3*, 1191–1198.

[45] Dyson, F. (1962b). Statistical theory of the energy levels of complex systems I. *Journal of Mathematical Physics*, *3*, 140–156.

[46] Dyson, F. (1962c). Statistical theory of the energy levels of complex systems II. *Journal of Mathematical Physics*, *3*, 157–165.

[47] Dyson, F. (1962d). Statistical theory of the energy levels of complex systems III. *Journal of Mathematical Physics*, *3*, 166–175.

[48] Dyson, F. (1962e). The threefold way. Algebraic structure of symmetry groups and ensembles in quantum mechanics. *Journal of Mathematical Physics*, *3*, 1199–1215.

[49] Esposti, M. D., O'Keefe, S., & Winn, B. (2005). Asemi-classical study of the casatiprosen triangle map. *Nonlinearity*, *18*, 1073–1094.

[50] Euler, L. (1741). Solutio problematis ad geometriam situs pertinentis [The solution of a problem relating to the geometry of position], *8*, 128–140.

[51] Euler, L. (1956). The seven bridges of Königsberg. In J. Newman (Ed.), *The world of mathematics* (Vol. 1, pp. 573–580). New York: Simon & Schuster.

[52] Exner, P., & Šeba, P. (1990). Trapping modes in a curved electromagnetic waveguide with perfectly conducting walls. *Physics Letters A*, *144*, 347–350.

[53] Faal, H. T. (2019a). A multiset version of determinants and the coin arrangements lemma. *Theoretical Computer Science*, *793*, 36–43.

[54] Faal, H. T. (2019b). A multiset version of even-odd permutations identity. *International Journal of Foundations of Computer Science*, *30*, 683–691.

[55] Forrester, P. J., Snaith, N. C., & Verbaarschot, J. J. M. (2003). Development in random matrix theory. *Journal of Physics A: Mathematical and Theoretical*, *36*, R1–R10.

[56] Fulling, S. A., Kuchment, P., & Wilson, J. H. (2007). Index theorems for quantum graphs. *Journal of Physics A: Mathematical and Theoretical*, *40*, 14165–14180.

[57] Gamburd, A. (2003). Eigenvalue spacings for quantized cat maps. *Journal of Physics A: Mathematical and Theoretical*, *36*, 3487–3499.

[58] García-Planas, M. I., & Magret, M. (2015). Eigenvalues and eigenvectors of monomial matrices. In *Proceedings of the XXIV congress on differential equations and applications* (pp. 963–966).

[59] Gnutzmann, S., & Altland, A. (2004). Universal spectral statistics in quantum graphs. *Physical Review Letters*, *93*, 194101.

[60] Gnutzmann, S., Keating, J. P., & Piotet, F. (2010). Eigenfunction statistics on quantum graphs. *Annals of Physics*, *352*, 2595–2640.

[61] Gnutzmann, S., & Smilansky, U. (2006). Quantum graphs: Applications to quantum chaos and universal spectral statistics. *Advances in Physics*, *55*, 527–625.

[62] Grabherr, M. G., Haas, B. J., Yassour, M., Levin, J. Z., Thompson, D. A., Amit, I., ... Regev, A. (2011). Full-length transcriptome assembly from RNA-seq data without a reference genome. *Nature Biotechnology*, *29*, 644–654.

[63] Gutzwiller, M. (1967). Phase-integral approximation in momentum space and the bound states of an atom. *Journal of Mathematical Physics*, *8*, 1979–2000.

[64] Gutzwiller, M. (1969). Phase-integral approximation in momentum space and the bound states of an atom. II. *Journal of Mathematical Physics*, *10*, 1004–1020.

[65] Gutzwiller, M. (1970). Energy spectrum according to classical mechanics. *Journal of Mathematical Physics*, *11*, 1791–1806.

[66] Gutzwiller, M. (1971). Periodic orbits and classical quantization conditions. *Journal of Mathematical Physics*, *12*, 343–358.

[67] Gutzwiller, M. (1992). Quantum chaos. *Scientific American*, *266*, 78–85.

[68] Haake, F. (2010). *Quantum signatures of chaos*. Heidelberg, Germany: Springer.

[69] Hannabuss, K. (1997). *An introduction to quantum theory*. New York: Oxford University Press, Inc.

[70] Harary, F. (1969). *Graph theory*. Reading, Massachusetts: Addison-Wesley.

[71] Harrison, J. M., Smilansky, U., & Winn, B. (2007). Quantum graphs where back-scattering is prohibited. *Journal of Physics A: Mathematical and Theoretical*, 14181–14193.

[72] Heusler, S., Müller, S., Altland, A., Braun, P., & Haake, F. (2007). Periodic-orbit theory of level correlations. *Physical Review Letters*, *98*, 044103.

[73] Hornan, J. (1993). Linus C. Pauling: Stubbornly ahead of his time. *Scientific American*, *268*, 36, 40.

[74] Hugenschmidt, C., Burdette, J., Morgan, A., Williamson, J., Kritchevsky, S., & Laurienti, P. (2014). Graph theory analysis of functional brain networks and mobility disability in older adults. *Journals of Gerontology Series A: Biomedical Sciences and Medical Sciences*, *69*, 1399–1406.

[75] Keating, J. P., Marklof, J., & Winn, B. (2003). Value distribution of the eigenfunctions and spectral determinants of quantum star graphs. *Communications in Mathematical Physics*, *241*, 421–452.

[76] Klingsberg, P. (n.d.). *A formula for the sign of a permutation*. Retrieved from http://people.sju.edu/~pklingsb/signumform.pdf

[77] Kostrykin, V., & Schrader, R. (1999). Kirchoff's rule for quantum wires. *Journal of Physics A: Mathematical and General*, *32*, 595–630.

[78] Kottos, T., & Schanz, H. (2001). Quantum graphs: A model for quantum chaos. *Physica E: Low-dimensional Systems and Nanostructures*, *9*, 523–530.

[79] Kottos, T., & Smilansky, U. (1997). Quantum chaos on graphs. *Physical Review Letters*, *79*, 4794–4797.

[80] Kottos, T., & Smilansky, U. (1999). Periodic orbit theory and spectral statistics for quantum graphs. *Annals of Physics*, *274*, 76–124.

[81] Kottos, T., & Smilansky, U. (2000). Chaotic scattering on graphs. *Physical Review Letters*, *85*, 968–971.

[82] Kottos, T., & Smilansky, U. (2003). Quantum graphs: A simple model for chaotic scattering. *Journal of Physics A: Mathematical and Theoretical*, *36*, 3501.

[83] Kozma, R., & Puljic, M. (2015). Random graph theory and neuropercolation for modeling brain oscillations at criticality. *Current Opinion in Neurobiology*, *31*, 181–188.

[84] Kuchment, P. (2002). Graph models for waves in thin structures. *Waves in Random Media*, *12*, R1–R24.

[85] Kuchment, P. (2004). Quantum graphs. I. Some basic structures. *Waves Random Media*, *14*, S107–S128.

[86] Kurasov, P., & Nowaczyk, M. (2005). Inverse spectral problem for quantum graphs. *Journal of Physics A: Mathematical and General*, *38*, 4901–4915.

[87] Kurasov, P., & Nowaczyk, M. (2006). Corrigendum to "Inverse spectral problem for quantum graphs". *Journal of Physics A: Mathematical and General*, *39*, 993.

[88] Kurasov, P., Ogik, R., & Rauf, A. (2014). On reflectionless equi-transmitting matrices. *Opuscula Mathematics*, *34*, 483–501.

[89] Laprise, J. F., Kroger, J., Kroger, H., Louis, P. Y. S., Dube, L. J., Endress, E., ... Moriarty, K. J. M. (2008). Universality of level spacing distributions in classical chaos. *Physics Letters A*, *372*, 4574–4577.

[90] Lee, G. T. (2018). *Abstract algebra: An introductory course*. Springer.

[91] Legrand, O. (1992). Quantum chaos methods applied to high-frequency plate vibrations. *Europhysics Letters*, *18*, 101–106.

[92] Lonsdale, K. (1937). Diamagnetic and paramagnetic anisotropy of crystals. *Reports on Progress in Physics*, *4*, 368–389.

[93] Lothaire, M. (1983). *Combinatorics on words*. Reading, Massachusetts: Addison-Wesley.

[94] Marklof, J. (1998). Spectral form factors of rectangle billiards. *Communications in Mathematical Physics*, *199*, 169–202.

[95] Marklof, J. (2003). Pair correlation densities of inhomogeneous quadratic forms. *Annals of Mathematics*, *158*, 419–471.

[96] Marklof, J., & Yesha, N. (2018). Pair correlation for quadratic polynomials mod 1. *Compositio Mathematica*, *154*, 960–983.

[97] Medvedev, P., Pham, S., Chaisson, M., Tesler, G., & Pevzner, P. (2011). Paired de Bruijn graphs: A novel approach for incorporating mate pair information into genome assemblers. *Journal of Computational Biology*, *18*, 1625–1634.

[98] Mehta, M. L. (2004). *Random matrices* (3rd ed.). San Diego, California: Elsevier.

[99] Müller, S., Heusler, S., Altland, A., Braun, P., & Haake, F. (2009). Periodic-orbit theory of universal level correlations in quantum chaos. *New Journal of Physics*, *11*, 103025.

[100] Müller, S., Heusler, S., Braun, P., Haake, F., & Altland, A. (2004). Semiclassical foundation of universality in quantum chaos. *Physical Review Letters*, *93*, 014103.

[101] Müller, S., Heusler, S., Braun, P., Haake, F., & Altland, A. (2005). Periodic-orbit theory of universality in quantum chaos. *Physical review. E, Statistical, nonlinear, and soft matter physics*, *72*, 046207.

[102] Musyt, O., Nadtochij, O., Stepanchiuk, A., & Beljatynskij, A. (2010). Modelling traffic flows using graph theory. *Mokslas: Lietuvos Ateitis*, *2*, 86–89.

[103] Omnés, R. (1999). *Understanding quantum mechanics*. Princeton, New Jersey: Princeton University Press.

[104] Pakoński, P., Tanner, G., & Życzkowski, K. (2003). Families of line-graphs and their quantization. *Journal of Statistical Physics*, *111*, 1331–1352.

[105] Pattabiraman, V., & Parvathi, R. (2018). Social network analysis using graph theory. *International Journal of Mathematics, Game Theory, and Algebra*, *27*, 45–65.

[106] Pauling, L. (1936). The diamagnetic anisotropy of aromatic molecules. *The Journal of Chemical Physics*, *4*, 673–677.

[107] Petersen, K. (1983). *Ergodic theory*. New York: Cambridge University Press.

[108] Pham, S., & Pevzner, P. (2010). DRIMM-Synteny: Decomposing genomes into evolutionary conserved segments. *Bioinformatics*, *26*, 2509–2516.

[109] Prot, D., Rapine, C., Constans, S., & Fondacci, R. (2010). Using graph concepts to assess the feasibility of a sequenced air traffic flow with low conflict rate. *European Journal of Operational Research*, *207*, 184–196.

[110] Pullirsch, R., Rabitsch, K., Wettig, T., & Markum, H. (1998). Evidence for quantum chaos in the plasma phase of QCD. *Physics Letters B*, *427*, 119–124.

[111] Quaintance, J., & Gould, H. W. (2016). *Combinatorial identities for Stirling numbers: The unpublished notes of H.W. Gould*. Hackensack, NJ: World Scientific.

[112] Quas, A. (2009). Ergodicity and mixing properties. In R. Meyers (Ed.), *Encyclopedia of complexity and systems science*. New York, NY: Springer.

[113] Räz, T. (2018). Euler's Königsberg: The explanatory power of mathematics. *European Journal for Philosophy of Science*, *8*, 331–346.

[114] Riedel, T., & Brunner, U. (1994). Traffic control using graph theory. *Control Engineering Practice*, *2*, 397–404.

[115] Robnik, M. (1992). Improved energy level statistics for a family of billiards with analytic boundaries. *Journal of Physics A: Mathematical and General*, *25*, 3593–3602.

[116] Roth, J. P. (1983). Le spectre du laplacien sur un graphe, Théorie du potentiel. In *Lecture notes in math* (Vol. 1096, pp. 521–539). Springer.

[117] Rueckriemen, R., & Smilansky, U. (2012). Trace formulae for quantum graphs with edge potentials. *Journal of Physics A: Mathematical and General*, *45*, 475205.

[118] Sagan, B. (1991). *The symmetric group: Representations, combinatorial algorithms, and symmetric functions*. New York: Springer.

[119] Sherman, S. (1960). Combinatorial aspects of the Ising model for ferromagnetism. I. A conjecture of Feynman on paths and graphs. *Journal of Mathematical Physics*, *1*, 202–217.

[120] Sieber, M. (2002). Leading off-diagonal approximation for the spectral form factor for uniformly hyperbolic systems. *Journal of Physics A: Mathematical and General*, *35*, L613–L619.

[121] Sieber, M., & Richter, K. (2001). Correlations between periodic orbits and their role in spectral statistics. *Physica Scripta*, *2001*, 128–133.

[122] Steward, E. (2012). *Quantum mechanics: Its early development and the road to entanglement and beyond*. London, United Kingdom: Imperial College Press.

[123] Stöckmann, H. J. (1999). *Quantum chaos: An introduction*. Cambridge, United Kingdom: Cambridge University Press.

[124] Tanner, G. (2000). Spectral statistics for unitary transfer matrices of binary graphs. *Journal of Physics A: Mathematical and General*, *33*, 3567–3585.

[125] Tanner, G. (2001). Unitary-stochastic matrix ensembles and spectral statistics. *Journal of Physics A: Mathematical and General*, *34*, 8485–8500.

[126] Tanner, G. (2002). The autocorrelation function for spectral determinants of quantum graphs. *Journal of Physics A: Mathematical and General*, *35*, 5985–5995.

[127] Turek, O., & Cheon, T. (2011). Quantum graph vertices with permutation-symmetric scattering probabilities. *Physics Letters A*, *375*, 3775–3780.

[128] Webb, J., Docemmilli, F., & Bonin, M. (2015). Graph theory applications in network security. Retrieved from https://arxiv.org/pdf/1511.04785.pdf

[129] Whiteman, K. J. (1977). Invariants and stability in classical mechanics. *Reports on Progress in Physics*, *40*, 1033–1069.

[130] Wigner, E. (1951). On the statistical distribution of the widths and spacings of nuclear resonance levels. *Mathematical Proceedings of the Cambridge Philosophical Society*, *47*, 790–798.

[131] Wigner, E. (1955). Characteristic vectors of bordered matrices with infinite dimensions. *Annals of Mathematics*, *62*, 548–564.

[132] Wishart, J. (1928). The generalised product moment distribution in samples from a normal multivariate population. *Biometrika*, *20A*, 32–52.

[133] Xia, J. (1992). Quantum wave-guide theory for mesoscopic structures. *Physical Review B*, *45*, 3593–3599.

[134] Zelditch, S. (2019). Mathematics of quantum chaos in 2019. *Notices of the American Mathematical Society*, *66*, 1412–1422.

[135] Zhu, J. (2009). *Power systems applications of graph theory.* New York: Nova Science Publishers.